

EFFECTS OF ENHANCING PERFORMANCE IN  
FIBER-WIRELESS NETWORKS

Wan Hafiza Binti Wan Hassan  
B.Eng., M.Sc.

College of Engineering and Science  
Victoria University

Submitted in fulfilment of the requirements for the degree of  
**Doctor of Philosophy**

December 2015



© Copyright by Wan Hafiza Binti Wan Hassan 2016

All Rights Reserved

*In loving memory of my precious still-born daughter, **Nouwar Nadhrah**, whom I carried for 40 weeks and 6 days while I was struggling with my PhD. I am grateful to Allah for granting me the strength in regaining my momentum to endeavour in this journey, amid the sadness of such enormous loss.*

*Till we unite again in the highest heaven, Ameen.*

*“Allah does not charge a soul except [with that within] its capacity”*

*- Al Baqarah:286-*

## DOCTOR OF PHILOSOPHY DECLARATION

I, Wan Hafiza Wan Hassan, declare that the PhD thesis entitled ‘Effects of Enhancing Performance in Fiber-Wireless Networks is no more than 100,000 words in length including quotes and exclusive of tables, figures, appendices, bibliography, references and footnotes. This thesis contains no material that has been submitted previously, in whole or in part, for the award of any other academic degree or diploma. Except where otherwise indicated, this thesis is my own work.

---

Wan Hafiza Binti Wan Hassan

Date: December 1, 2015

# Abstract

The convergence of optical and wireless technologies has given rise to the fiber-wireless (Fi-Wi) network. This network combines the huge capacity of optical fiber with the ubiquity and mobility of wireless networks. Fiber to the premises (FTTP) combined with wireless local area network (WLAN) in home distribution is now becoming a reality. However, network congestion in the wireless access link still limits end user performance, especially in dense residential areas. Therefore, this thesis focuses on the enhancement of the wireless media in Fi-Wi networks.

The thesis considers the realisation of Fi-Wi networks using the gigabit passive optical network (GPON) and the infrastructure based WLAN. The study shows the binary exponential backoff (BEB) adopted in the medium access control (MAC) protocol for the IEEE 802.11 WLAN standard is the key factor inhibiting WLAN performance. The standard distributed coordination function (DCF) access method used by WLAN today provides equal chance of transmissions to all stations. This equality can lead to unfairness between uplink (UL) and downlink (DL) transmissions because the number of active wireless users normally exceeds the number of access points. Generally the Fi-Wis access point (AP) requires greater media access than any of its associate wireless users (WUs) because of the predominance of downlink traffic. Thus, techniques to maximize the network throughput and provide fairness between UL and DL transmissions are proposed. Traffic information obtained from monitoring both GPON and WLAN networks is utilized in the proposed schemes.

The thesis first proposes an optimized constant contention window (OCCW) scheme to improve throughput. The standard BEB algorithm is modified by holding the contention window (CW) size constant irrespective of successful or unsuccessful transmissions. The optimized CW size is determined by the total traffic load passing through the GPON network. In comparison to the legacy BEB, the scheme shows up to 50% improvement in throughput and nearly a five-fold reduction in media access delay under heavy traffic conditions. Subsequently, the OCCW scheme is further improved to ensure the AP in each BSS is given priority. As a result, both UL and DL transmissions are equally probable.

Secondly, the thesis proposes a novel transmission priority scheme with an adaptive backoff technique known as ATxPriority. An adjustable factor is introduced to allow any required AP transmission priority within an infrastructure WLAN network. Expressions for optimum AP and WU contention window size are derived as a function of the number of contending APs and the number of contending WUs, both of which are unknown quantities. However, the scheme capitalizes on information from both GPON and WLAN networks to provide appropriate estimates for these quantities. A new convergence function was then developed to maintain the CW sizes of all WUs within a maximum standard deviation of 2.3% of the mean value at a cost of a 3% reduction in throughput.

Finally, the thesis proposes a scheme based on the well known *Idle Sense* (IS) algorithm that does not require the intermediate step of estimating the number of wireless stations (WUs). IS is a simple distributed control algorithm which seeks to optimize system throughput. However, the thesis shows the additive increase multiplicative decrease (AIMD) algorithm used in IS causes instability under certain conditions which are then identified. The scheme is extended to include multiple basic service sets (BSSs) operating under different transmission priority factors. A network with 30 BSSs responds within 5 seconds to any changes of the priority factor

while maintaining fairness among all BSSs.

# Dedications

*“... He who fear Allah He will hold for him a way out. And give him sustenance from unexpected directions-but thought nothing. And whoever put his **trust in Allah**, Allah will suffice (purpose) it. Allah implement affair (desired) Him. Allah has appointed a measure for all things.” Surah Ath-Thalaq: 2-3*

- **To my Almighty God** - Having **faith in Allah**, my Creator is the vital reason that keeps me going until the completion of this PhD journey.
- **To my loyal bodyguards, my beloved husband and son** - They are always with me through thick and thin. My dearest husband, **Rosmizu Ali** who always keep an eye on my relationship with Allah and without fail supervise my PhD progress, even more than my supervisors. My devoted son, **Ahmad Umair Ziyad** who grew up way much faster than my research; the joy of cuddling him always soothes me after a trying day at uni, which reminds me that it was all worth it.
- **My dearest mom, Siti Fatimah Ismail**- who showered me with infinite love and countless prayer. Her blessings and prayers flows with every heartbeat that shaped the person I am today.

# Acknowledgements

*“Surely, with hardship comes ease”*

*-Al Insyarah:6-*

First and foremost, I thank Allah (SWT) for this PhD journey. Indeed this quest is a huge learning curve full of lifetime lesson; that ultimately made me realize the supreme power of the Almighty Creator. Therefore, I am eternally grateful to Allah the Almighty God for bestowing upon me wisdom, perseverance, and continuously making the impossible possible until completion of this thesis.

I would like to express my utmost gratitude to my main supervisor Prof. Mike Faulkner. This thesis could not be done without his invaluable guidance, dedication, and patience throughout my candidature period. His humbleness and down to earth character amazed me despite the hard time he gave me due to our knowledge gap. I wish him be in best of health, happiness and a blissful life ahead. I am also thankful to my associate supervisor, Dr. Horace King for his constant support, insight and positive remarks irrespective my level of progress and achievement. I am indebted to Dr. Shabbir Ahmed for his technical support and highly appreciate his sincere advice and opinion especially when my steps almost faltered.

My deepest gratitude to Associate Professor Aladin Zayegh, Abdulrahman, Angela and Liz Smith for their kind assistance and support. I want to acknowledge all my past and current colleagues in TEPS (Sirma, Robab, Geordie, Hojjat, Reza, Bhadra,

Baharuddin, Abdul Hadi, Sara, Marziyeh and Pooneh) who have made my PhD journey more memorable through this colourful companionship. A special thank to Raheleh, my loyal GPS guide in tracking Mike and my best write-up buddy who always have more confidence in me than myself. Not forgotten to Nithila who always shared the ‘excitement’ of running simulations as well as for the refreshment during our time-out session. May each of you have a wonderful life ahead.

I would like to express my appreciation to my employer, Universiti Malaysia Terengganu and my sponsor, Malaysian Ministry of Education for their financial support and kind consideration for allowing my study leaves from December 2010 until February 2015.

A heartfelt thanks to members of KVNM community, who have been our extended big family in Melbourne. Their unconditional support, warmth and encouragement always made us feel loved. To the lovely ladies in my beautiful circle of *Usrah Kaum Ibu KNVM*, thank you very much for everything. My special thanks to Ima, Syam and their joyful daughters for laughs and tears, endless supports and understanding. My sincere thanks to Hah & War, Intan & Zuhair and all my friends back home in Malaysia for being there for me and family especially during our trying time coping with the loss of our beloved daughter.

Most importantly, my deepest gratitude to my dearest husband, mother, son, grandmother and the whole clan of Hjh Limah & Co for their endless love, support and prayers. Even though we are thousand miles apart, they remind me to persevere this uphill journey and above all the view from top is all worth it.

# Contents

<b>Doctor of Philosophy Declaration</b>	<b>iv</b>
<b>Abstract</b>	<b>v</b>
<b>Dedications</b>	<b>viii</b>
<b>Acknowledgements</b>	<b>ix</b>
<b>Contents</b>	<b>xi</b>
<b>List of Tables</b>	<b>xvi</b>
<b>List of Figures</b>	<b>xvii</b>
<b>List of Abbreviations</b>	<b>xx</b>
<b>List of Symbols</b>	<b>xxiv</b>
<b>1 Introduction</b>	<b>1</b>
1.1 Overview of Broadband Access Networks . . . . .	1
1.2 Research Aims . . . . .	3
1.3 Research Contributions . . . . .	4
1.4 Thesis Outline . . . . .	5

<b>2</b>	<b>Gigabit Passive Optical Networks</b>	<b>9</b>
2.1	Evolution of Passive Optical Networks . . . . .	10
2.1.1	Comparison between GPON and EPON . . . . .	11
2.1.2	Next Generation PON . . . . .	12
2.2	GPON Architecture . . . . .	13
2.2.1	GPON Identities . . . . .	15
2.3	GPON Frame Format . . . . .	17
2.3.1	Potential Indicators . . . . .	18
2.4	Summary . . . . .	18
<b>3</b>	<b>Wireless Local Area Networks</b>	<b>20</b>
3.1	The Evolution of IEEE 802.11 WLAN standard . . . . .	21
3.1.1	History of IEEE 802.11(b/a/g) . . . . .	21
3.1.2	IEEE 802.11e . . . . .	23
3.1.3	Advent of IEEE 802.11n . . . . .	24
3.1.4	Development of Gigabit WLANs . . . . .	25
3.1.4.1	IEEE 802.11ac . . . . .	25
3.1.4.2	IEEE 802.11ad . . . . .	27
3.2	The General WLAN Standard . . . . .	28
3.2.1	WLAN Architecture . . . . .	28
3.2.2	MAC Protocol . . . . .	30
3.2.2.1	Distributed Coordination Function (DCF) . . . . .	31
3.2.2.2	Point Coordination Function (PCF) . . . . .	34
3.3	Performance Evaluation of IEEE 802.11 WLAN DCF . . . . .	34
3.3.1	MAC Frames Indicator . . . . .	37
3.3.1.1	ACK Frame . . . . .	37
3.3.1.2	RTS and CTS Frames . . . . .	38

3.3.2	Wireless Channel Status Indicator . . . . .	39
3.3.2.1	History Based Backoff . . . . .	39
3.3.2.2	Number of Backoff Pauses . . . . .	39
3.3.3	Number of Idle Slots . . . . .	40
3.3.4	Number of Contending Stations . . . . .	40
3.3.5	Limitations . . . . .	41
3.4	Uplink and Downlink Priority Schemes . . . . .	41
3.4.1	Control CW size . . . . .	42
3.4.2	Reduce Interframe Space (IFS) Period . . . . .	42
3.4.3	Adjust TXOP limit . . . . .	43
3.4.4	Other Schemes . . . . .	44
3.4.5	Limitations . . . . .	44
3.5	Fiber-Wireless Networks . . . . .	46
3.6	Summary . . . . .	48
<b>4</b>	<b>Modified Backoff Technique in Fiber-Wireless Networks</b>	<b>49</b>
4.1	Proposed Fiber Wireless Networks . . . . .	50
4.2	Preliminary Works: Analysis of WLAN Performance . . . . .	52
4.3	Optimized Constant Contention Window Scheme . . . . .	53
4.3.1	Analysis of Constant Contention Window Size . . . . .	54
4.3.2	Optimum Contention Window Size . . . . .	55
4.3.3	Performance Analysis . . . . .	58
4.4	Transmission Priority Scheme . . . . .	61
4.4.1	Uplink and Downlink Transmission Analysis . . . . .	61
4.4.2	Transmission Priority Technique . . . . .	62
4.4.3	Performance Analysis . . . . .	64
4.5	Summary . . . . .	67

<b>5</b>	<b>Transmission Priority Scheme with Adaptive Backoff Technique</b>	<b>69</b>
5.1	Transmission Priority (TxPriority) Scheme . . . . .	70
5.1.1	Derivation of Optimum CW sizes . . . . .	70
5.1.2	Model Validation . . . . .	76
5.1.2.1	Validation to adhoc network in [60] . . . . .	76
5.1.2.2	Validation of Simplification . . . . .	76
5.1.3	Performance Evaluation . . . . .	78
5.2	Adaptive Backoff Technique with Transmission Priority (ATxPriority) scheme . . . . .	81
5.2.1	Measurement of $P_{tr}$ . . . . .	81
5.2.2	Estimate of $n$ . . . . .	83
5.2.3	The Convergence Function . . . . .	85
5.3	ATxPriority Performance . . . . .	90
5.4	Summary . . . . .	92
<b>6</b>	<b>Transmission Priority Scheme using Idle Sense Method</b>	<b>94</b>
6.1	Idle Sense . . . . .	96
6.2	Bias in Idle Sense Method . . . . .	98
6.3	The Accuracy of $\hat{I}$ . . . . .	100
6.4	Fairness Analysis . . . . .	101
6.5	<i>Idle Sense</i> with Transmission Priority in Multiple BSSs WLAN . . . . .	107
6.6	Throughput Performance . . . . .	111
6.7	The Choice of $M$ . . . . .	113
6.8	AP Self-adapting algorithm . . . . .	116
6.9	Wireless User Adjustment Algorithm (WUA) . . . . .	121
6.10	Summary . . . . .	124

<b>7</b>	<b>Conclusions and Future Works</b>	<b>126</b>
7.1	Conclusions . . . . .	126
7.2	Future Works . . . . .	130
<b>A</b>	<b>Full Derivation of Saturation Throughput <math>S</math></b>	<b>132</b>
	<b>References</b>	<b>134</b>

# List of Tables

1.1	Global IP traffic usage ( $10^{15}$ bytes (petabytes,PB) per month) for 2013-2018 [3]. . . . .	2
1.2	Mobile data and internet traffic usage ( $10^{15}$ bytes (petabytes, PB) per month for 2013-2018 [3]. . . . .	3
2.1	Comparison between current GPON and EPON specifications [15]. . . . .	11
2.2	Comparison between mid-term next generation PONs (NG-PON1) [15]. . . . .	13
2.3	GPON nominal transmission rate. . . . .	15
2.4	Types of T-CONT. . . . .	16
3.1	The evolution of IEEE 802.11 standards [26]. . . . .	22
3.2	802.11b OPNET simulation parameters (saturated condition). . . . .	35
4.1	802.11a OPNET simulation parameters (non saturated condition). . . . .	52
5.1	List of Notations . . . . .	72
5.2	802.11a OPNET simulation parameters (saturated condition) . . . . .	78
6.1	$CW_{ap}^{opt}$ (6.22) and $CW_{wu}^{opt}$ (6.24) for varying sizes of BSSs. . . . .	110
6.2	Performance comparison for $M =5,20$ and 1000 . . . . .	115
6.3	Equilibrium throughput for 5 BSSs having different target $k$ . . . . .	120
6.4	Equilibrium throughput for 5 BSSs having different target $k$ and $n^j$ . . . . .	120

# List of Figures

1.1	(a) Physical description of the problem. (b) Thesis structure and links between the chapters. . . . .	6
2.1	Transmission mechanism of GPON. . . . .	14
2.2	Three types of GPON identifiers. . . . .	15
2.3	GPON frame format [13]- [24] . . . . .	17
3.1	Primary and secondary channel selection [26] . . . . .	26
3.2	IEEE 802.11 LAN architecture [25, 27, 41] . . . . .	29
3.3	IEEE 802.11 basic access scheme [25, 42] . . . . .	32
3.4	Four handshakes scheme [42] . . . . .	33
3.5	Point coordination function [43, 47] . . . . .	34
3.6	Effect of network size on saturation throughput . . . . .	36
3.7	BEB saturation throughput versus $CW_{min}$ . . . . .	37
3.8	The dotted circle BSSs are potential interferers to the AP and WUs in BSS 1 (solid circle). . . . .	45
3.9	The Fi-Wi network scenario using the <i>RoF</i> technology [90]. . . . .	47
4.1	Proposed fiber-wireless network scenario . . . . .	50
4.2	Proposed fiber-wireless network scenario with traffic indicators. . . . .	51
4.3	BEB throughput normalized to offered load vs. number of active BSSs. . . . .	53

4.4	Normalized throughput for constant CW size . . . . .	54
4.5	The optimized CW size vs. offered load. . . . .	56
4.6	Comparison of throughput performances vs. offered load. . . . .	57
4.7	Lost bits due to dropped packets caused by buffer overflow. Note: Each packet contains 8184 bits . . . . .	58
4.8	Lost bits due to dropped packets when exceeding retransmission thresh- old (6 retransmissions). Note: Each packet contains 8184 bits . . . . .	59
4.9	Average media access delay. . . . .	60
4.10	The normalized throughput for uplink and downlink transmissions . . . . .	62
4.11	Non-overlapped contention window . . . . .	62
4.12	The optimized contention window size . . . . .	64
4.13	The fairness index . . . . .	65
4.14	The overall normalized throughput . . . . .	66
4.15	The media access delay . . . . .	66
5.1	Discrete markov chain model of the backoff counter $P \{b(t) = 0\} = p$ . . . . .	71
5.2	Normalized throughput, $S$ vs $CW_{wu}$ . . . . .	77
5.3	Comparison of normalized saturation throughputs. . . . .	79
5.4	Comparison of media access delay per packet transmission. . . . .	80
5.5	Estimating $\hat{P}_{tr}$ over one observation period as measured by station Y. . . . .	82
5.6	Average $P_{tr}$ values as measured by one user. . . . .	83
5.7	The convergence of $\bar{n}$ for one station. . . . .	85
5.8	Effect of the convergence factor, $h$ on system throughput. . . . .	86
5.9	The change in $\bar{n}$ per iteration( $c(\bar{n}) = (1 + \frac{h}{\sqrt{\bar{n}}})$ ). . . . .	87
5.10	The change in $\bar{n}$ per iteration ( $c(m, \bar{n}) = (1 + \frac{h+2\log_{10}m}{\sqrt{\bar{n}}})$ ). . . . .	87
5.11	The convergence of $\hat{C}W_{wu}$ toward $CW_{wu}^{opt}$ . . . . .	90
5.12	Comparison of normalized saturation throughputs. . . . .	91

5.13	The cumulative distribution function of $CW_{wu}$ .	92
5.14	Comparison of the measured transmission ratio factor.	93
6.1	Non-productive (wasted) time.	95
6.2	The cumulative distribution function of $I$ .	101
6.3	The Jain fairness index (6.14) vs. number of stations.	102
6.4	The probability distribution functions (pdfs) of $I$ for 2 classes of stations	103
6.5	The cumulative distribution function of CW with 136 contending stations	105
6.6	The cumulative distribution function of CW with 16 contending stations	106
6.7	Normalized saturation throughput vs. number of BSSs	111
6.8	The Jain fairness index (6.14) vs. the number of BSSs.	112
6.9	The cumulative distribution function of $CW_{wu}$ with 120 WUs	114
6.10	The cumulative distribution function of $CW_{ap}$ for different $P_{set}$	116
6.11	The convergence time for of one AP for different $P_{set}$	117
6.12	The fairness between 30 APs for networks with $k = 0.5, 1$ and $2$ .	119
6.13	The normalized saturation throughputs as the network's target $k$ varies	119
6.14	The network (30 BSSs) responses to the changes of the target $k$ ( $\alpha = 1$ ).	123

# List of Abbreviations

AAP	Assymmetric Access Point
AC	Access Category
ACK	Acknowledgement
AIFS	Arbitration Inter-Frame Space
AIMD	Additive Increase Multiplicative Decrease
AP	Access Point
APC	Adaptive Priority Control
APSA	Access Point Self-adapting
ATM	Asynchronous Transfer Mode
AWA	Adaptive Window Algorithm
BEB	Binary Exponential Backoff
BER	Bit Error Rate
BPON	Broadband PON
BSS	Basic Service Set
CAGR	Compound Annual Growth Rate
CCA	Clear Channel Accessment
CSMA/CA	Carrier Sense Multiple Access with Collision Avoidance
CTS	Clear To Send
CW	Contention Window
DCF	Distributed Coordination Function

DDCWC	Dynamic Deterministic Contention Window Control
DIDD	Double Increment Double Decrement
DIFS	DCF Interframe Space
DL	Downlink
DSL	Digital Subscriber Loop
EBA	Estimation Based Backoff Algorithm
EDCA	Enhanced Distributed Channel Access
EFM	Ethernet in the First Mile
EIED	Exponential Increase Exponential Decrease
EPON	Ethernet PON
ESS	Extended Service Set
Fi-Wi	Fiber-Wireless
FSAN	Full Service Access Network
GEM	GPON Encapsulation Method
GPON	Gigabit Passive Optical Network
HBAB	History Based Adaptive Backoff
IBSS	Independent BSS
ID	Identifier
IEEE	Institute of Electrical and Electronics Engineers
IP	Internet Protocol
IS	Idle Sense
ITU	International Telecommunication Union
MAC	Medium Access Control
MANET	Mobile Adhoc Network
MIMO	Multiple Input Multiple Output
NAV	Network Allocation Vector
NAVC	Network Allocation Vector Count

NBN	National Broadband Network
NG-PON	Next Generation PON
OCCW	Optimized Constant Contention Window
OCDM	Optical Code Division Multiplexed
OECD	Organisations for Economic Cooperation and Development
OFDM	Orthogonal Frequency Division Multiplexed
OLT	Optical Line Terminal
ONT	Optical Node Terminal
PC	Point Coordinator
PCB	Pause Count Backoff
PCF	Point Coordination Function
PHY	Physical
PIFS	PCF Inter-Frame Space
PLI	Payload Length Indicator
PMD	Physical Medium Dependent
PON	Passive Optical Network
QoS	Quality of Service
RAU	Remote Access Unit
<i>R&amp;F</i>	Radio and Fiber
<i>RoF</i>	Radio over Fiber
RTS	Request to Send
SDM	Spatial Division Multiplexing
SIFS	Short Inter-Frame Space
SNR	Signal to Noise Ratio
TDM	Time Division Multiplexed
TDMA	Time Division Multiplexing Access
TXOP	Transmission Opportunity Priority

UFB	Ultra Fast Broadband
UL	Uplink
UP	User Priorities
US BW Map	Upstream Bandwidth Mapping
VHT	Very High Throughput
WDM	Wavelength Division Multiplexed
WLAN	Wireless Local Area Network
WU	Wireless User
WUA	Wireless User Adjustment

# List of Symbols

$CW_{min}$	Minimum CW size
$CW_{ap}$	CW size of an AP
$CW_{wu}$	CW size of a WU
$x_1$	downlink normalized throughput
$x_2$	uplink normalized throughput
$p$	probability of a station transmitting
$p_{ap}$	probability of an AP transmitting
$p_{wu}$	probability of a WU transmitting
$m$	total number of APs
$n$	total number of WUs
$w$	random backoff value
$P_s$	probability of a successful transmission given that there is a transmission
$P_s^{ap}$	probability of a successful AP transmission given that there is a transmission
$P_s^{wu}$	probability of a successful WU transmission given that there is a transmission
$k$	transmission priority factor
$k_{mea}$	measured transmission priority factor
$T$	packet transmission time (measured in slots)
$\gamma$	fraction of time used for payload transmission
$E[I]$	average number of consecutive idle slots

$T_{Header}$	Header transmission time
$T_{Payload}$	Payload transmission time
$S$	Normalized saturation throughput
$S_{wu}$	Normalized uplink saturation throughput
$S_{ap}$	Normalized downlink saturation throughput
$Q$	simplification variable
$N$	Total number of stations
$CW_{ap}^{opt}$	optimum $CW_{ap}$
$CW_{wu}^{opt}$	optimum $CW_{wu}$
$CW^{opt}$	optimum $CW$
$\overline{CW}$	average CW size
$\overline{CW}_{wu}$	average CW size size of a WU
$\overline{CW}_{ap}$	average CW size of an AP
$F_B$	number of times the channel is busy
$F_I$	number of times the channel is idle
$\hat{P}_{tr}$	Estimated transmission probability
$\bar{P}_{tr}$	the average of the estimated transmission probability
$\hat{n}$	estimated number of WUs
$\bar{n}$	the average of estimated number of WUs
$\hat{C}W_{ap}$	estimated $CW_{ap}$
$\hat{C}W_{wu}$	estimated $CW_{wu}$
$\alpha$	smoothing factor
$h$	convergence factor
$\sigma_{\overline{CW}_{wu}}$	the measure standard deviation of the $\overline{CW}_{wu}$
$\mu_{\overline{CW}_{wu}}$	the measured mean of the $\overline{CW}_{wu}$
$\hat{I}$	the estimate number of idle slots per transmission
$I_t$	the target number of idle slots per transmission

$M$	the number of transmission attempts over which the measurement is taken.
$\psi$	decrement factor for AIMD algorithm
$\phi$	increment constant for AIMD algorithm
$I_{median}$	median idle slots per transmission
$x$	number of slots to produce $M$ transmission attempts
$CW_t$	optimum CW size
$CW_{eq}$	equilibrium point in terms of CW size
$F$	fairness index
$p_i$	probability of an idle slot
$p_i^{opt}$	optimum probability of an idle slot
$\Omega$	constant probability when all stations in adhoc WLAN using IS
$\beta$	constant probability when only WUs in infrastructure WLAN using IS
$T_i$	idle slot time
$T_s$	average time the channel is sensed busy due to collision
$T_c$	average time the channel is sensed busy due to successful transmission
$\bar{I}$	mean of estimate $I$
$P_d$	number of successfully transmitted packets by AP
$P_u$	number of successfully received packets by AP
$\delta$	alteration size of $CW_{ap}$
$P$	number of AP transmissions
$P_{set}$	maximum number of AP transmissions
$\Delta$	the difference between target $k$ and measure $k_{mea}$
$\delta$	reduction/increment size of CW in APSA algorithm
$n^j$	number of WUs in $j^{th}$ BSS
$p_s^j$	probability of a successful transmission in $j^{th}$ BSS
$p_{s_wu}^j$	probability of a successful WU transmission in $j^{th}$ BSS

# Chapter 1

## Introduction

### 1.1 Overview of Broadband Access Networks

Broadband access networks connect millions of users to the internet, providing various services, including voice, data and video [1]. According to the latest study carried out by the Organisations for Economic Cooperation and Development<sup>1</sup> (OECD), 97% of the internet access in the OECD countries has been upgraded almost entirely to broadband leaving only 3% of the total subscribers still using the dial-up links [2]. Cisco reported that global internet protocol (IP) traffic in 2013 stands at 51.2 exabytes ( $10^{18}$  bytes) per month and will nearly triple by 2018. Table 1.1 indicates that the IP traffic across the globe will grow at a compound annual growth rate (CAGR) of 21% from 2013 to 2018 [3].

This ever increasing internet usage has strongly motivated the necessity of upgrading the access network infrastructure. As of now, the network remains a bottleneck in efforts to deliver services to customers due to the limitation of available bandwidth.

Networks are categorized into fixed and wireless segments, In essence, there are two

---

<sup>1</sup>An international economic organisation of 34 countries across the globe founded in 1961 to stimulate economic progress and world trade.

Table 1.1: Global IP traffic usage ( $10^{15}$  bytes (petabytes,PB) per month) for 2013-2018 [3].

(By Geography PB per month)	2013	2014	2015	2016	2017	2018	CAGR 2013-2018
Asia Pacific	17,950	22,119	26,869	32,383	39,086	47,273	21%
North America	16,607	20,293	24,599	29,377	34,552	40,545	20%
Western Europe	8,396	9,739	11,336	13,443	16,051	19,257	18%
Latin America	3,488	4,361	5,318	6,363	7,576	8,931	21%
Central Eastern Europe	3,654	4,416	5,443	6,666	8,332	10,223	23%
Middle East Africa	1,074	1,546	2,174	3,027	4,108	5,324	38%
<b>Total</b>	51,168	62,476	75,739	91,260	109,705	131,553	21%

distinct substances used for fixed broadband access networks: copper and fiber optics. Digital subscriber loop (DSL) is one of the dominant services offered by twisted pair (copper) networks. The DSL technologies are now matured and close to achieving their maximum performance. They evolve into higher speeds but at the cost of a shorter reach. Theoretically, DSL only will be able to provide 200 Mbps to the home if there is a node close to each house which is apparently an impractical solution [4]. In contrast, fiber optics offer virtually unlimited carrying capacity as the speed can exceed 100 terabits ( $10^{15}$  bits) per second over hundreds of kilometres [89]. Gigabit passive optical network (GPON) is preferred for low cost residential users, now has access rates of 2.5 Gbps, and will increase to 10 Gbps [15]. Even though optical fibers are an ideal media for high-speed broadband networks, the deployment cost was considered prohibitive in the access area, and copper wires still dominate in the current market place. However, due to the fact that the copper wire has reached its maximum speed, fiber will eventually become the dominant access technology in the near future.

On the other hand, wireless is most convenient for users and gaining popularity. Statistics in Table 1.1 show that the global mobile data traffic will grow three times faster than fixed IP traffic from 2013 to 2018. This is mainly because the wireless networks offer end users great flexibility and mobility. Wireless local area network

Table 1.2: Mobile data and internet traffic usage ( $10^{15}$  bytes (petabytes, PB) per month for 2013-2018 [3].

<b>(By Geography PB per month)</b>	2013	2014	2015	2016	2017	2018	CAGR 2013-2018
Asia Pacific	524	953	1,670	2,777	4,442	6,718	67%
North America	389	625	969	1,453	2,101	2,954	50%
Western Europe	254	389	593	888	1,310	1,900	50%
Latin America	92	177	308	505	789	1,158	66%
Central Eastern Europe	117	231	420	705	1,115	1,619	69%
Middle East Africa	106	207	378	651	1,031	1,490	70%
<b>Total (PB per month)</b>	1,480	2,582	4,337	6,981	10,788	15,838	61%

(WLAN) is the most favoured wireless network due to its low cost and ease of installation. However, it is limited to a much lower bandwidth than the fixed network and the transmission channel is susceptible to a variety of impairments [5]. Wireless usage will saturate unless these issues are addressed.

Interestingly, optical and wireless networks can be viewed as complementary: fiber has a sufficient bandwidth but does not go everywhere while wireless can go everywhere but has a limited bandwidth. Therefore, fiber-wireless (Fi-Wi) broadband access networks are realized by combining the huge capacity of fiber with the ubiquity and mobility of wireless networks. The development of Fi-Wi networks makes the enhancement of both optical and wireless networks important. This thesis studies the Fi-Wi networks scenario by focusing on the enhancement of the wireless side, which is seen as the critical bottleneck.

## 1.2 Research Aims

The main aim of the research is to improve WLAN (multiple basic service sets (BSSs)) performance of Fi-Wi networks based on GPON and WLAN integration by increasing media access efficiency, improving fairness and exploiting the synergies between

optical and wireless media. The specific aims are as follows:

- To study the media access control (MAC) protocol of the GPON and identify potential traffic indicator(s) that can be used in the WLAN enhancement. (Chapter 2)
- To study the MAC protocol of the existing IEEE 802.11 WLAN and identify the factors that affect the throughput performance. (Chapter 3)
- To modify the legacy binary exponential backoff (BEB) algorithm in a WLAN in order to allow the network to improve network capacity. (Chapter 4)
- To investigate the causes of fairness problem in a multiple BSSs network scenario. (Chapter 4)
- To derive expressions that optimize the CW sizes of an access point (AP) and wireless users (WUs) for maximum throughput while achieving the desired fairness between uplink and downlink transmissions. (Chapter 5)
- To develop a distributed algorithm that dynamically tracks changes in the network while maintaining optimum CW sizes in a robust and simple way. (Chapter 6)

### 1.3 Research Contributions

The research has led to the following peer-reviewed publications:

- W. H. W. Hassan, M. Faulkner, and H. King, “Integration of a modified distributed coordination function (DCF) in Wireless LAN using IEEE 802.11n to mitigate interference and optimise transmission capacity in full duplex gigabits passive optical network (GPON), in *8th International Conference on Information, Communications and Signal Processing (ICICS)*, 2011. IEEE, pp. 1-4.

- W. H. W. Hassan, H. King, and M. Faulkner, “Modified backoff technique in fiber-wireless networks, in *IEEE 23rd International Symposium on Personal Indoor and Mobile Radio Communications (PIMRC)*, 2012. IEEE, pp. 431-435.
- W. H. W. Hassan, H. King, S. Ahmed, and M. Faulkner, Modified back-off technique with transmission priority scheme in fiber-wireless networks, in *AFRICON*, 2013. IEEE, pp. 1-4.
- W. H. W. Hassan, H. King, S. Ahmed, and M. Faulkner, “Transmission Priority Scheme with Adaptive Backoff Technique in Fiber-Wireless Networks,” *EURASIP Journal on Wireless Communications and Networking*, 2015, no. 1 (2015), pp. 1-14
- W.H.W. Hassan, H. King, S. Ahmed and M. Faulkner, “WLAN Fairness with Idle Sense,” in *IEEE Communication Letters*, IEEE , vol.19, no.10, Oct. 2015, pp. 1794-1797.
- W.H.W. Hassan, H. King, S. Ahmed and M. Faulkner, “Idle Sense with Transmission Priority Scheme in Fiber-Wireless Networks,” in *IEEE Transactions on Mobile Computing* (Manuscript Preparation).

## 1.4 Thesis Outline

Fig. 1.1(a) shows a physical description of the problem. The fibre GPON network provides high speed connections into individual residences. The data is then re-distributed from an access point (AP) to the respective wireless user (WU) using a wireless LAN. It is assumed the spectrum is owned by the service provider, and is limited to a single channel. The WLANs therefore interfere with each other, causing throughput degradation and fairness problems. The thesis uses traffic information

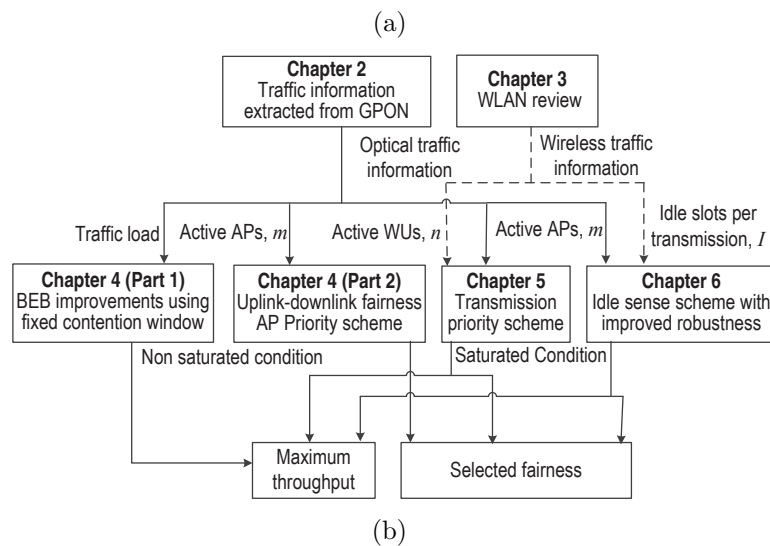
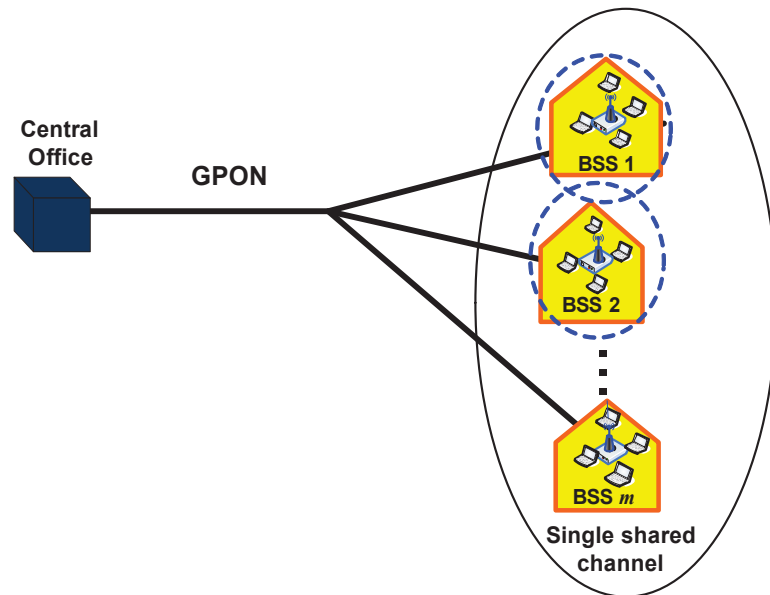


Figure 1.1: (a) Physical description of the problem. (b) Thesis structure and links between the chapters.

from the GPON headers combined with wireless channel activity measurements to optimise the MAC parameters for maximum throughput and fairness. The structure of the thesis and links between the chapters is shown in Fig. 1.1(b). The chapter contents are summarised below.

- Chapter 2 reviews the progress of the passive optical networks starting from the first PON standard until the next generation PON. The chapter then focuses on the gigabit optical networks (GPON), discussing its architecture and frame format. In addition, the chapter also identifies the potential traffic indicators extracted from GPON.
- Chapter 3 reviews the relevant WLAN literature. The chapter first studies the evolution of the IEEE 802.11 WLAN standard. Then, the chapter explores the pertinent features of IEEE 802.11 including the architecture and medium access control. Further, it reviews the techniques to improve the throughput performance. The chapter also investigates the uplink and downlink priority schemes. Finally, the chapter discusses the development of the fiber-wireless networks (the studied network scenario in this thesis).
- Chapter 4 addresses the idea of integrating the gigabit passive optical network (GPON) with the wireless local area network (WLAN). The chapter proposes two techniques to improve the end user performance. The first technique: optimized contention window size (OCCW) modifies the BEB scheme by introducing fixed contention window (CW) sizes and exploiting the content of the GPON control frame in order to assign the optimum CW sizes for maximum throughput. The second technique: AP priority (APPriority) investigates the fairness between uplink (UL) and downlink (DL) transmissions of the OCCW scheme and proposes a transmission priority scheme.

- Chapter 5 proposes a novel approach known as the TxPriority scheme. The scheme introduces a transmission priority factor that can be adjusted to allow AP transmission priorities. The chapter derives the optimum AP and WU contention window sizes and shows that the optimum CW sizes depend on the number of active APs and WUs: unknown quantities. The chapter then demonstrates that the information from both the GPON and WLAN networks can be capitalized to provide appropriate estimates and makes the system adaptive. Finally, a new convergence function is introduced to improve the reliability of the adaptive system.
- Chapter 6 first investigates the robustness of the previously proposed *Idle Sense* (IS) method in [67] by varying CW sizes in the network and identifies the causes of the fairness problem in IS. The chapter then proposes a potential solution to improve the fairness. Next, the chapter incorporates the IS scheme with the existing *Asymmetric Access Point* scheme and analytically extends them to a scenario with multiple BSSs. Furthermore, the chapter presents two additional algorithms: access point self adapting (APSA) and wireless user adjustment (WUA), to ensure all the APs achieve their set priorities while maintaining bandwidth fairness amongst BSSs.
- Finally, Chapter 7 summarizes the key outcomes and findings of the thesis, and gives direction for future work.

## Chapter 2

# Gigabit Passive Optical Networks

Passive optical network (PONs) are considered the most promising technology for fixed local access. This is mainly because the signals in PON are replicated passively by a splitter without involving any electric component. Hence, the PON deployment incurs less cost since it does not require any electrical power or backup batteries. In addition, it also offers higher reliability due to the absence of the electronic components, which are prone to failure [6, 7]. Above all, the simplicity and the flexibility in the deployment makes PON become a favourite access technology.

This chapter reviews the progress of the passive optical networks starting from the first PON standard up to the next generation PON. The chapter then focuses on the gigabit optical networks (GPON), discussing its architecture and frame format. In addition, the chapter also identifies the potential traffic indicators extracted from GPON.

Section 2.1 presents the evolution of PONs and Section 2.2 describes the GPON architecture. Finally, Section 2.3 discusses the GPON frame format and presents the potential traffic indicators.

## 2.1 Evolution of Passive Optical Networks

The first PON standard was introduced in 1995 by the Full Service Access Network (FSAN) consortium [8]. It is based on an asynchronous transfer mode (ATM) framing and known as APON. In 1999, the ITU-T body enhanced APON into broadband PON (BPON) and standardised them in the G 983 series of recommendation. It supported 32-64 users per PON with a maximum data rate of 622 Mbps and 155 Mbps in the downstream and the upstream directions respectively. While maintaining ATM as its main protocol, BPON was also allowing non-ATM traffic by encapsulating it within the ATM cells [9]. Although the architecture of BPON was flexible and adapted well to different types of service, it started to lose its popularity when the IP-based traffic became more popular and it proved to be further inefficient due to the complexity in the ATM protocol [10].

As a solution to cater to the need for a larger bandwidth, FSAN proposed gigabit passive optical networks (GPON) in late 2001. In 2003, the ITU-T body approved the first two GPON standards, i.e., the basic architecture (G 984.1) [11] and the physical-medium-dependent (PMD) layer (G984.2) [12]. Then, the last two standards, GPON transmission convergence layer (G 984.3) [13] and ONT management and control interface specification (G 984.4) [14] were approved in 2004. In comparison to BPON, GPON offers higher transmission rates and provides a much simpler frame format known as the GPON encapsulation method (GEM) to support video, voice and data services. Therefore, GPON has a capability to encapsulate different frame protocols into their native GEM frames before they get transmitted [10].

On the other hand, the IEEE body assigned the Ethernet in the First Mile (EFM) task force to work on their own PON system, known as ethernet PON (EPON) shortly before GPON was proposed by FSAN in 2001. EPON was ratified by IEEE in September 2004 (after GPON had been approved by ITU-T) and released as an

Table 2.1: Comparison between current GPON and EPON specifications [15].

Feature/PON	GPON	EPON
Standards	ITU-T G984.X	IEEE 802.3ah
Maximum rates	1.25 Gbps(↑) 2.5 Gbps(↓)	1.25 Gbps (↓ ↑)
Frame Format	GPON Encapsulation Method (GEM)	Ethernet
Number of users per PON	32-64	16-32
Bandwidth per user	40-80 Mbps	30-60 Mbps
Video	RF/IP	RF/IP
Cost	Medium	Low

IEEE 802.3ah standard. The key goal of EPON is to achieve a full compatibility with other ethernet based networks.

### 2.1.1 Comparison between GPON and EPON

Currently, GPON and EPON are the two dominant standards in PON which share the same objective: to improve the transmission speed at gigabit line rates. Both standards evolved heavily from the BPON standard as their general concept [8]. However, there are significant differences between them as summarized in Table 2.1.

In comparison to EPON, the current GPON offers higher capacity, allows more subscribed users per PON and allocates more bandwidth per user. Thus, GPON is more popular with the Telecommunications service providers, most adopted in Europe and North America [16]. Indeed, Australian and New Zealand governments employed GPON as the backhaul network for their respective National Broadband Network (NBN) and Ultra-Fast Broadband (UFB) projects [17]. Nevertheless, EPON is deployed in many Asian countries, including Japan, due to its low cost [7].

### 2.1.2 Next Generation PON

Despite the fact that the current PON technology offers data rate up to 2.5 Gbps, the end users only get access to limited megabits per second data rate because the maximum bandwidth is shared by all users in the PON. Therefore, the allocated bandwidth per user is insufficient to cater for bandwidth-hungry applications such as video on demand, voice over IP, video conferencing, high-definition TV (HDTV), online gaming and others [15, 18].

To meet the anticipated capacity, next generation PONs (NG-PONs) have been proposed by the telecommunications interest group, i.e., IEEE and FSAN. In comparison to the current GPON/EPON architectures, NG-PONs are mainly envisioned to achieve higher performance parameters such as higher bandwidth per user, increased number of users and extended maximum reach [19]. NG-PON can be divided into NG-PON1 and NG-PON2, known as mid-term next generation PON and long-term next generation PON respectively. Table 2.2 compares the NG-PON1 standards offered by IEEE and FSAN. NG-PON1 enhances the current generation PON by increasing the data rate from 2.5 Gbps to 10 Gbps without affecting their coexistence on the same optical distribution network (ODN). However, it is predicted that the NG-PON1 will still be insufficient to accommodate the rapid growth in the new applications and services. Therefore, NG-PON2 has been proposed by FSAN as an enhancement to the NG-PON1 and a solution to the bandwidth-hungry applications. At present, NG-PON2 is expected to offer a maximum bandwidth of 40/10 Gbps (downstream/upstream) and will reach 160/80 Gbps in future [15].

The existing TDM-PON architecture employed in the current PON system is incapable of supporting the huge bandwidth increment in NG-PON2. Thus, it requires a new access technology that is capable of delivering higher bandwidth and supporting a major number of users while lowering down the energy consumption and cost [16]. Many research studies have been carried out to study the potential

Table 2.2: Comparison between mid-term next generation PONs (NG-PON1) [15].

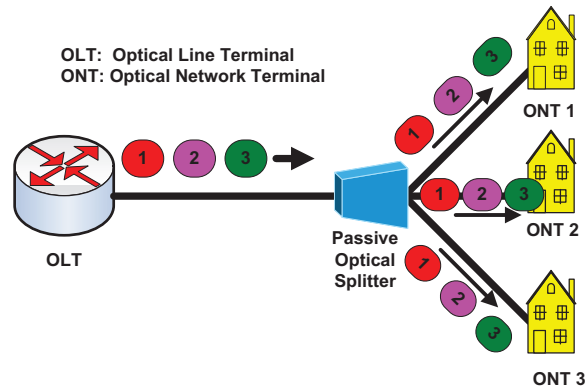
Feature/PON	10 GE-PON	XG-PON1	XG-PON2
Current PON	EPON	GPON	GPON
Standards	IEEE 802.3 av	FSAN	FSAN
Maximum rates	10 Gbps ( $\downarrow \uparrow$ )	2.5 Gbps( $\uparrow$ ) and 10 Gbps( $\downarrow$ )	10 Gbps ( $\downarrow \uparrow$ )
Frame Format	Ethernet	GEM	GEM
Number of users per PON	$\geq 64$	$\geq 64$	$\geq 64$
Bandwidth per user	$\geq 100$ Mbps	$\geq 100$ Mbps	$\geq 100$ Mbps
Video	RF/IP	RF/IP	RF/IP
Cost	High	High	High

technologies for NG-PON2 namely, wavelength division multiplexed PON (WDM-PON) [7, 18], hybrid WDM/TDM-PON [7, 16, 20], optical code-division multiplexing PON (OCDM-PON) [19] and orthogonal frequency division multiplexing PON (OFDM-PON) [16, 21]. Among these technologies, hybrid WDM/TDM-PON has the brightest potential because it supports backward compatibility, flexibility and static sharing [15]. In addition, it is important to note that NG-PON2 requires a revolutionary upgrade of current PONs' infrastructure to allow higher splitting ratio and longer maximum reach. Therefore, it is a big challenge for network operators to ensure gradual and smooth migration capability for existing users to NG-PON2 system [22].

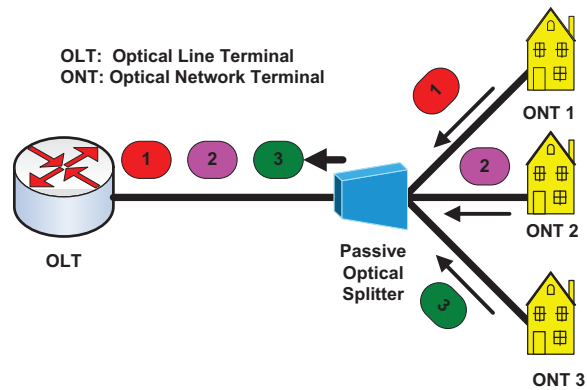
From the above discussion, it is concluded that the current GPON has a promising future and will become an elegant legacy for its successor. Therefore, the rest of the chapter is now focusing on GPON.

## 2.2 GPON Architecture

Fig. 2.1 illustrates the gigabit passive optical network (GPON) architecture including its transmission mechanism for downstream and upstream transmissions. The optical line terminal (OLT) at the central office is connected to a passive optical power



(a) Downstream transmission of GPON



(b) Upstream transmission of GPON

Figure 2.1: Transmission mechanism of GPON.

splitter using a single-mode optical fiber which divides the optical power into  $N$  ( $N$  varies from 16 up to 128) separate paths to the subscribed optical network terminals (ONTs). An individual single-mode fiber strand runs from the optical splitter to each ONT and the physical reach from the OLT to ONTs can go up to 20 km.

GPON employs a time division multiplexing (TDM) for downstream (1480-1500 nm) and a time division multiplexing access (TDMA) for upstream (1260-1360 nm) transmissions. Besides, the wavelength 1550-1560 nm is used for downstream video transmission. Several transmission rates for the downstream and the upstream lines are defined in the GPON standard [11] as summarized in Table 2.3. All rates combination are made possible except for downstream 1.2 Gbps and upstream 2.4 Gbps.

However, most often, vendor offer only 2.4 Gbps in downstream and 1.2 Gbps in upstream [23].

Table 2.3: GPON nominal transmission rate.

Transmission Line	Rate (Gbps)
Downstream	1.244
	2.488
Upstream	0.155
	0.622
	1.244
	2.488

The downstream traffic is broadcast to all ONTs and each frame is labeled with the address of its target ONT as depicted in Fig. 2.1. The OLT has full control of upstream transmissions by allocating fixed or variable time slots to each ONT.

### 2.2.1 GPON Identities

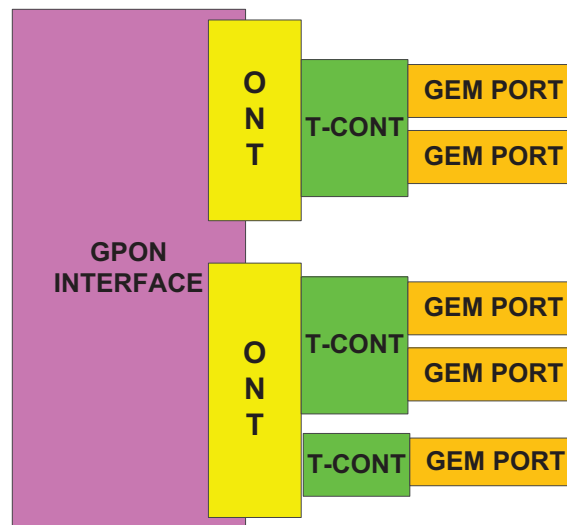


Figure 2.2: Three types of GPON identifiers.

At the GPON interface, Fig. 2.2 shows three identities used at the end user, namely: optical network terminal ONT, transmission containers (T-CONT) and GPON encapsulation method (GEM) port. An ONT is identified by a unique ONT-ID (ranges from 0 to 256) assigned by the OLT. Within each ONT, there is at least one T-CONT, a traffic-bearing object. Each T-CONT is assigned a unique Alloc-ID as its identity that ranges from 0 to 4095. T-CONT is used by ONT to buffer the upstream traffic before it gets transmitted to the OLT. T-CONTs are mainly employed to improve the upstream bandwidth management by enabling quality of service (QoS) implementation in the upstream direction. This is achieved by allocating five types of T-CONTs to the user as classified in Table 2.4.

On the other hand, GEM Ports are virtual ports for transmitting frames between OLT and ONT. Each T-CONT consists of one or more GEM ports because each different traffic class per ONT is assigned a different GEM port. A unique 12 bit number known as a GEM port identifier (port ID) is assigned by the OLT to each GEM port for identification purposes.

Table 2.4: Types of T-CONT.

BW Type	Delay Sensitive	Applicable T-CONT Types				
		Type 1 (Voice)	Type 2 (Video)	Type 3 (Data Higher Priority)	Type 4 (Data)	Type 5
Fixed	Yes	X				X
Assured	No		X	X		X
Non-assured	No			X		X
Best effort	No				X	X



subframe to the OLT.

### 2.3.1 Potential Indicators

The broadcast nature of downstream transmissions allow ONTs to retrieve network traffic information. Three traffic indicators are defined within the integrated ONT-AP. First, the downstream traffic load indicator is obtained by extracting the contents of the PLI subfield in the GEM headers. This provides the size of the downstream traffic going into the ONTs, which in turn is the total traffic transmitted from APs to wireless users (WUs). Second, the traffic load indicator is defined by analyzing the US BW Map subfield; the sum of the lengths of each allocated time slot provides an estimate for the total size of upstream traffic. However, this indicator is lagging because the traffic load has already been transmitted across the WLAN. Assuming the traffic statistics are relatively constant over the measuring period, this indicator corresponds to the total traffic transmitted from WUs to APs. The third indicator gives the total number of active integrated ONT-APs at the air interface by combining the estimate of active ONTs on the upstream and the downstream lines, extracting information from the Port-ID and the US BW Map subfields respectively.

At the air interface of the integrated ONT-AP, these three traffic indicators (i.e. upstream traffic size, downstream traffic size and total number of active APs) can be exploited to enhance the performance in the wireless side of Fi-Wi networks.

## 2.4 Summary

In summary, the chapter first discusses the evolution of PONs. It starts with APON, is followed by BPON, GPON and EPON. The comparison between two dominant standards of PON: GPON and EPON, is presented and subsequently, the future of PON technology is discussed. Then, the study of GPON architectures and protocols

revealed that the broadcast nature of GPON's architecture allows users to gain traffic information. Thus, three traffic indicators are identified within GPON: upstream traffic size, downstream traffic size and total number of active ONTs. These indicators can be used to enhance the network performance.

The next chapter studies the basics of the wireless part and investigates the literature concerning the performance enhancement of the wireless networks.

# Chapter 3

## Wireless Local Area Networks

A wireless local area network (WLAN) connects at least two devices and usually operates in unlicensed radio frequency spectrum bands. After being introduced nearly two decades ago, the demand for WLAN deployments has continuously increased due to their low cost and ease of installation. The applications of WLAN range from the provision of internet access to the unified interconnection of electronic devices [25].

This chapter reviews the literature relevant to WLAN in order to form a solid foundation for the thesis. The pertinent features of IEEE 802.11, including the architecture and medium access control, are studied and presented. Prior to that, the evolution of the WLAN standard is reviewed to give the information on the progress that has been made by the WLAN since its first appearance. The throughput performance of WLAN is analysed through simulations to illustrate the well known performance degradation at high user density. Then, a critical review of the techniques to improve the performance is presented by classifying them according to the network indicators they use. The unfairness between uplink and downlink transmissions is another identified problem in an infrastructure WLAN. Therefore, a literature review on the transmission priority schemes is carried out. Finally, the development of the fiber-wireless networks (the studied network scenario in this thesis) is presented

towards the end of the chapter.

This chapter is organized as follows. Section 3.1 presents the evolution of the IEEE 802.11 WLAN standard. Section 3.2 discusses the general WLAN standards including the architectures and MAC protocols. Section 3.3 analyses the throughput performance of the WLAN and reviews the existing adaptive backoff techniques. Section 3.4 investigates the uplink and downlink priority schemes. Lastly, Section 3.5 studies the fiber-wireless networks.

## **3.1 The Evolution of IEEE 802.11 WLAN standard**

A new IEEE committee was set up in 1990 to draft the WLAN standard known as IEEE 802.11. The standard was first published in 1997, at a time when the demand for wireless devices was high. Since then, IEEE 802.11 has become a widely used WLAN standard.

The IEEE 802.11 standard defines an over-the-air interface between a wireless client and an access point, or at least two wireless clients. It covers the medium access control (MAC) sub-layer and the physical layer of the open system interconnection (OSI) reference model. Table 3.1 summarizes and compares the main specification of each standard: IEEE 802.11a, b, g, n, ac and ad.

### **3.1.1 History of IEEE 802.11(b/a/g)**

The first two generations, IEEE 802.11b and IEEE 802.11a, were ratified in 1999 and operated in the unlicensed 2.4 GHz industrial, scientific and medical (ISM) band and the unlicensed 5 GHz national information infrastructure (U-NII) band respectively.

Table 3.1: The evolution of IEEE 802.11 standards [26].

Feature/IEEE Standard	802.11b	802.11a/g	802.11n	802.11ac	802.11ad
Maximum data rate per stream (Mb/s)	11	54	>100	>500 (Assuming 80 MHz channels)	7000
Frequency band (GHz)	2.4	5/ 2.4	2.4 and 5	5	60
Channel width (MHz)	20	20/20	20 and 40 (40 is optional)	20, 40,80,160, and 80+80 (last two are optional)	2160
Antenna technology	SISO	SISO	MIMO	MIMO/MU-MIMO	SISO/MIMO
Transmission technique	DSSS	DSSS OFDM	OFDM	OFDM	OFDM
Maximum number of spatial streams	1	1	4	8	
Beamforming	No	No	Yes	Yes	Yes
Date ratified by IEEE	1999	1999/2003	2009	2013	2013

Later in 2003, the third standard was ratified called IEEE 802.11g utilizing the same band as IEEE 802.11b. IEEE 802.11b employs direct sequence spread spectrum as the transmission technique and achieves a maximum data rate of 11 Mbps. On the other hand, IEEE 802.11a and IEEE 802.11g use a more advanced technique known as orthogonal frequency division multiplexing (OFDM), allowing them to reach speeds of up to 54 Mbps [27]. Despite having some major differences in the physical layer, these three standards use the same medium access protocol and frame structure in the MAC layer as generally discussed in the next section.

### 3.1.2 IEEE 802.11e

IEEE 802.11e standard was proposed in 2005 to alleviate the limitations of quality-of-service (QoS) in the conventional IEEE 802.11 standards. The standard provides QoS stations with a prioritized protocol by introducing a contention based enhanced distributed channel access (EDCA) mechanism [28]. EDCA provides differentiated, distributed channel accesses for frames with 8 different user priorities (UP) ranging from 0 to 7. Each frame arrives at the MAC layer with a defined UP will be mapped into one of four access categories (AC): including background traffic (UP1 and UP2), best effort traffic (UP0 and UP3), video traffic (UP4 and UP5), and, finally voice traffic (UP 6 and UP 7), that is the highest priority level. Unlike the conventional IEEE 802.11 standards, EDCA uses contention parameters, namely arbitration inter-frame space (AIFS [AC]),  $CW_{min}[AC]$  and  $CW_{max}[AC]$  instead of DIFS,  $CW_{min}$  and  $CW_{max}$  of the DCF to transmit a frame belonging to AC. In addition, one distinctive feature is introduced in EDCA which is an interval of time when a particular station has the right to initiate multiple transmissions separated by SIFS, known as transmission opportunity (TXOP). The interval limit of TXOP is specified for each AC using the parameter TXOPlimit[AC]. Basically, the highest priority AC is assigned with the least values of contention parameters and the longest duration of TXOPlimit. The standard EDCA capability seems to be limited because it relies on the fixed default EDCA parameters. Hence, [29] believes the standard EDCA can be further enhanced by incorporating a dynamic EDCA parameter adaptation through the negotiation among the participating stations. Further, [30] concludes that default parameter values in the EDCA mechanism are just able to guarantee industrial communications requirements for a number of real time stations smaller than 10 stations. Recently, [31] claimed that most research work was concentrated on optimising EDCA in ad-hoc scenarios, while in reality all WLAN deployments were in infrastructure networks. Hence, a detailed analysis of latencies and packet loss

ratios for a typical EDCA infrastructure WLAN is presented in [31].

### 3.1.3 Advent of IEEE 802.11n

Due to an increasing demand for a higher data rates, the fourth standard, IEEE 802.11n was ratified in October 2009. Relative to IEEE 802.11a/g, IEEE 802.11n approximately quadruples the throughput up to 300 Mbps by enhancing physical layer and MAC layer mechanisms.

In the physical layer, multiple input and multiple out [MIMO] air interface technology is introduced. MIMO employs a technique called spatial division multiplexing (SDM) to transport two or more data streams simultaneously in the same frequency channel. IEEE 802.11n further increases the physical transfer rate by doubling the legacy bandwidth of IEEE 802.11 channels from 20 MHz to 40 MHz (i.e. channel bonding). The combination of MIMO architecture with channel bonding is a cost effective approach for increasing the physical transfer rate [32].

In the MAC layer, three major enhanced mechanisms are introduced: frame aggregation, block acknowledgement and reverse direction [33–35]. First, frame aggregation combines and sends multiple MAC data frames in one PHY layer packet to reduce overhead. Second, the block acknowledgement mechanism bundles all corresponding ACKs of aggregate data frames into a single collective ACK. These two mechanisms provide significant efficiency gains, particularly for voice traffic where inter-frame gaps and ACK frames sent for every short voice frame make traditional voice streams highly inefficient [35]. Third, a reverse direction protocol improves the efficiency of the transmission opportunity (TXOP) mechanism. This protocol allows the holder of TXOP to allocate the unused TXOP time to its receivers without the need for the receivers to initiate a data transfer.

### 3.1.4 Development of Gigabit WLANs

The exponential growth of mobile subscribers forces the mobile data traffic to expect an 11-fold increase between 2013 and 2018 [3] which will be beyond the capability of IEEE 802.11n. Therefore, the Very High Throughput (VHT) study group was formed in 2007 to work on the next generation WLAN which was ratified in 2013. Two new standards, IEEE 802.11ac and IEEE 802.11ad were introduced for VHT operation. Specifically, IEEE 802.11ac was aimed to increase the throughput to at least 1 Gbps with multiple links and up to 500 Mbps for a single link, while IEEE 802.11ad was targeted for a single-link performance of at least 1 Gbps in the 60 GHz band [32].

#### 3.1.4.1 IEEE 802.11ac

IEEE 802.11ac is designed to operate in the 5 GHz band because this band faces less interference than the 2.4 GHz band. It aims to become the leading access technology for houses, small businesses, and public Wi-Fi, by providing gigabit transmission rates. Multi-user capability is introduced in the form of downlink multi-user MIMO (DL MU-MIMO) [36], which enables an access point to transmit to four users simultaneously.

In addition, IEEE 802.11ac also supports a wider channel by expanding the channel bonding feature in IEEE 802.11n. It supports 20, 40 and 80 MHz channels as well as provides optional support for operation on 160 MHz channels. Similar to IEEE 802.11n, a primary 20 MHz subchannel is required for carrier sensing to ensure no other device is transmitting. The relationship between the primary and secondary subchannels based on the different bandwidth selections is demonstrated in Fig. 3.1

However, it should be noted that having wider channels makes it harder to avoid overlap between neighbouring BSSs as well as to choose a primary subchannel common to all overlapping networks [36]. Hence, IEEE 802.11ac proposes three MAC

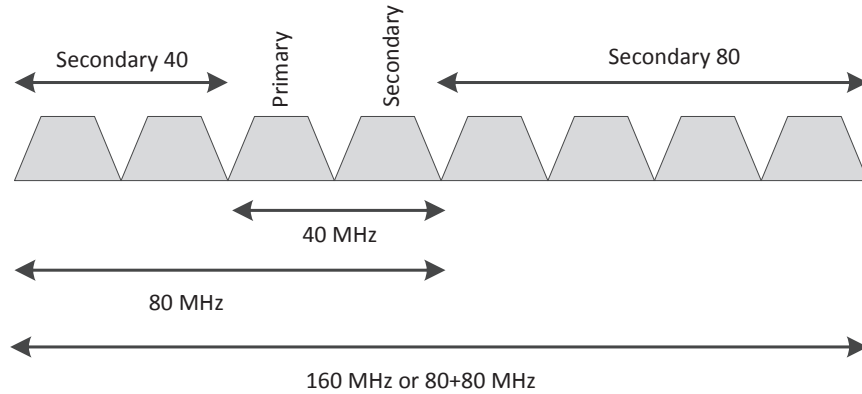


Figure 3.1: Primary and secondary channel selection [26]

enhancements to overcome this problem: 1) enhanced secondary subchannel Clear Channel Assessment (CCA), 2) improved dynamic channel width operation and 3) a new operating mode notification frame.

In common, the CCA mechanism is employed in IEEE 802.11 to detect other signals and defer transmission appropriately. In IEEE 802.11ac, a valid signal detect on the secondary subchannel is improved from  $-62$  dBm (IEEE 802.11n) to  $-72$  dBm as a means to improve CCA performance on the secondary subchannel. The basic request to send (RTS) and clear to send (CTS) mechanism of IEEE 802.11 is modified in IEEE 802.11ac to improve the dynamic channel width operation when dealing with the hidden node interference scenario. The modification involves adding bandwidth signalling to the RTS and CTS frames. Finally, an Operating Mode notification frame is introduced to mitigate the interference problem. It allows the WU to send the notification frame to its corresponding AP informing about the changing of its operating bandwidth. Successively, the AP will send the frames at the new operating bandwidth provided the WU can still use the same primary subchannel as the AP [36].

### 3.1.4.2 IEEE 802.11ad

IEEE 802.11ad is claimed to be a perfect complement to IEEE 802.11ac as it provides a feasible solution in delivering 7 Gbps data rate for short distance transmission (i.e, within a room or less than 10 meters) and personal area networking. The development of IEEE 802.11ad is mainly motivated by the plentiful amount of available unlicensed spectrum at the 60 GHz millimeter-wave band. In comparison to 2.4 GHz microwave band, it has 83 times more free space than the 83.5 MHz of free space available in the unlicensed 2.4 GHz band [32,37]. Apart from enormous bandwidth, the much smaller wavelength in 60 GHz band enables the employment of a very small antenna array size (roughly 2.5 mm) with many elements. As a result, it makes the beam of the antenna array narrower and more directional which allows spatial reuse, a property that can be used to increase network capacity by increasing the deployment density with reduced interference between nearby devices [36].

However, the millimeter wave operation suffers more attenuation and path loss than in the microwave band when passing through walls or over distances due to the oxygen absorption and atmospheric attenuation [38]. Hence, IEEE 802.11ad standard proposes a directional transmission technique in order to utilize the high gain and less interference of directional antennas as a solution to overcome this limitation. Furthermore, a few PHY and MAC amendments are made in IEEE 802.11ad. The IEEE 802.11ad PHY layer defines three different packet structures to fulfil differing requirements of applications [39]. The first structure is known as the control PHY, used for low SNR operation prior to beamforming. The second structure is the Single Carrier, designed for low power and low complexity transceiver. Finally, the third structure is the OFDM PHY, which enables high performance in frequency selective channels and achieves the maximum data rates.

IEEE 802.11ad also modifies the MAC protocols to support directional transmission. A MAC protocol in IEEE 802.11ad is not solely based on random access

CSMA/CA (carrier sense multiple access/collision avoidance) but is extended to allow scheduled access, where the station gets to know beforehand the periods of time when it is expected to be awakened and towards which direction it should point its antenna pattern [40]. Further, a new architecture known as personal BSS (PBSS) is introduced while retaining the infrastructure and independent BSS network architectures. One station takes the role of PBSS Control Point (PCP) which is responsible for scheduling access and transmitting beacon frames.

## 3.2 The General WLAN Standard

### 3.2.1 WLAN Architecture

The main entities defined in the WLAN architecture are the station (also known as wireless user (WU)) and the access point (AP). The station connects to the wireless medium via a network interface card (NIC) embedded in electronic devices (i.e. desktop, laptop or mobile phone). On the other hand, an AP is an entity that forms a bridge between the wireless medium and a wired network like the IEEE 802.3 LAN. The AP acts as a base station for the IEEE 802.11 devices and aggregates them on to the wired network such as the LAN [41].

In general, the IEEE 802.11 architecture consists of basic service set (BSS) which is a collection of stations that communicate among themselves. The architecture can be classified into three operating modes as illustrated in Fig. 3.2.

The first operating mode is the independent basic service set (IBSS), shown in Fig.3.2(a). In the IBSS mode, stations are communicating with each other without any connection to an external network (i.e. access point) and creates an ad hoc network. It has a short lifespan and only serves a specific purpose such as exchanging or sharing files [25]. Hence, in a real-world WLAN deployment, the second operating

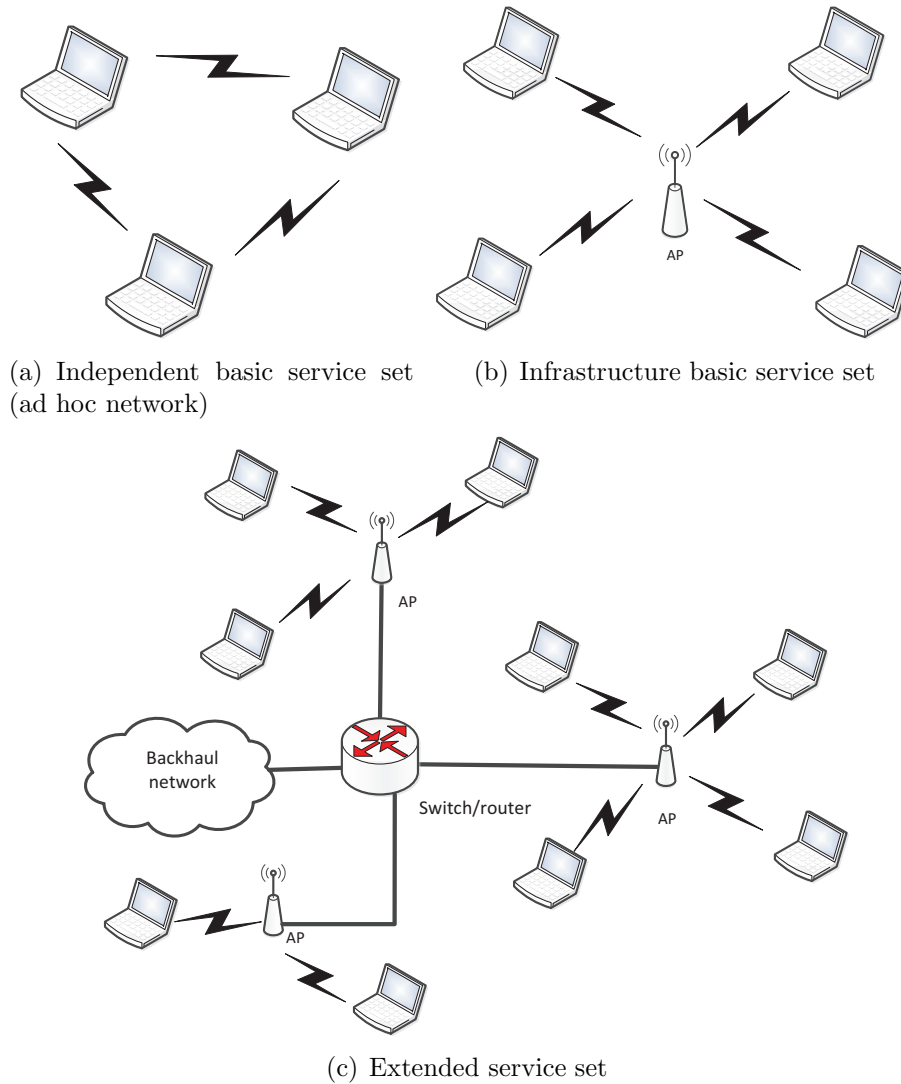


Figure 3.2: IEEE 802.11 LAN architecture [25, 27, 41]

mode which is an infrastructure BSS (referred to as BSS throughout this thesis) is more preferable to an ad hoc type of network. BSS allows a station to communicate with any other stations irrespective of their location and distance. Fig. 3.2(b) illustrates the architecture of a BSS that includes the presence of a single access point (AP), which provides connectivity to a wired network and eventually to the internet [25, 41]. Practically, the AP relays the received frames from the source stations

to the intended destination within its serving BSS. Therefore, all stations must communicate through the AP though the destination station is in the same BSS. Prior to initiating a transmission, a station must be associated with the AP by exchanging important information such as radio synchronization and supported data rates.

Finally, the third operating mode defined in the IEEE 802.11 standard is an extended service set (ESS). Fig. 3.2(c) demonstrates the architecture of ESS which comprises a set of two or more BSSs that form a single sub network. ESS architecture extends the network coverage by allowing inter networking among APs in the joint BSSs via a wired local area network to forward traffic and facilitate movement of stations. It is commonly deployed in large public or corporate places such as university campuses, corporations, airports or shopping malls [25].

### 3.2.2 MAC Protocol

WLAN adopted the IEEE 802.11 standard as described in [43]. The standard specifies two important layers in WLAN deployment namely physical (PHY) and media access control (MAC) layers. PHY specifies the modulation scheme used and signaling characteristics for the transmission through radio frequencies and its specification varies from one protocol to another (i.e. IEEE 802.11a, IEEE 802.11b and IEEE 802.11g). On the other hand, the latter is responsible for moving data packets across a shared wireless channel. The MAC protocols specify a channel access control mechanism to allow several stations to communicate without colliding with each other. These protocols are known as coordination functions and can be classified into two access methods. The fundamental method is called distributed coordination function (DCF) which uses a distributed algorithm, where all stations run the algorithm. The second method is known as point coordination function (PCF) which employs a centralized algorithm, where the AP runs the algorithm [44–46].

### 3.2.2.1 Distributed Coordination Function (DCF)

The distributed coordination function (DCF) is the main medium access control protocol adopted by IEEE 802.11 standard. It is a random access scheme, based on the carrier sense multiple access with collision avoidance (CSMA/CA) [43]. DCF employs two approaches to sense the channel which are physical sensing and virtual sensing. In physical sensing, a station senses the channel to determine the condition of the channel (i.e. busy or idle). On the other hand, virtual carrier sensing is a logical abstraction which minimizes the need for physical carrier-sensing at the air interface in order to save power. The MAC layer frame headers contain a duration field that specifies the transmission time required for the frame, in which time the medium will be busy. The stations listen on the channel by reading the duration field in the MAC layer frame headers. The duration field provides information on the transmission time required for the frame. Then, each station updates their network allocation vectors (NAVs), which is an indicator for a station on how long it must defer from accessing the channel due to packet transmissions from other stations. The station can switch off to save power, for the duration of their NAV setting. It is only allowed to initiate a transmission after the channel is sensed idle for a period defined as DCF interframe space (DIFS) by means of either physical or virtual sensing mechanisms. If the channel is sensed busy either immediately or within the DIFS period, the station keeps on listening on the channel until it is sensed idle for a DIFS period. Consequently, the station generates a backoff interval which is randomly chosen from the backoff window (known as contention window (CW) size) [48]. The window size begins with a minimum CW size and it is doubled at each retransmission up to a maximum CW size. Retransmission takes place whenever there is a packet collision, indicated by the absence of acknowledgement frame (ACK) from the receiver. This backoff algorithm is known as binary exponential backoff (BEB) technique. In general, two schemes for packet transmissions are defined in DCF protocol, as presented in the following

subsections.

a) Basic Access Scheme

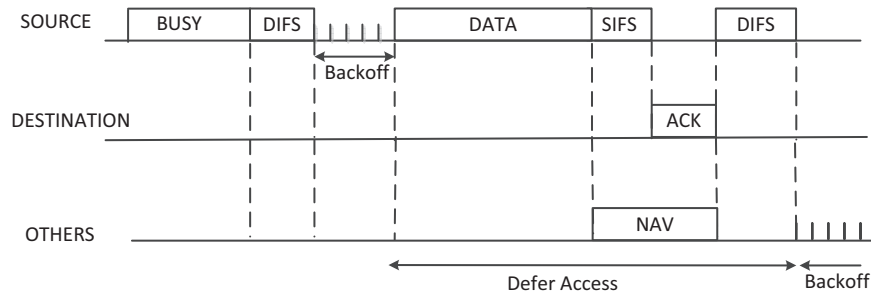


Figure 3.3: IEEE 802.11 basic access scheme [25, 42]

Fig. 3.3 illustrates the default mechanism for packet transmission, known as basic access scheme. In this scheme, only DATA and ACK frames are involved. Upon DATA frame transmission from the source station, other stations update their NAV value after hearing the frame transmission. In this scheme, the NAV value is set based on the duration field in the DATA frame includes the short inter frame spacing (SIFS) period and the ACK frame transmission following the DATA frame as shown in Fig.3.3 [42]. When the destination station has successfully received the DATA frame, it immediately waits for a SIFS duration and is followed by ACK transmission to the source station indicating a successful transmission.

b) Four Handshakes Scheme

The four handshakes method is considered as an optional scheme in the DCF protocol to reserve the channel before transmission and as a solution to the hidden station problem. As illustrated in Fig. 3.4, this method uses a four-phase RTS-CTS-DATA-ACK handshake, which is also known as request-to-send/clear-to-send (RTS/CTS) scheme [25, 42]. Initially, after sensing the channel is idle for a DIFS duration, the source station broadcasts an RTS frame to notify the destination and other stations the total time required to transmit the DATA and ACK frames. Upon successful transmission of the RTS frame, the destination station replies by broadcasting a CTS

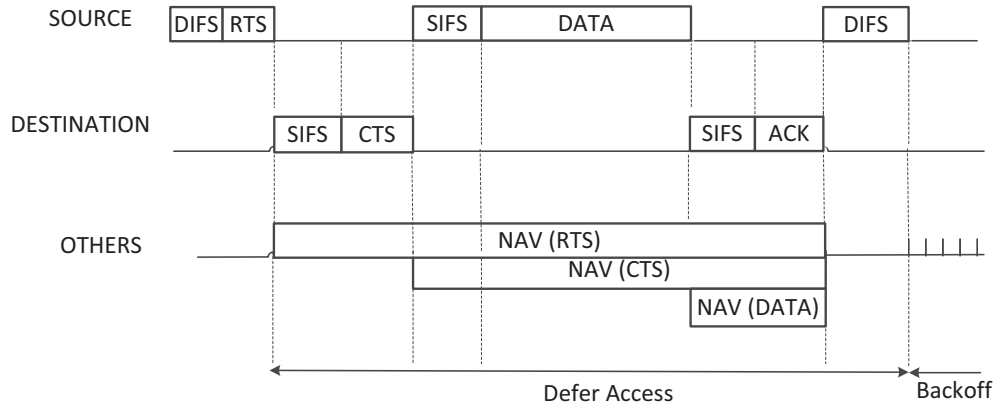


Figure 3.4: Four handshakes scheme [42]

frame to give the source station explicit permission to send DATA frame and inform other stations not to send for the reserved duration [27]. After receiving the CTS frame, the source station waits for a SIFS duration before it proceeds to transmit the DATA frame. Meanwhile, other stations which hear the RTS and CTS frames update their NAV value according to the duration fields in those frames.

In general, this four handshakes scheme is able to solve the hidden station problem because the DATA frame is transmitted only after the channel has been reserved. Moreover, it also reduces the collision duration since the collisions may only occur for the RTS or CTS frames which are definitely shorter size than the DATA frame. Once the RTS and CTS frames are correctly transmitted, the following DATA and ACK frames should be successfully transmitted. However, this scheme also introduces delay and consumes channel resources due to the additional overheads involved. Hence, this scheme is only employed to transmit a long DATA frame. In practice, each station can set an RTS threshold such that the scheme is only implemented if the DATA frame is longer than the threshold [27].

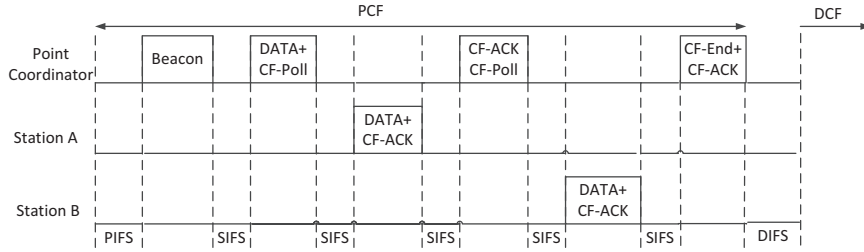


Figure 3.5: Point coordination function [43, 47]

### 3.2.2.2 Point Coordination Function (PCF)

The point coordination function is an optional access protocol defined in the standard to support time bounded services. It is achieved by letting stations have priority accessing the channel, coordinated by a station called point coordinator (PC). The PC is implemented in the AP and it arranges the packet transmissions of stations by polling them one at a time as shown in Fig.3.5. Despite the fact that the PCF has the priority to access the channel, in practise, the majority of vendors do not implement PCF mode in their APs because it requires additional coordinations, mainly when multiple APs are deployed within interference range [25].

## 3.3 Performance Evaluation of IEEE 802.11 WLAN DCF

This section studies the WLAN performance by evaluating the normalized saturation throughput of IEEE 802.11 DCF. Bianchi has proposed an accurate analytical model in [48] to analyse the saturation throughput of the BEB algorithm. He defines the normalized throughput as the fraction of time the channel is used to successfully transmit payload bits. The saturation throughput indicates that the throughput has reached the limit despite the increase in offered load.

In order to allow a comparison to the analysis in [48] (for a validation purpose),

all the simulation parameters and assumptions for the IEEE 802.11 performance evaluation are following the specifications in [48]. The throughput performance of IEEE 802.11b adhoc WLAN is now verified using OPNET<sup>1</sup> simulation software [49]. The main OPNET simulation parameters are listed in Table 3.2 and the following assumptions are made: 1) all stations always have packets to transmit (greedy stations) 2) the channel is ideal 3) all stations can hear each other (no hidden stations).

Table 3.2: 802.11b OPNET simulation parameters (saturated condition).

Parameter	Value
Payload size	8184 bits
MAC header	272 bits
PHY header	128 bits
ACK	112 bits + PHY
Channel bit rate	1 Mbps
Network type	Infrastructure
Slot time	50 $\mu$ s
SIFS time	28 $\mu$ s
DIFS time	128 $\mu$ s
ACK Timeout	300 $\mu$ s

Fig. 3.6 shows the saturation throughput gradually decreases as the number of stations increases from 5 to 50. It is shown that the obtained simulation results matched with the analysis established in [48]. As more stations contend the channel, there is an increase in collisions that deteriorates the whole system utilization. It is also observed (Fig. 3.7) that the selection of initial CW ( $CW_{min}$ ) size gives a significant impact to the throughput performance. The throughput for a small number of stations (5 stations) is severely deteriorated when  $CW_{min}$  is set to a high value, 1024. In contrast, bigger network size (50 stations) gained maximum throughput

<sup>1</sup>OPNET is a commercial packet level simulator. It accurately models the behaviour for any kind of networks.

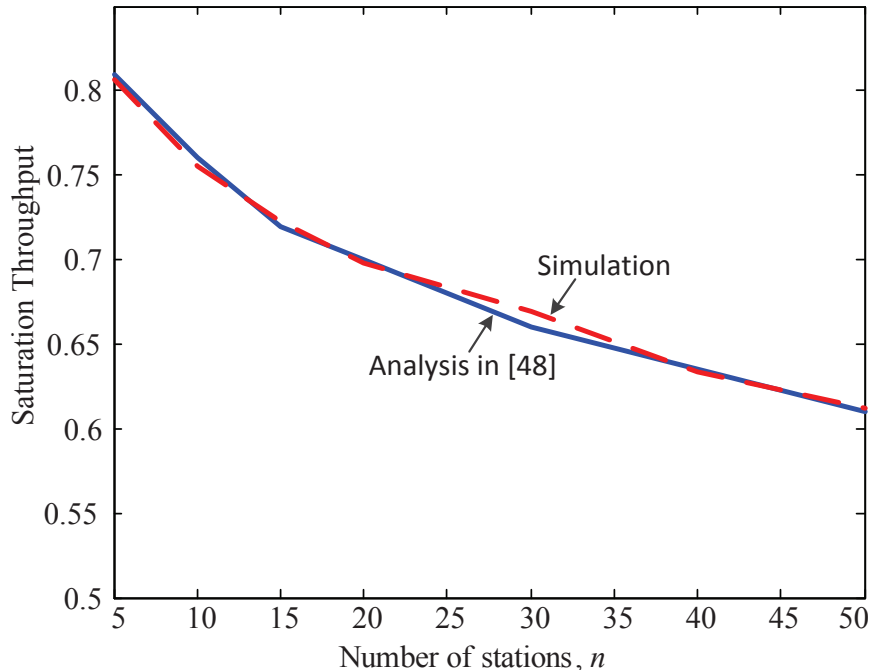


Figure 3.6: Effect of network size on saturation throughput in comparison to analysis in [48].

when  $CW_{min}$  is assigned to 1024. The best choice of  $CW_{min}$  strongly depends on the network size.

Further, it is extensively agreed in the literature that the BEB algorithm adopted in the IEEE 802.11 standard is the key factor to WLAN performance degradation [48, 50–53, 55–60]. There are two major drawbacks found in BEB that cause the network degradation [61]. First, the contention window is increased upon transmission failure regardless of the cause of failure. Second, after a successful packet transmission, the contention window is reset to the minimum size, thus forgetting its knowledge of the current congestion level in the network and increasing its collision chances.

Numerous modifications have been proposed in the literature to improve the legacy BEB algorithm. In common, all modifications are made to adjust the contention window size according to the network condition. A number of approaches have been proposed in the literature to identify the network condition using different types of

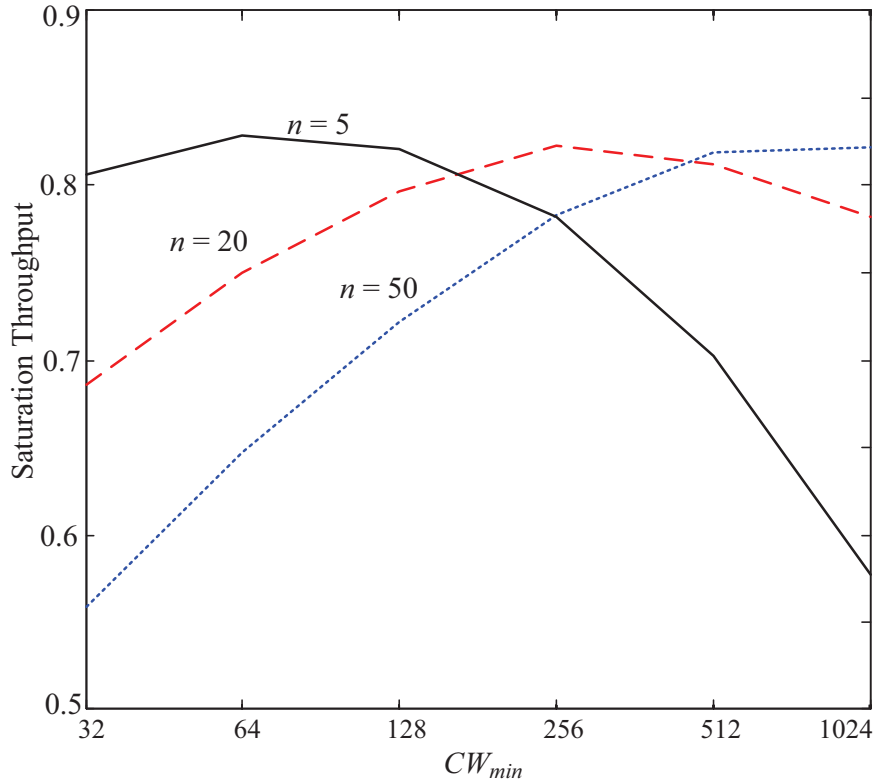


Figure 3.7: BEB saturation throughput versus  $CW_{min}$

traffic indicators as classified below.

### 3.3.1 MAC Frames Indicator

The proponents of the first category take advantage of the least overhead size information carried by MAC frames including ACK, RTS and CTS frames.

#### 3.3.1.1 ACK Frame

Stations continuously monitor the traffic on the channel to identify collisions. The presence or absence of an ACK can be used to identify the success or otherwise (collision) of a transmission [50–52, 58].

In [50], the authors propose to exponentially increase the CW size when there is a

collision and exponentially decrease the CW size when there is a successful transmission, known as the EIED (exponentially increases exponentially decreases) algorithm. The exponential factors are then optimized to get maximum throughput. The proponents of [51] use a more conservative approach, they linearly decrease the CW size when there is a successful transmission. Similarly, [58] proposes to halve the CW size (unlike BEB where the CW size is reset to minimum) to increase the overall throughput. Further, the work in [52] proposes a fairness based algorithm for mobile adhoc networks (MANETs) by adjusting the CW size according to the number of successful transmissions.

In common, all of the above techniques steadily decrease the CW after a successful transmission to retain the overall network state information. Though this approach may have a positive correlation, it usually falls short of predicting the overall network status.

### **3.3.1.2 RTS and CTS Frames**

The schemes [53, 55] proposed in this category use the network allocation vector (NAV) information embedded in RTS and CTS packets as the overall network traffic indicator. The transmitting station explicitly indicates the length of time that it will be using the channel. Consequently, all stations will update their NAV by checking RTS and CTS frames from their transmitting neighbours.

Initially, the authors in [54] utilized NAV information to analytically derive an interference aware metric named network allocation vector count (NAVC). A function is derived to predicate the possible delay and the available bandwidth for a dynamic interference aware routing protocol in a MANET. Later, [55] employed NAVC to adjust the contention window size in the routing protocol. Similarly, Wang and Song in [53] used NAV information to approximate the intensity of surrounding traffic and the density of stations.

Though NAV information can be a good traffic indicator to tune the CW sizes, this approach is only limited to the four handshakes mode (RTS/CTS reservation mechanism) and not available in the basic access mode of IEEE 802.11 DCF access method.

### **3.3.2 Wireless Channel Status Indicator**

All contending stations can listen to each other, allowing them to identify whether the channel is idle or busy. The resultant channel status becomes a traffic indicator of the overall network [56, 57, 60, 62–66]. The CW sizes can be manipulated in various ways for throughput enhancement as below.

#### **3.3.2.1 History Based Backoff**

Authors in [64, 65] use the past channel status to control the current CW size. The work in [65] proposed history based adaptive backoff (HBAB) algorithm that checks the last two states of the channel and decides whether to increase or decrease the CW sizes based on the channel's tendency to being free or busy. Further, a dynamic, deterministic contention window control (DDCWC) scheme [64] extended the algorithm to include the last three states in a channel state vector. The backoff range is divided into several small sub-ranges which are selected based on the channel state vector.

#### **3.3.2.2 Number of Backoff Pauses**

The pause count backoff (PCB) algorithm proposed in [62] observed the number of backoff pauses (due to busy channel) until its backoff counter becomes zero and sets an appropriate CW size that matches the estimated traffic status. However, [63] claimed the PCB algorithm could not adjust to dramatically changing traffic loads

because the algorithm could not estimate the number of active stations. Hence, [63] took one step forward by introducing the estimation-based backoff (EBA) algorithm which estimates the number of active stations by observing the number of idle slots during the backoff period.

### 3.3.3 Number of Idle Slots

The works in [67–70] dynamically control the CW sizes by monitoring the estimated mean number of idle slots between transmission attempts  $\bar{I}_i$ . This method is known as *Idle Sense*, a distributed control method where all contending stations in IS compare their  $\bar{I}_i$  with the target value  $I_t$ , a common value to all stations, and adapt their CW size using the additive increase multiplicative decrease (AIMD) algorithm. The station gradually increases its CW size when  $\bar{I}_i < I_t$  or multiplicatively decrease the CW if  $\bar{I}_i > I_t$ . The CW sizes of all stations will converge to the same value. However, as will be shown later in the thesis, if the initial CW sizes are significantly different then IS can go unstable as explained in Section 6.4.

### 3.3.4 Number of Contending Stations

The techniques in this category use an analytical approach based on Markov models to determine the optimum CW sizes for maximum throughput as a function of the number of  $n$  contending stations.

For example, the adaptive window algorithm (AWA) proposed by Bianchi et al. [60], used the number of active stations in the network to control the CW size; the number of active stations were estimated by observing the activity on the channel. A similar approach is employed in [56] and [57] to control a complex  $p$ -persistent MAC protocol that selects the optimum backoff interval. More recently, [66] identified the relationship between backoff parameters, contention level, and channel bit error rate

(BER) in order to propose a distributed algorithm that allows a station to dynamically adjust its contention window size based on turn-around-time measurement of channel status.

These analytical approaches may result in better network performance because the algorithms allow each station to independently tune the backoff window size at run time. However, complex computations are required that lead to high power consumption, which is in many cases considered unaffordable in wireless networks context [64, 65]

### 3.3.5 Limitations

In common, the above studies focused on the enhancement of the IEEE 802.11 protocol in an adhoc configuration; with all stations having an equal chance to transmit. However, in infrastructure networks, the AP requires more transmission opportunities to give fairness to the uplink/downlink performance. The following section reviews on the performance enhancements for infrastructure based WLAN.

## 3.4 Uplink and Downlink Priority Schemes

In practice, the majority of WLAN deployments operate in an infrastructure mode where an access point (AP) serves its own basic service set (BSS) of associated wireless users (WUs). The AP acts as a bridge between the wired network and the associated WUs. Therefore, AP requires more transmission opportunities than WUs. However, in the standard DCF access method, every station including the AP is given an equal chance of transmission which leads to unfairness between uplink and downlink transmissions and consequently degrades the overall performance of the WLAN. Extensive works have been carried out to mitigate the uplink and downlink unfairness. The following subsections discuss several types of techniques proposed in the literature.

### 3.4.1 Control CW size

The schemes proposed in [69, 73–76] control the contention window sizes of the contending stations (i.e. AP or WUs or both) in order to achieve the desired fairness between uplink and downlink transmissions. The work in [69] provides the AP with a higher transmission priority by scaling the CW size to a constant value while allowing the associated WUs to dynamically control their CW sizes according to the *Idle Sense* method [67].

Abeysekera et.al [73] introduced a simpler technique which modifies the well known BEB MAC protocol. The minimum CW size,  $CW_{min}$  of the AP is adaptively adjusted based on the target packet ratio between uplink and downlink flows. Nevertheless, this scheme does not consider throughput maximization and dynamics in WLAN (e.g. channel condition and traffic loads) when deriving the optimal  $CW_{min}$ . Therefore, [76] improves the scheme by considering the dynamics of WLAN environment.

The most recent work in [74] analytically derived the optimum  $CW_{min}$  sizes for an AP and associated WUs in order to achieve the target downlink/uplink ratio and the optimum network throughput. The derived formulations show that  $CW_{min}$  sizes depend on the number of WUs. However, the scheme does not propose any algorithm to estimate this number.

In common, this approach always sets the CW size of an AP lower than WU's to give the AP priority access. The limitation is that it increases the collision rate due to the smaller CW size and consequently deteriorates the overall WLAN performance.

### 3.4.2 Reduce Interframe Space (IFS) Period

Priority access for an AP is obtained in [77, 78] by reducing its sensing time. In [78], the AP performs carrier sensing only for a PCF interframe space (PIFS) period instead

of DIFS (in the default IEEE 802.11), where the length of PIFS is shorter than DIFS but longer than SIFS.

The same approach is also proposed in guaranteed access mode mechanisms [77] to solve the unfairness problem in IEEE 802.11e. In this scheme, when the AP perceives unfairness problem, the enhanced distributed channel access (EDCA) protocol is modified by fixing the arbitration interframe space (AIFS) period equals to 1 and the backoff algorithm is ignored. Though this has immediate effect and gives the AP the greatest amount of required bandwidth, it may cause AP hogging before the desired ratio is achieved.

### 3.4.3 Adjust TXOP limit

The authors in [79–81] utilizes this approach based on a concept of transmission opportunity (TXOP) in the IEEE 802.11e [28]. It allows a station gaining the channel to transmit multiple frames without any contention within the predefined TXOP limit. The TXOP limit is typically fixed by the IEEE 802.11e standard. Therefore, [79] introduces an adaptive priority control (APC) which dynamically adjusts the TXOP limit of an AP according to the traffic volume of uplink and downlink. It is shown that APC balances the uplink and downlink delay effectively in VoIP traffic without additional overhead.

However, it should be noted that if the transmission of any frame in TXOP fails, the burst transmission is terminated (losing a considerable amount of data) and is retransmitted after the next channel access. Therefore, the TXOP approach is not suitable for error prone environments [82]. As an alternate solution, Clifford et.al in [80] proposed to use a smaller TXOP limit with multiple transmission opportunities and a smaller value of  $CW_{min}$  to improve the AP's access priority.

### 3.4.4 Other Schemes

Xiao [83] used an analytical approach to model the backoff-based priority schemes for IEEE 802.11 and IEEE 802.11e WLANs. Three backoff based metrics including the initial window size, the retry limit and the backoff window-increasing factor are differentiated to achieve the target throughput and priority. However, this work does not propose any specific algorithm to adaptively tune the metrics. In contrast, the work in [84] proposed a novel dynamic EDCA parameter adaptation algorithm to achieve a predetermined fairness ratio in IEEE 802.11e where the initial parameters (i.e. AIFS,  $CW_{min}$  and TXOP limit) are calculated from their analytical model. Other schemes are proposed in [85] to support the fairness between uplink and downlink while maintaining the maximum throughput. The schemes usually involve improving the AP's transmission probability. Techniques such as ACK-piggybacked data and replacing the DIFS waiting period with the shorter SIFS waiting period are occasionally applied as control methods.

Conversely the UL priority can be reduced [86, 87], or the AP can establish a contention free period by spoofing the 'duration' field in the MAC header; effectively forcing large NAV values in the WUs [88].

### 3.4.5 Limitations

In summary, it is worth noting that all the above priority schemes have been proposed for a single BSS infrastructure network; that is one AP and  $n$  associate WUs sharing the same radio resource.

The demand for high data rate WLAN services has resulted in reduced transmission ranges caused by the use of high order QAM modulations. However, the carrier-sensing range remains essentially constant, set by the -82 dBm CCA specification (Fig. 3.8). Any co-channel BSSs located within the carrier sensing zone will need

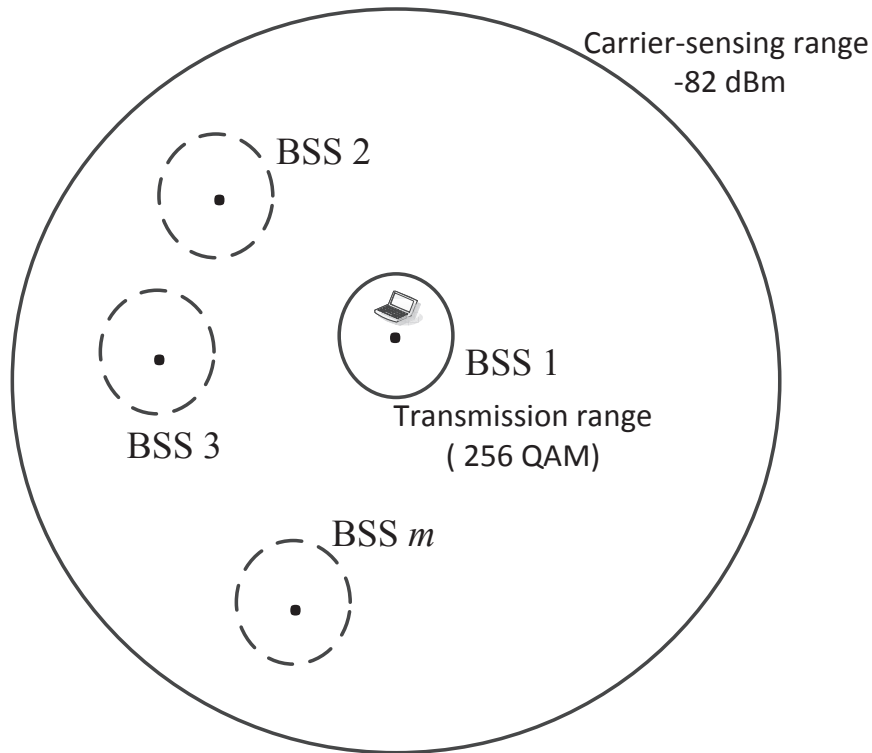


Figure 3.8: The dotted circle BSSs are potential interferers to the AP and WUs in BSS 1 (solid circle).

to share the same frequency resource. Unfortunately, in today's high density urban environment the spectrum is so crowded that many BSSs are forced to share the same channel. The problem of overlapping coverage areas potentially increases collisions and reduces saturated throughput as is evident in the BEB algorithm used in today's IEEE802.11 standards. There are now a number of fairness issues to consider: uplink-downlink fairness for each BSS, fairness between BSSs and fairness among WUs.

These issues will be addressed later in the thesis.

## 3.5 Fiber-Wireless Networks

The convergence of optical and wireless technology creates the fibre-wireless (Fi-Wi) networks. It combines the reliability, robustness and high capacity of optical fiber networks with the flexibility, ubiquity and cost savings of wireless networks. Remarkable progress has been made on the design of Fi-Wi networks architecture over the decade. It initially evolves from the proposal of the integration between EPON and WiMAX. This integration has attracted much research [91–94] due to both networks having a point to multipoint topology with a centralized system (OLT in PON and base station in WiMAX) [95].

In [94], the authors classified the network architecture proposed by [93] into three significant categories: independent, radio-over-fibre and hybrid. The independent architecture is the most intuitive but it is expected to be costly since it requires two independent devices, an optical network unit (ONU) and a WiMAX base station. Radio-over-fibre (*RoF*) scheme (Fig. 3.9) uses an analog optical link to transmit radio signals between the central office and a remote access unit (RAU) with the central office controlling both optical (EPON) and wireless (WiMAX) media. This mechanism imposes additional fibre propagation delays which might exceed certain wireless media timeouts. Furthermore, despite the RoF system having low attenuation loss and reduced power consumption, it is prone to noise and distortion due to the analog nature of its transmission [93].

In contrast, the hybrid architecture (also known as radio and fiber (*R&F*) system) reduces cost because it integrates the ONU and the WiMAX base station into a single device. The device acts as a gateway translating media access control (MAC) frames from the PON to the WiMAX networks and vice versa. Two distinct separate MAC protocols are used to access optical and wireless media respectively. Thus, the wireless MAC frames do not have to travel along the optical fibre to be processed at the central

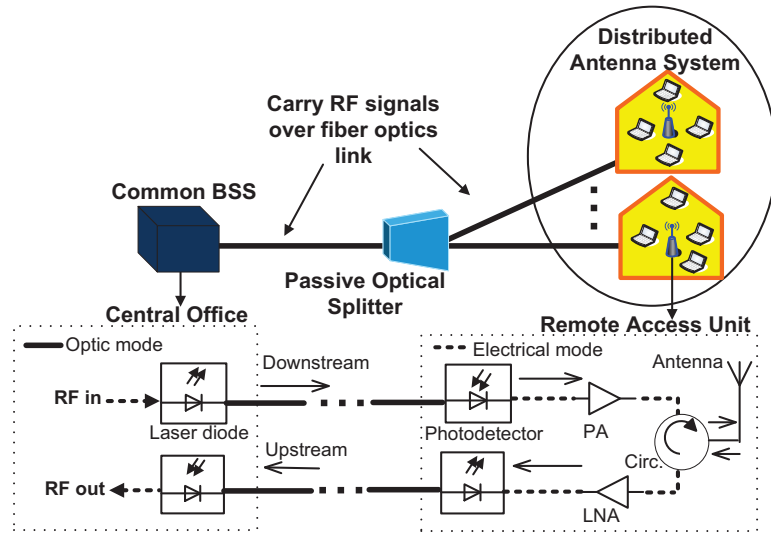


Figure 3.9: The Fi-Wi network scenario using the *RoF* technology [90].

office.

On the other hand, the authors in [95] doubted the integration between EPON and WiMAX would be practical because WiMAX has a metropolitan reach where as PON optical network brings fibre closer to the end users. WiMAX is not the right choice for realizing short distance wireless access inside offices and homes. As a result, [95, 96] proposed to integrate the optical networks with a mesh connected wireless local area networks (WLAN). However, one significant challenge in employing a mesh network in Fi-Wi networks is the end users may suffer performance degradation as the number of wireless hops increases. Therefore, a routing protocol is required to optimize the network performance.

Anticipating the exponential growth of mobile data in the future, the current research trend is moving towards high-capacity Fi-Wi networks by seamlessly integrating next generation PON with gigabit WLAN technologies [97–99].

## 3.6 Summary

This chapter has reviewed the evolution of WLAN standard from the first variant till the latest proposed variant. Since its first appearance more than a decade ago, the maximum data rate has significantly improved from the original 11 Mbps to 7 Gbps in the near future. Next, the fundamentals of WLAN were discussed, focusing on the architectures and MAC protocols. The DCF protocol was studied and its performance analysed via OPNET simulations. The simulation validated that the BEB algorithm combined with the DCF protocol causes significant throughput degradation as the number of stations increases. Therefore, a literature survey of alternate backoff and priority schemes was undertaken. The schemes are classified according to their traffic indicators. The findings provide a variety of possible solutions to solve the fairness problem in an infrastructure WLAN. Finally, the development of Fi-Wi networks (the studied network scenario in this thesis) is presented. Of architectures compared, *R&F* solution is preferred because of lower delays. Nearly all *R&F* studies considered optimising MAC issues without including any of the limitations experienced by the WLAN on the radio channel. Interference between Fi-Wi AP's is not considered, yet increasing wireless LAN data rates are assumed. The latter implies wider bandwidth channels, increased noise ( $kTB$ ) and therefore reduced cell size and a lower number of channels to choose from. (The spectrum resource is essentially fixed). Multiple overlapping BSSs are therefore unavoidable.

The next chapter presents the proposed Fi-Wi network, identifies the problems on the wireless side and proposes techniques to improve performance in dense environments.

# Chapter 4

## Modified Backoff Technique in Fiber-Wireless Networks

This chapter studies the idea of integrating the gigabit passive optical network (GPON) with the wireless local area network (WLAN). Such integration enables the end user to enjoy the large capacity of a GPON network with the mobility of a WLAN network [100, 101]. However, a limitation in the WLAN is anticipated considering the fact that a wireless channel is shared by many wireless users (WUs) and access points (APs), resulting in packet collisions and likely loss of transmitted data. Thus, two techniques are proposed to overcome the limitations and improve the end user performance. The first technique exploits the accessible content of the GPON control frame and modifies the standard binary exponential backoff (BEB) scheme in the IEEE 802.11 WLAN by introducing fixed near-optimum contention window (CW) sizes. The second technique is a transmission priority scheme that provides fairness between uplink and downlink transmissions for end user terminals and their serving access points. Section 4.1 discusses the architecture of the multi-BSS Fi-Wi network. Section 4.2 evaluates the performance of the Fi-Wi scenario when employing the standard IEEE 802.11 WLAN protocol. Section 4.3 proposes an optimized constant

contention window (OCCW) scheme for a given BSS density. Finally, Section 4.4 presents a transmission priority scheme for providing fairness between APs.

## 4.1 Proposed Fiber Wireless Networks

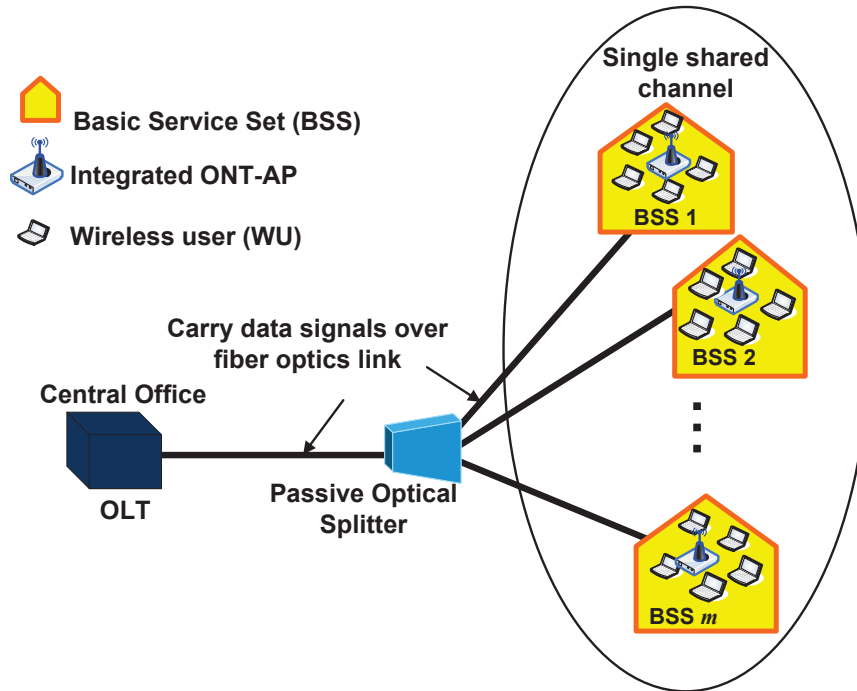


Figure 4.1: Proposed fiber-wireless network scenario

This thesis studies the integration of GPON with a ‘closed’ WLAN system as shown in Fig. 4.1. The network is ‘closed’ in the sense that the operator has a dedicated spectrum allocation for all WLAN access points connected to the same GPON fiber. The integration is employed at the end-user terminal where an optical network terminal (ONT) of GPON and an access point (AP) of WLAN are incorporated into a single device, forming a Fi-Wi hybrid system (also known as radio and fiber (R&F) system) [93, 95]. The integrated ONT-AP device acts as a gateway translating media access control (MAC) frames from the optical network to the wireless network

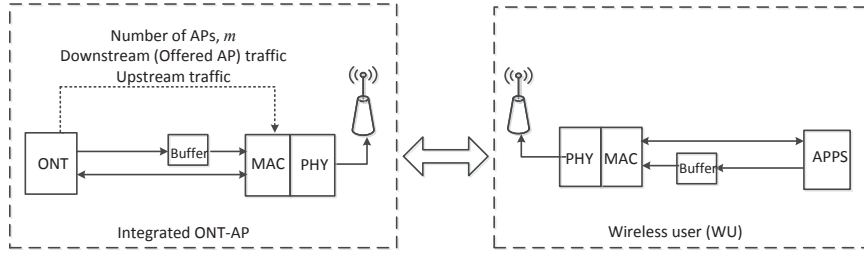


Figure 4.2: Proposed fiber-wireless network scenario with traffic indicators.

and vice versa. Two distinct separate MAC protocols are used to access GPON and WLAN respectively. Thus, the wireless MAC frames only traverse the WLAN and do not have to travel along the optical fibre to be processed at the central office. Consequently, the negative impact of the fiber propagation delay on the network can be avoided. This conclusion is also supported in [95].

The study considers the worst case scenario for the wireless media in terms of frequency availability in densely populated urban areas. All BSSs are within close proximity, i.e. all wireless stations, APs and WUs, share one single channel and can hear each other, albeit being potential interferers. The spectrum is considered ‘closed’, that is a single 20 MHz channel entirely dedicated to this Fi-Wi network.

The simulation scenario is designed to closely resemble the proposed fiber-wireless network shown in Fig. 4.1. For simplification, two assumptions are made in this work. First, all the GPON’s traffic goes directly to the WLAN and the WLAN channel is only dedicated to the GPON traffic. As such, each ONT from the splitter is directly connected to the corresponding AP in the WLAN. Second, a perfect transmission is assumed from the OLT to each ONT with the extracted GPON traffic information made available in the AP of each basic service set (BSS) through the networks integration process (Fig. 4.2).

## 4.2 Preliminary Works: Analysis of WLAN Performance

In this section, preliminary works are carried out to analyse the effects of increasing the number of BSSs. A 802.11a WLAN network scenario is modelled using OPNET software [49]. Each scenario consists of a different number of BSSs ranging from 1 to 32. Each BSS comprises of one access point (AP) and five associate wireless users (WUs). Every station continuously generates packets following an exponential distribution with the constant packet size of 1024 bytes. The packets are then transmitted over the WLAN channel at the data rates of 54 Mbps. Each AP is modeled to generate packets 5 times more than its associated users with the inter arrival time of 0.01 sec and 0.05 sec respectively. The main OPNET simulation parameters are listed in Table 4.1.

Table 4.1: 802.11a OPNET simulation parameters (non saturated condition).

Parameter	Value
Packet size	1024 bytes (constant size)
Packet distribution	exponential
Inter-arrival time	0.05 sec (WU) and 0.01 sec (AP)
Data rate	54 Mbps
Channel bandwidth	20 MHz
Network type	Infrastructure
Slot time	9 $\mu$ s
SIFS time	16 $\mu$ s
DIFS time	34 $\mu$ s

The normalized throughput is analysed to evaluate the network performance; defined as the number of packets successfully received from the transmitters divided by

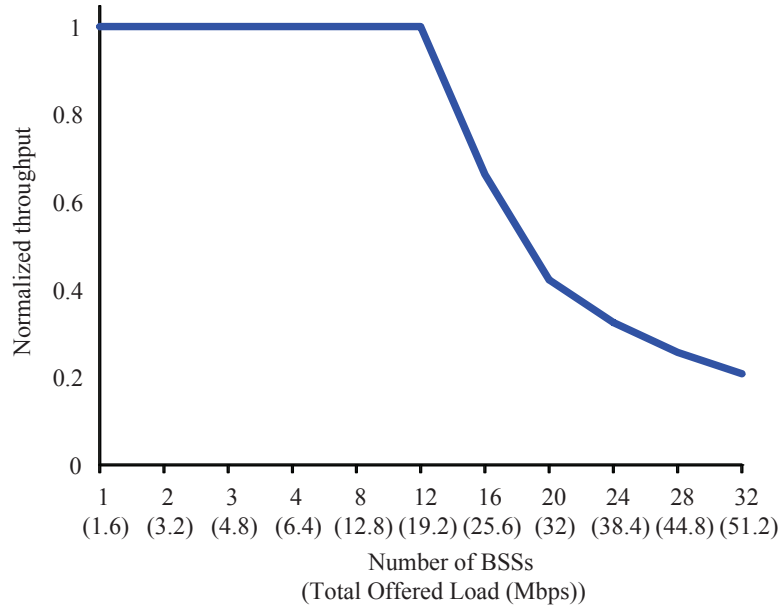


Figure 4.3: BEB throughput normalized to offered load vs. number of active BSSs.

the offered load. The curve in Fig. 4.3 shows the normalized throughput of the multiple BSSs networks employing the binary exponential backoff (BEB) scheme. Perfect transmission is achieved when the network is operating within 1 to 12 BSSs. Beyond 12 BSSs, the overall throughput performance gradually decreases. In short, it is evident the WLAN performance is poorly degraded by having more BSSs in the network. The observation is consistent with the analysis made in the preceding Section 3.3

Hence, in the next section the legacy BEB is modified by exploiting the traffic information, which is obtained directly from the GPON frame in each ONT.

### 4.3 Optimized Constant Contention Window Scheme

This section proposes an optimized constant contention window (OCCW) scheme. An exhaustive search is used to develop a map of optimum CW sizes for different traffic loads in the network. This method takes advantage of GPON's centralized structure to extract traffic information and make it available to all wireless stations. Based

on the information, wireless stations select the required CW size from the developed table.

### 4.3.1 Analysis of Constant Contention Window Size

In order to analyze the effects of CW size in the backoff technique, the BEB is modified by making the CW size constant throughout the transmission regardless of whether it is successful or not. The simulation is begun by assigning the CW size of 16 slots to the WLAN network scenario. Then, the same scenario is repeatedly simulated while gradually increasing the CW size from 16 up to 2048 slots. In each scenario, the traffic size is varied from light to heavy as specified in Fig. 4.4. The total offered traffic load is directly proportional to the number of BSSs. On average, one BSS carries approximately 1.6 Mbps of traffic load.

Fig. 4.4 depicts the normalized throughput analysis of the simulated network scenar-

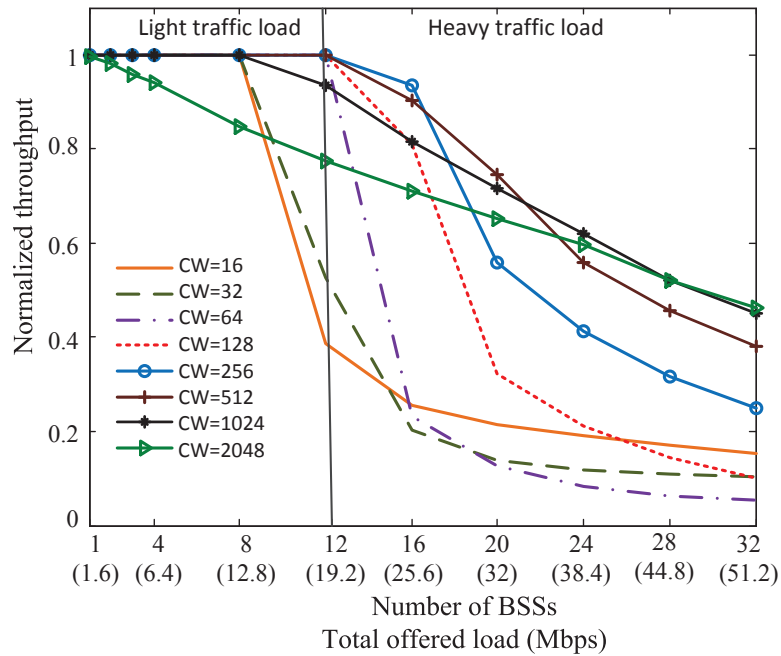


Figure 4.4: Normalized throughput for constant CW size

ios. The figure is divided into two regions representing light and heavy (or saturated) traffic load. Light traffic load is up to 19.2 Mbps (approximately 1 to 12 BSSs). Meanwhile, heavy traffic load is more than 19.2 Mbps. Light traffic loads yield almost identical patterns even though different CW sizes (16 to 1024 slots) are assigned. However, there is an exception when the CW size of 2048 is assigned. The throughput performance is significantly lower because the channel is forced into the idle state for longer periods reducing the carrying capacity of the channel. Consequently, the offered traffic is greater than the carried traffic and incoming new packets are dropped due to buffer overflow. Apart from that, it is observed that a wide range CW sizes (between 54 and 512) do not have any effect on the throughput performance for the light traffic scenarios. Hence, the smaller CWs are preferred because they result in shorter transmission delay.

Conversely, the CW size has a huge impact to the network performance for the heavy traffic loads where the network saturates. As the offered traffic increases, the capacity of the lower CWs drop when retransmissions slow the throughput to the point where the input buffers overflow, so packets are lost both when contesting the medium and overflowing the buffer. Heavier traffic loads require longer backoff intervals.

### 4.3.2 Optimum Contention Window Size

This section proposes a near-optimized backoff technique. In this technique, once the CW size is assigned at the beginning of every transmission, it will remain constant throughout the transmission. The assignment of the constant CW size depends on the filtered gross traffic load. The simulation results of the previous subsection are taken as the sole reference for CW size selection in this technique. The best CW size is chosen on the basis of throughput performance for the offered load. Fig. 4.5 summarizes the selection of the best CW size for each traffic scenario. The CW size quickly increases as the traffic rises above 25.6 Mbps, 47% of the maximum nominal

throughput of 54Mbps.

Fig. 4.6 shows the normalized throughput of the network which employs this op-

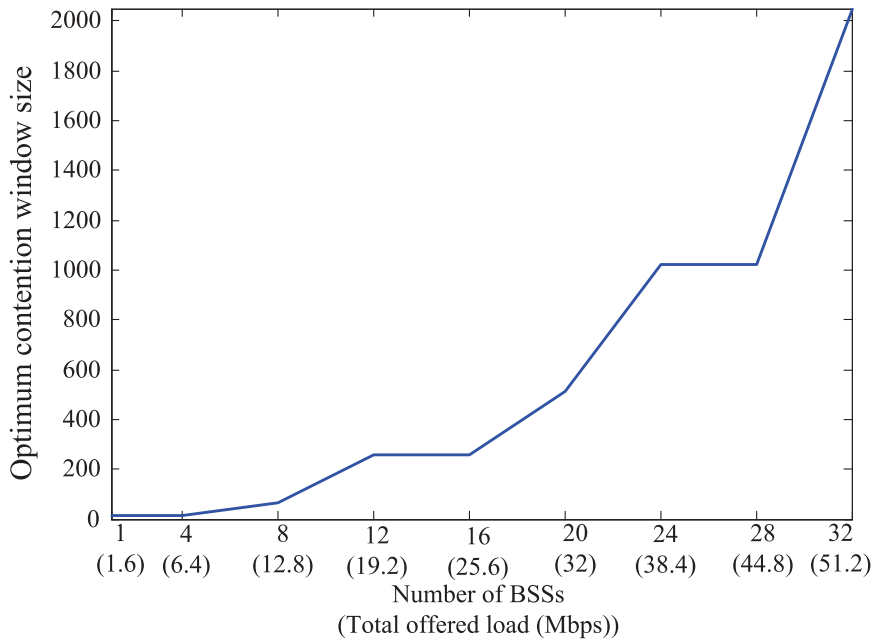


Figure 4.5: The optimized CW size vs. offered load.

timized backoff technique in comparison to the standard BEB and double increment double decrement (DIDD) techniques [58]. DIDD technique is similar to BEB except for the case of a successful transmission: it halves the CW (BEB resets to  $CW_{min}$ ). In addition, it does not discard packets that reach the maximum number of retransmission attempts. This smooth decrease of the CW is claimed to be able to avoid potential packet collisions especially when the number of contending stations increases. However, in this performance analysis, the DIDD scheme is modified such that it discards any packet that exceeds the maximum number of retransmission attempts. This modification is necessary in order to do the performance comparison among all the three schemes.

It seems the throughput performance for all the schemes are almost identical for light traffic scenarios (less than or equal to 12 BSSs (19.2 Mbps)). This is because the CW

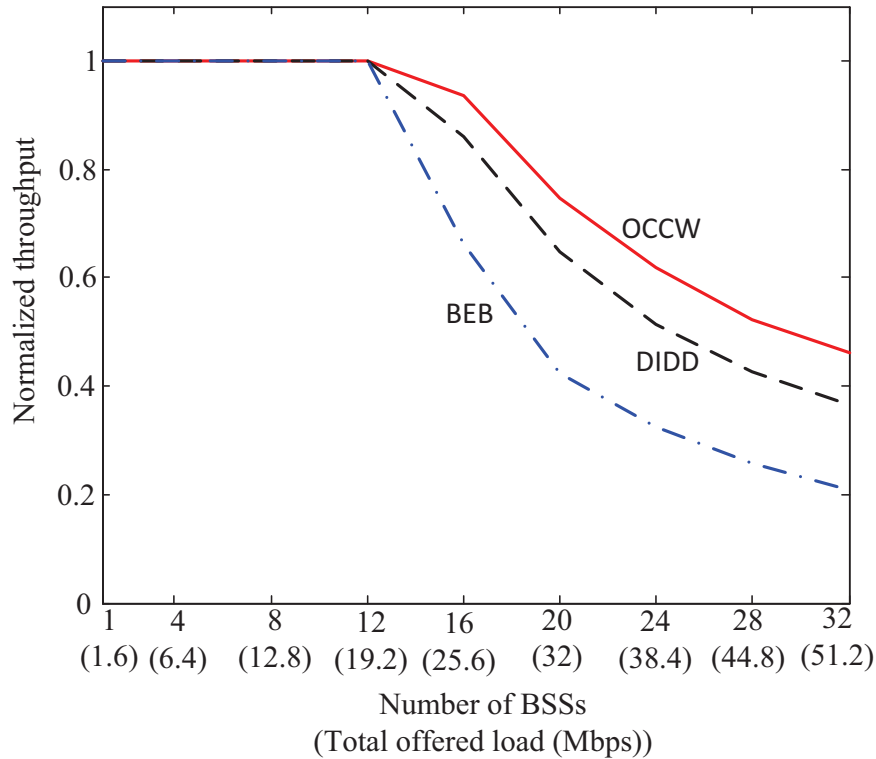


Figure 4.6: Comparison of throughput performances vs. offered load.

size does not have any impact on the network throughput as has been discussed in the preceding subsection. Conversely, it is evident this scheme outperforms the BEB and DIDD schemes for heavy traffic scenarios (more than 12 BSSs (19.2 Mbps)). Interestingly, this technique shows a significant 50% throughput improvement relative to BEB at an offered load of 32Mbps, which is 0.6 of the maximum nominal transmission rate (54Mbps). The improvement increases to close to 100% at the maximum offered load in the simulation. Further performance analysis will be discussed in the next subsection.

### 4.3.3 Performance Analysis

In this subsection, the performance analysis is extended by analysing other statistics. Fig. 4.7 shows the total dropped packets due to buffer overflow and Fig. 4.8

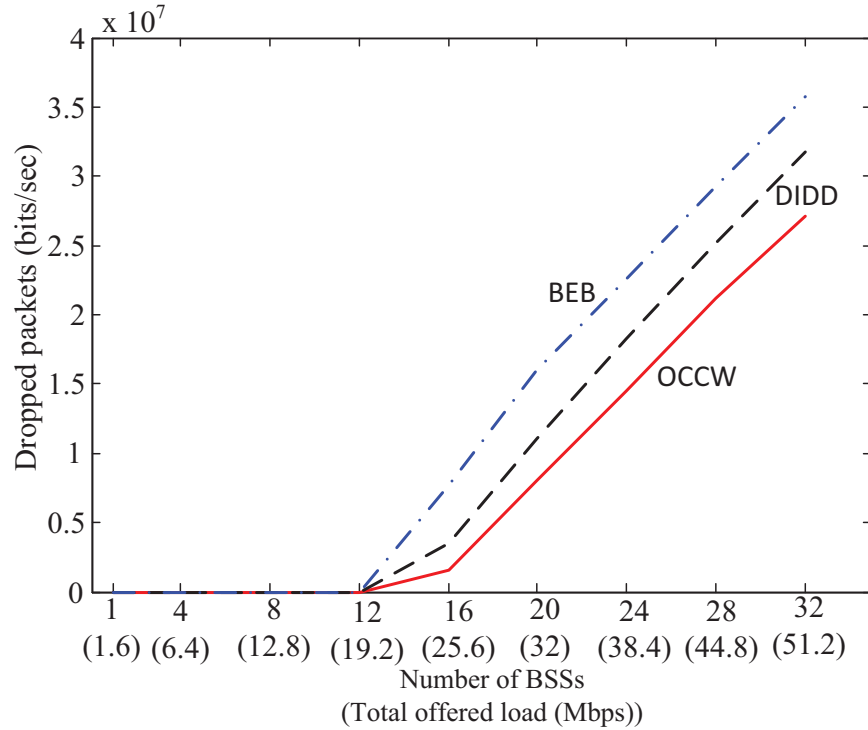


Figure 4.7: Lost bits due to dropped packets caused by buffer overflow. Note: Each packet contains 8184 bits

presents the packets dropped as a result of failing retransmissions. The sum of these two statistics is the total packet loss, which causes the throughput reduction. When the heavy offered load saturates the wireless channel; the wireless cannot keep up. Thus, the buffers fill up and then overflow as numerically demonstrated in Fig. 4.7. Among all three schemes, the OCCW scheme results in the least number of dropped packets from buffer overflow.

Meanwhile, Fig. 4.8 shows that this proposed scheme consistently maintains the

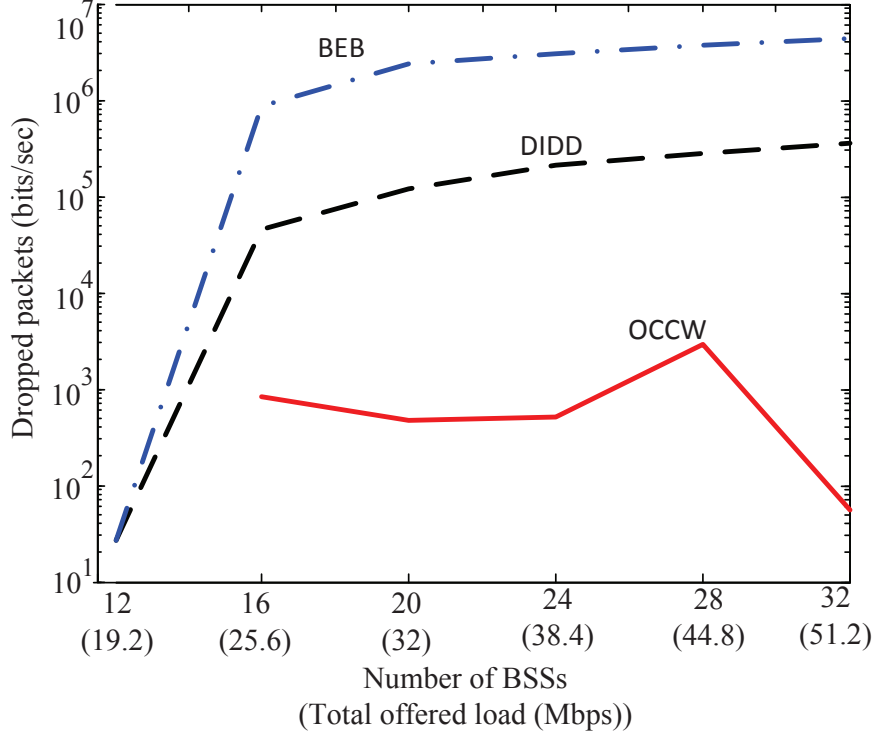


Figure 4.8: Lost bits due to dropped packets when exceeding retransmission threshold (6 retransmissions). Note: Each packet contains 8184 bits

minimum amount of dropped packets that exceed the retransmissions threshold, regardless of the traffic size. On the other hand, BEB and DIDD schemes show a nearly linear increase in this statistic. With regard to the BEB scheme, the statistic shows a similar trend to the results obtained in [102]. The linear increase in both BEB and DIDD schemes is expected because both schemes always reduce the CW for every new packet transmission, regardless of the station density. The lower values of CW can be too small for the increasing number of stations, because it accelerates the collision rate and consequently increases the number of the packets dropped. However, the DIDD scheme shows better performance than BEB because it modifies the aggressive behavior of BEB by avoiding setting the CW to  $CW_{min}$  after a successful transmission [102].

Statistically, the OCCW scheme manages to eliminate almost all dropped packets caused from transmission collisions. The DIDD scheme also shows promising performance but the OCCW scheme is still the best among all three schemes. This performance improvement was gained by assigning the closest optimized CW size based on traffic knowledge derived from the GPON headers. This allows a reduction in packet collisions and increases the number of successful packet transmissions.

Fig. 4.9 depicts the average media access delay. It records the waiting time in the

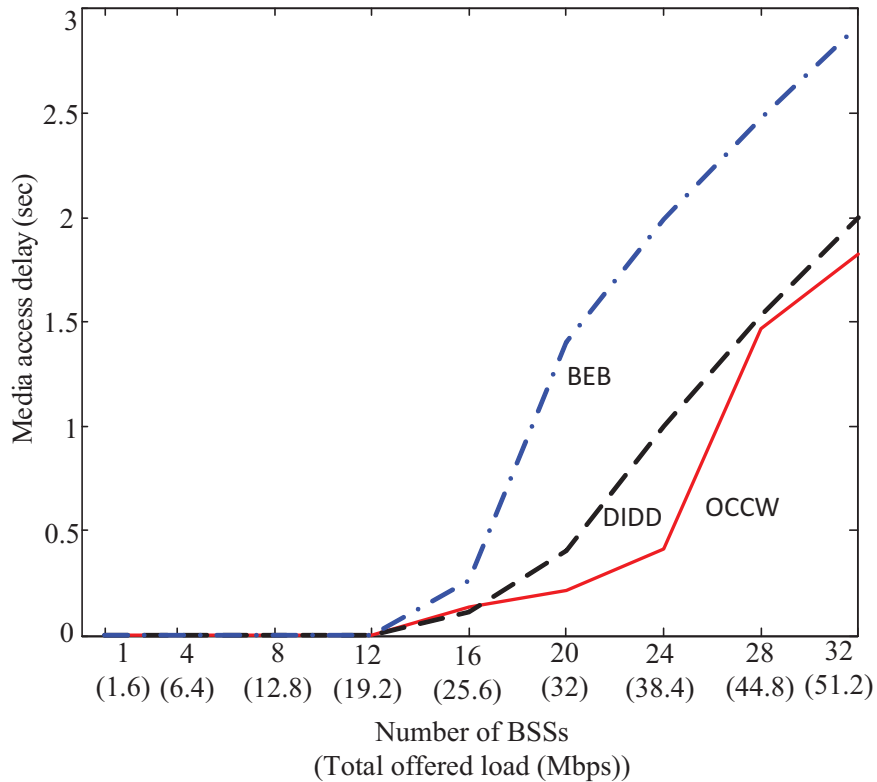


Figure 4.9: Average media access delay.

buffer queue and contention delays on the wireless air-interface, encountered by each packet when it is sent to the physical layer for transmission. Among all the schemes, the proposed scheme results in the shortest delay particularly when the network carries heavy traffic loads.

Despite the fact that the CW size increases as the traffic size grows, OCCW still attained minimum delay relative to the BEB and DIDD schemes. Clearly, the downside of a longer idle time is more than outweighed by the benefits of increased successful packet transmission. Thus, the collision rates are reduced and the packets do not have to be retransmitted again as experienced by the BEB and DIDD schemes.

## 4.4 Transmission Priority Scheme

This section presents further improvement of the OCCW scheme in Section 4.3 by introducing a transmission priority scheme in order to improve the fairness between UL and DL transmissions of the WLAN in fiber-wireless networks. The next subsection (4.4.1) illustrates the unfairness problem. Subsection 4.4.2 describes the AP transmission priority (APPriority) scheme where the AP in each BSS is given priority to select smaller backoff slots from the lower part of the optimized CW. On the contrary, WUs are bound to select longer backoff slots. Subsection 4.4.3 shows the performance of the new scheme.

### 4.4.1 Uplink and Downlink Transmission Analysis

In this section, an analysis of the UL and DL transmissions of the OCCW scheme is performed. Fig. 4.10 presents the normalized throughput for the UL and DL transmissions respectively. The figure suggests that there is an extreme unfairness; it is evident that UL transmissions have dominated the channel and caused DL transmissions to suffer from performance degradation particularly when the traffic starts to saturate after 19.2 Mbps. When the number of BSSs increase (more than 16 BSS) and carry more traffic (more than 25.6 Mbps), the DL performance worsens. Even at maximum load (51.2 Mbps) where the UL throughput has deteriorated to 0.75, there exists a performance gap of 0.6 (with the DL throughput at 0.15). There is a skewed

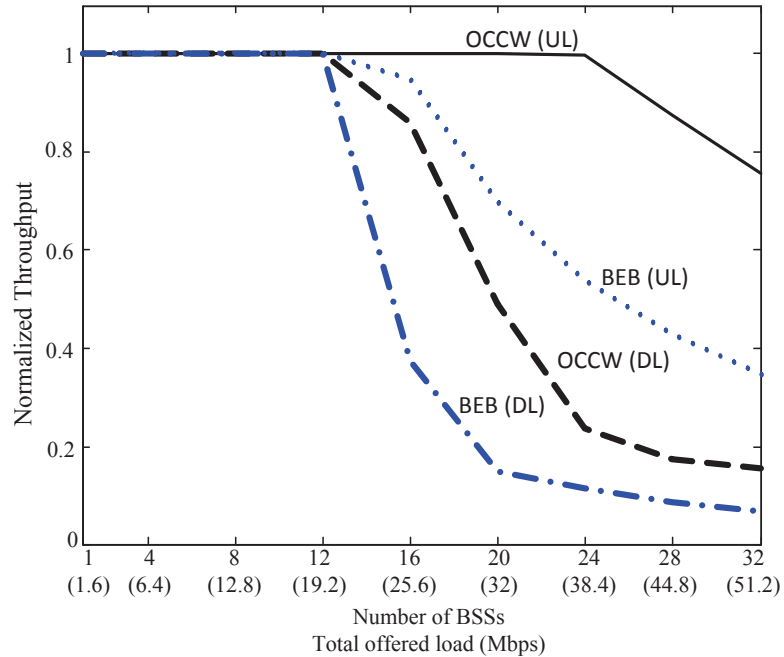


Figure 4.10: The normalized throughput for uplink and downlink transmissions

capacity distribution which creates unfairness in transmission. This unfairness occurs because all stations in each BSS are given an equal chance of a transmission opportunity regardless whether they are an AP or WU. In reality, the AP requires more transmission opportunities because it is the only station which is responsible for downlink transmissions in each BSS. Hence, this work proposes to assign a transmission priority to the AP by reducing the size of its contention window (CW) [103].

#### 4.4.2 Transmission Priority Technique

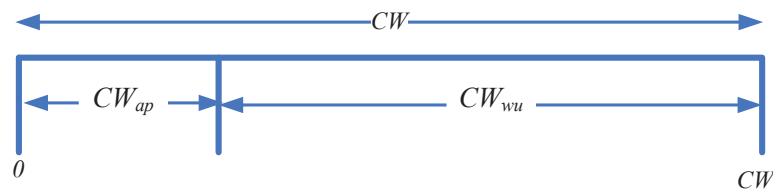


Figure 4.11: Non-overlapped contention window

The APPriority scheme reduces the CW size for the APs based on  $n^j$ , the active number of WUs in the  $j^{\text{th}}$  BSS $^j$ . The scheme is arranged in a manner that the CW of the AP ( $CW_{ap}$ ) and the CW of the WU ( $CW_{wu}$ ) do not overlap. In this scheme, as depicted in Fig. 4.11, APs are given the priority to select a backoff slot from 0 to  $CW_{ap}$  (exclusive) while the WUs are going to select from  $CW_{ap}$  to  $CW$  ( $= CW_{ap} + CW_{wu}$ ), thus, using different intervals of the optimized CW. This forces the APs to select a lower number of backoff slots than the WUs. Hence, the APs get earlier transmission chances which results in better throughput and less delay. Fairness requires the probability of AP transmission,  $p_{ap}$ , to be  $n^j$  times greater than the probability of WU transmission:  $p_{ap} = n^j p_{wu}$ . For  $CW \gg 1$ ,

$$p_{ap} = \frac{1}{CW_{ap}/2} \quad (4.1)$$

$$p_{wu} = \frac{1}{CW_{ap} + (CW - CW_{ap})/2} \quad (4.2)$$

from which

$$CW_{ap} = \frac{CW}{(n^j - 1)}. \quad (4.3)$$

For  $n^j = 5$ , then  $CW_{ap} = CW/4$ .

The value of the CW is initially obtained from the OCCW scheme in Section 4.3 and further improved by considering the APPriority scheme, as shown in Fig. 4.12. It is observed that changes to the CW size only occur when the number of BSSs is between 16 to 20 (25.6 to 32 Mbps). This is because the CW size (256 and 512 slots) in the early saturation region is too small to be applied in this transmission priority scheme especially for the  $CW_{ap}$ .

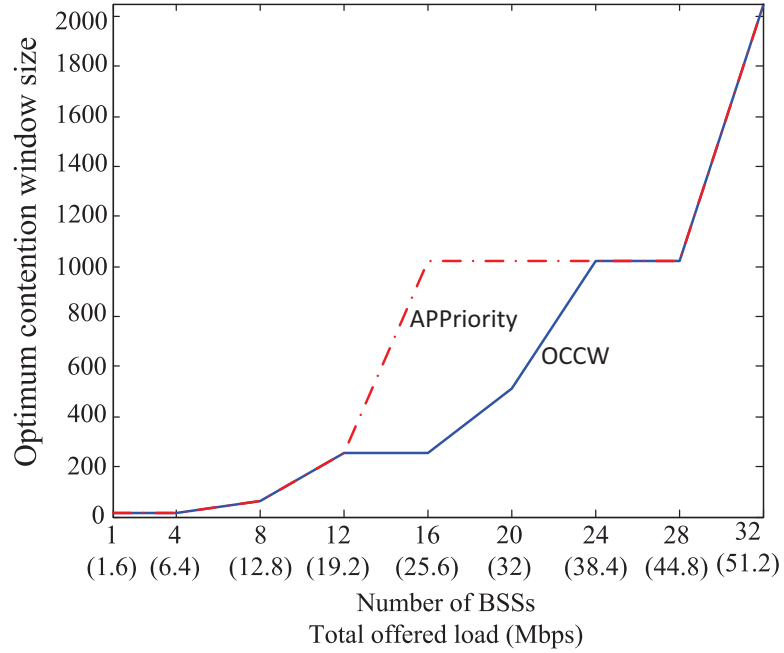


Figure 4.12: The optimized contention window size

### 4.4.3 Performance Analysis

A simple fairness index is introduced in equation (4.4) with  $x_1$  and  $x_2$  as the normalized throughput for the DL and the UL transmission respectively.

$$\text{Fairness Index} = \begin{cases} x_1/x_2, & \text{if } x_1 < x_2 \\ 1, & \text{if } x_1 = x_2 \\ x_2/x_1, & \text{if } x_2 < x_1 \end{cases} \quad (4.4)$$

The value for this fairness index is bounded within the interval  $[0,1]$ . A unity fairness index is targeted as it indicates that the UL and the DL have an equal throughput performance which translates to the best fairness condition. Fig. 4.13 displays the fairness index of the APPriority scheme in comparison to the OCCW and BEB schemes. The APPriority scheme shows a promising performance, maintaining

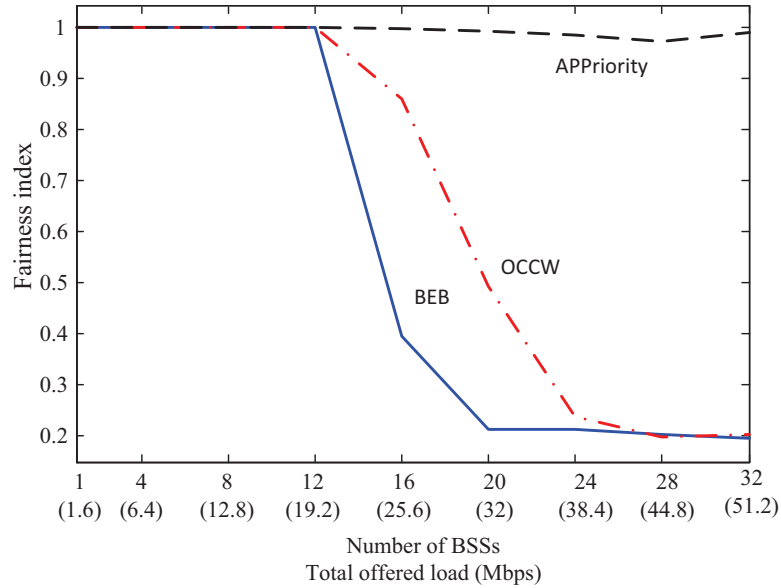


Figure 4.13: The fairness index

almost a unity fairness index irregardless of traffic size. Moreover, the unity fairness is gained without affecting the overall throughput performance as depicted in Fig. 4.14. It is shown that the overall normalized throughput of the scheme is at the same level as the OCCW scheme and much better than the legacy BEB scheme. This throughput performance is achieved because in the APPriority scheme, the DL throughput is improved at the price of a loss in UL throughput, keeping the overall throughput similar to that obtained in the OCCW scheme.

Conversely, Fig. 4.15 shows that the APPriority scheme encounters slightly higher overall media access delay in comparison to the OCCW scheme but is nevertheless superior to the standard BEB scheme. The longer delay is due to the WUs, having to select backoff slots from the upper 3/4ths of the selected CW resulting in longer idle durations. The APPriority scheme is a trade off between better fairness and longer media access delay.

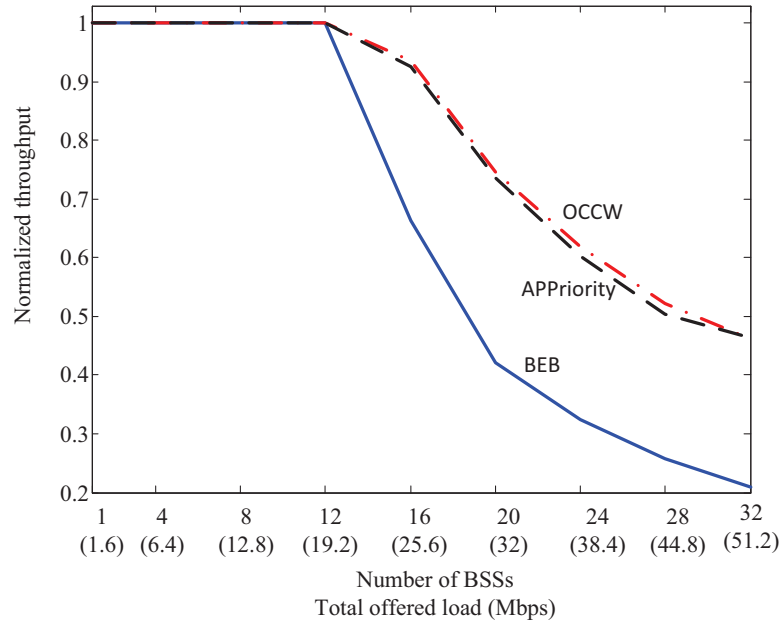


Figure 4.14: The overall normalized throughput

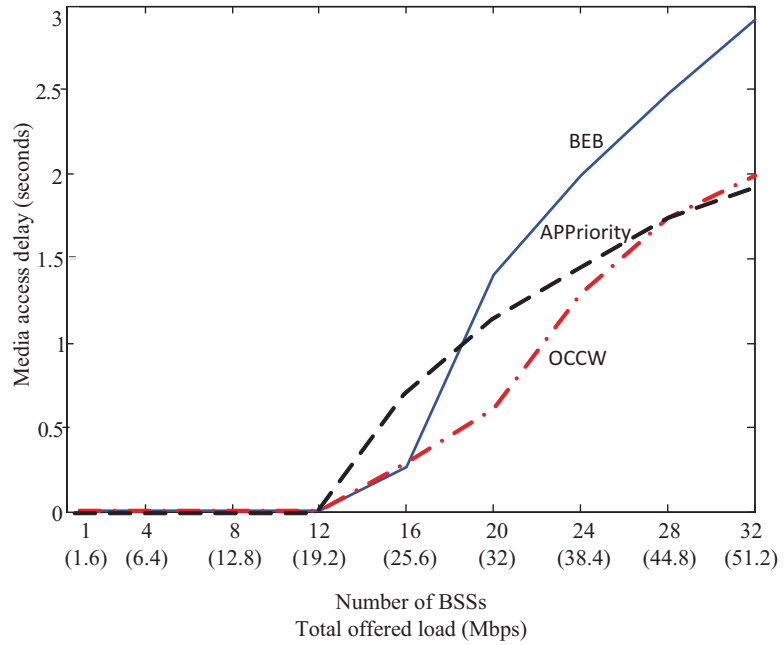


Figure 4.15: The media access delay

## 4.5 Summary

The chapter introduces a hybrid Fi-Wi network by integrating gigabit passive optical network (GPON) with wireless local area network (WLAN). The preliminary simulation results indicate that the BEB technique in the standard IEEE 802.11 WLAN performance is poorly degraded by having more BSSs in the network.

The optimum constant contention window (OCCW) scheme proposed in this chapter modifies the standard BEB algorithm by extracting traffic information from the GPON frame in order to enhance the WLAN performance in the proposed Fi-Wi network. The algorithm modification is made, by assigning the CW size based on traffic intensity, to achieve the best throughput performance. Most benefit in performance occurs when the offered traffic exceeds approximately 0.35 of the nominal maximum transmission rate (19Mbps). Beyond this, for a traffic rate of 0.6 of the maximum transmission rate, the throughput improves by up to 50% and the delay reduces by a factor of 5 compared to BEB.

Further, a transmission priority scheme is proposed to improve the fairness between UL and DL transmissions of the WLAN in fiber-wireless networks. The AP in each BSS is given priority to select smaller backoff slots from the lower one-fourth of the selected CW. On the contrary, WUs are bound to select longer backoff slots. As a result, a near unity fairness index is achieved irrespective of the traffic load. Interestingly, it is gained without affecting the overall throughput performance although it resulted in slightly longer delays.

Although the proposed schemes are able to improve the wireless performance of the Fi-Wi network, the schemes are dependent on accurate GPON estimates of ‘offered’ traffic. Only the downstream traffic estimate is accurate. Upstream traffic represents the ‘carried’ traffic not the offered traffic from the WU; adding these two figures together will underestimate the total ‘offered traffic’ required to select CW

optimum although it might be possible to correct for the underestimate by listening for collision on the channel (absence of ACK's), a different approach is taken in the next chapter.

Chapter 5 avoids the need for 'offered' traffic altogether and instead uses the number of active APs,  $m$ , available from the GPON network.

## Chapter 5

# Transmission Priority Scheme with Adaptive Backoff Technique

The previous chapter showed that under lightly loaded scenario the CW can vary over a wide range of values without degrading performance. Problems of throughput and fairness occur under heavily loaded conditions, when the channel reaches saturation and the offered traffic is significantly larger than the carried traffic. The remainder of the thesis will deal exclusively with the saturated condition.

The chapter proposes a novel transmission priority (TxPriority) scheme, that allows AP transmission priorities to be set as required within an infrastructure WLAN network. Mathematical analysis is carried out and expressions are derived for optimum AP and WU contention window sizes. The derived formulations show that the optimum CW sizes depend on the number of active APs and WUs; unknown quantities. Information from both the GPON and WLAN networks are capitalized to provide appropriate estimates and make the system adaptive. A new convergence function is introduced to improve the reliability of the adaptive system. The mathematical formulations are verified using network simulator software OPNET 16.1 [49].

The chapter is organized as follows. Section 5.1 describes the transmission priority

scheme and derives optimum contention window sizes. Section 5.2 estimates the number of active WUs and proposes an adaptive backoff technique with transmission priority (ATxPriority) scheme. Finally, Section 5.3 evaluates the performance of ATxPriority scheme.

## 5.1 Transmission Priority (TxPriority) Scheme

The proposed transmission priority scheme in Chapter 4 is further expanded in this section. The scheme is improved by introducing an adjustable transmission priority factor  $k$ . The parameter  $k$  allows the network to predefine its uplink to downlink throughput. The optimum sizes of an AP and a WU are derived respectively. In addition, the following analysis derives the optimum CW sizes which dynamically change in accordance to the network size. This study considers the same Fi-Wi network scenario shown in Fig. 4.1. For simplification, the assumptions made in Chapter 4 still hold.

### 5.1.1 Derivation of Optimum CW sizes

This section derives optimum contention window sizes for the two types of contending stations, an AP and a WU respectively. Consider a Fi-Wi network scenario which comprises of  $m$  integrated ONT-APs and  $n$  associate WUs. When a station wants to contend the channel, the backoff counter value  $b(t)$  is randomly selected within the range  $(0, CW - 1)$ , and then decremented at each subsequent idle slot.

The stochastic process  $b(t)$  is modeled with a simple discrete Markov chain as shown in Fig. 5.1 where  $w$  represents the value of the backoff counter in a state and  $p = P\{b(t) = 0\}$  is the probability of a station transmitting. The transition

probabilities are given as [60],

$$\begin{cases} P\{b(t) = w\} = P\{b(t-1) = w+1\} \\ \quad + \frac{P\{b(t-1)=0\}}{CW}, & \text{if } w = 0 \dots CW-2 \\ P\{b(t) = CW-1\} = \frac{P\{b(t-1)=0\}}{CW}, & \text{if } w = CW-1. \end{cases} \quad (5.1)$$

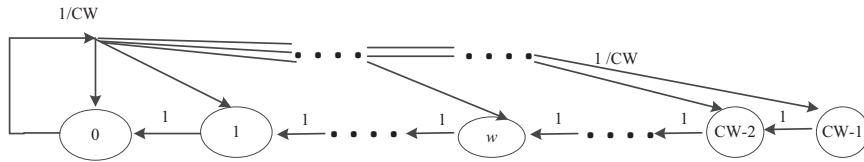


Figure 5.1: Discrete markov chain model of the backoff counter  $P\{b(t) = 0\} = p$ .

where  $P\{b(t-1) = w+1\}$  refers to the probability that the backoff counter was decremented due to an idle slot.  $\frac{P\{b(t-1)=0\}}{CW}$  corresponds to the previous event being a transmission and the selection of the randomly chosen value of  $w$ . Further, from (5.1), the probability of transmission,  $p$ , can be determined by imposing the normalization condition as follows,

$$\sum_{w=0}^{CW-1} P\{b(t) = w\} = \sum_{w=0}^{CW-1} \frac{CW-w}{CW} p = 1 \quad (5.2)$$

which gives

$$p = \frac{2}{(CW+1)}. \quad (5.3)$$

The probability that a station transmits in a slot is denoted as  $p_{ap}$  for an AP and  $p_{wu}$  for a WU. See Table 5.1 for a list of notations.

Since  $p_{ap}$  and  $p_{wu}$  are independent of each other, (5.3) can be employed to obtain,

$$p_{ap} = \frac{2}{(CW_{ap}+1)} \quad (5.4)$$

Table 5.1: List of Notations

Notation	Description
$p_{ap}$	probability of an AP transmitting
$p_{wu}$	probability of a WU transmitting
$m$	total number of APs
$n$	total number of WUs
$CW_{ap}$	current contention window size for an AP
$CW_{wu}$	current contention window size for a WU
$P_s^{ap}$	probability that a transmission is a successful AP transmission
$P_s^{wu}$	probability that a transmission is a successful WU transmission

and,

$$p_{wu} = \frac{2}{(CW_{wu} + 1)}. \quad (5.5)$$

Further, given  $m$  APs and  $n$  WUs are contending on the channel, the probability that there is at least one transmission is given by,

$$P_{tr} = 1 - (1 - p_{ap})^m (1 - p_{wu})^n. \quad (5.6)$$

The average number of consecutive idle slots  $E[I]$  can now be defined as,

$$E[I] = \frac{1 - P_{tr}}{P_{tr}}. \quad (5.7)$$

The probability that a transmission is a successful AP transmission  $P_s^{ap}$  is given by the probability that only one AP transmits on the channel provided that there is a transmission,

$$P_s^{ap} = \frac{mp_{ap}(1 - p_{ap})^{m-1}(1 - p_{wu})^n}{P_{tr}}. \quad (5.8)$$

Similarly, the probability that a transmission is a successful WU transmission is given by,

$$P_s^{wu} = \frac{np_{wu}(1-p_{ap})^m(1-p_{wu})^{n-1}}{P_{tr}}. \quad (5.9)$$

A transmission priority factor  $k$  can now be introduced. It is defined as the number of successful transmissions of WUs with respect to APs,

$$k = \frac{P_s^{wu}}{P_s^{ap}} = \frac{np_{wu}(1-p_{ap})}{mp_{ap}(1-p_{wu})}. \quad (5.10)$$

A value of  $k < 1$  implies higher downlink throughput; while a value of  $k > 1$  represents higher uplink throughput. Note, successful transmissions from an AP and a WU are mutually exclusive events. Thus, the probability that a transmission is successful is given by,

$$P_s = P_s^{ap} + P_s^{wu} = (1+k)P_s^{ap}. \quad (5.11)$$

The system throughput  $S$  is derived from the effective channel utilization. It is defined as the ratio of time taken to successfully transmit payload bits to the sum of the packet transmission time  $T$  and the idle slot time  $E[I]$ ,

$$S = P_s \frac{\gamma T}{T + E[I]} \quad (5.12)$$

where,  $T$  is measured in slot times,

$$T = T_{Header} + T_{Payload} + SIFS + ACK + DIFS \quad (5.13)$$

and,  $\gamma$  is the fraction of  $T$  used for payload transmission,

$$\gamma = \frac{T_{Payload}}{T}. \quad (5.14)$$

In addition, the uplink throughput  $S_{wu}$  and the downlink throughput  $S_{ap}$  are expressed as follows

$$S_{wu} = P_s^{wu} \frac{\gamma T}{T + E[I]} \quad (5.15)$$

and

$$S_{ap} = P_s^{ap} \frac{\gamma T}{T + E[I]}. \quad (5.16)$$

Using (5.10),  $p_{wu}$  can be substituted in terms of  $p_{ap}$ , thus, the system throughput in (6.25), can be evaluated as follows,

$$S = \frac{(1+k)m\gamma p_{ap}(1-p_{ap})^{m+n-1}}{(1+p_{ap}(\frac{km}{n}-1))^n + \frac{1-T}{T}(1-p_{ap})^{m+n}} \quad (5.17)$$

Equation (5.17) corroborates that  $S$  depends on  $p_{ap}$  which in terms of a function  $CW_{ap}$  by (5.4). An optimum value of  $CW_{ap}$  is obtained when  $S$  is maximized using the following equation,

$$\frac{dS}{dCW_{ap}} = \frac{dS}{dp_{ap}} \frac{dp_{ap}}{dCW_{ap}} = 0. \quad (5.18)$$

However, equation (5.4) verifies that  $\frac{dp_{ap}}{dCW_{ap}} \neq 0$  (except for the lower bound condition  $CW_{ap} \rightarrow \infty$ ). Hence, the solution for (5.18) is given by  $\frac{dS}{dp_{ap}} = 0$ , this equates to,

$$0 = \left( \left( 1 + \left( \frac{km}{n} - 1 \right) p_{ap} \right)^n + \frac{1-T}{T} (1-p_{ap})^{m+n} \right) (1 - (m+n)p_{ap}) - p_{ap} (1-p_{ap}) \left( \begin{array}{l} n \left( \frac{km}{n} - 1 \right) \left( 1 + \left( \frac{km}{n} - 1 \right) p_{ap} \right)^{n-1} \\ - \frac{1-T}{T} (m+n) (1-p_{ap})^{m+n-1} \end{array} \right). \quad (5.19)$$

Considering  $m+n > n \gg 1$ , the following approximation holds for small  $p_{ap}$ ,

$$(1-p_{ap})^{m+n} \approx 1 - (m+n)p_{ap} + \frac{(m+n)(m+n-1)}{2} p_{ap}^2. \quad (5.20)$$

Thus, (5.19) can be evaluated to give the following solution,

$$p_{ap} \approx \frac{\sqrt{(m+n)^2 + 2Q} - (m+n)}{Q} \quad (5.21)$$

where,

$$Q = \frac{n-1}{n}(km-n)^2T + (T-1)(m+n)(m+n-1) + 2T(km-n)(m+n-1). \quad (5.22)$$

$Q$  is a negative number, and so (5.21) becomes invalid when the term under the square root becomes negative, which (after some simplification) occurs when the larger of the two conditions holds

$$n > \max [((k+1)\sqrt{2T} - 1)m, 2(T-m)]. \quad (5.23)$$

Now, the optimum  $CW_{ap}$  can be approximated from (5.4),

$$CW_{ap}^{opt} \approx \frac{2Q}{\sqrt{(m+n)^2 + 2Q} - (m+n)}. \quad (5.24)$$

Further, (5.10) and (5.24) can be used to approximate the optimum value of  $CW_{wu}$  as,

$$CW_{wu}^{opt} \approx \frac{n(CW_{ap} - 1)}{km} + 2. \quad (5.25)$$

The optimum CW values depend on the active number of APs and WUs ( $m$  and  $n$ ) and also the values of  $T$  and  $k$ .

## 5.1.2 Model Validation

### 5.1.2.1 Validation to adhoc network in [60]

The following formulation extension is carried out to validate the derived formulations with the previous work published in [60]. The formulation can be extended to an adhoc network by letting  $p_{ap} = p_{wu} = p$ , which implies both stations are having equal chance of transmitting. As such, equation (5.10) becomes,

$$k = \frac{n}{m}. \quad (5.26)$$

Then, equation (5.21) becomes

$$p = \frac{\sqrt{(m+n)^2 + 2(T-1)(m+n)(m+n-1)} - (m+n)}{(T-1)(m+n)(m+n-1)} \quad (5.27)$$

$$\approx \frac{\sqrt{2}}{(m+n)\sqrt{T}}.$$

Let the total number of stations,  $m+n$  equals to  $N$  and so the optimum  $CW$  can be approximated from (5.5) as,

$$CW^{opt} \approx \sqrt{2TN}. \quad (5.28)$$

The above derived equation is identical to the optimum contention window size formulated in [60] for an adhoc network.

### 5.1.2.2 Validation of Simplification

The proposed scheme aims to keep the  $CW$  sizes as close as possible to the optimum values at all the time. Hence, after a successful transmission, the  $CW$  sizes of the stations remain constant; they are not reset to a minimum value as in the BEB scheme.

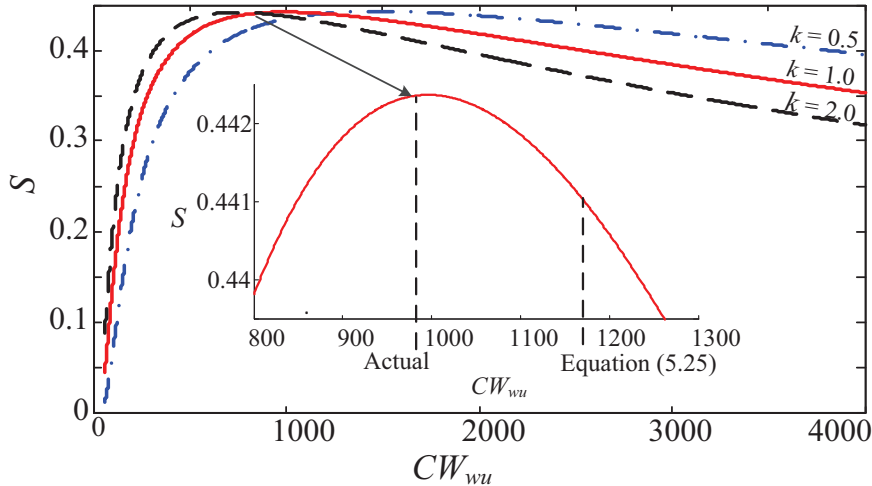


Figure 5.2: Normalized throughput,  $S$  vs  $CW_{wu}$  from equation (5.17) and equation (5.5) with transmission priority factor  $k = [0.5, 1, 2]$ .

Further, Fig. 5.2 illustrates the system throughput  $S$  with respect to the contention window size  $CW_{wu}$  for a network with  $m = 15$ ,  $n = 60$ ,  $T = 30$  and  $\gamma = 0.56$ . The latter applies to the simulation parameters of Table 5.1. The figure further verifies that there exists an optimum contention window size that maximizes throughput. It demonstrates a higher value of  $k$  ( $k = 2$ ) increases the probability of a WU transmission by reducing the optimum  $CW_{wu}^{opt}$  size, hence, increasing the overall uplink throughput  $S_{wu}$ . On the other hand, a lower value of  $k$  ( $k = 0.5$ ) reduces the probability of a WU transmission by increasing the optimum  $CW_{wu}^{opt}$  size. The figure also shows that the formulated optimum  $CW_{wu}^{opt}$  (5.25) is almost 20% higher than the actual  $CW_{wu}^{opt}$  (for  $k = 1$ ) based on brute force evaluations of equation (6.25). However, the difference has a negligible effect on the throughput with an error of 0.3%. The simplification required for (5.25) appear justified.

Table 5.2: 802.11a OPNET simulation parameters (saturated condition)

Parameter	Value
Packet size	8184 bits
MAC header	224 bits
PHY header	20 $\mu$ s
ACK length	134 bits/control rate + PHY header
Data rate	54 Mbps
Control rate	6 Mbps
Channel bandwidth	20 MHz
Slot time	9 $\mu$ s
SIFS time	16 $\mu$ s
DIFS time	34 $\mu$ s
ACK timeout	70 $\mu$ s
Packet transmission time (T)	30 slots
Transmission priority factor ( $k$ )	1

### 5.1.3 Performance Evaluation

Fig. 5.3 compares the uplink and downlink saturation throughputs for the BEB [43] and AWA [60] schemes with the proposed TxPriority scheme having transmission priority factor  $k = 1$ . The simulations are carried out in OPNET 16.1 software using IEEE 802.11a standard parameters as summarized in Table 5.2. Noted that the same IEEE 802.11a MAC parameters from Table 4.1 are used but this time under saturated condition.

The normalized throughput is measured as the total bits/second successfully received by each station over the channel capacity (data rate=54Mbps). The traffic load is increased by increasing the number of basic service sets (BSSs) ranging from 1 to 30; each BSS comprises of one integrated ONT-AP and four associate wireless users (WUs).

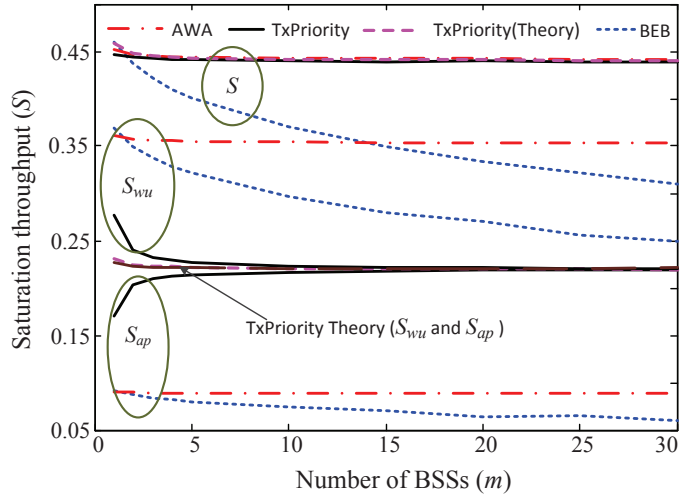


Figure 5.3: Normalized saturation throughput vs. number of BSSs for BEB, AWA and TxPriority (simulation and theory) schemes.

As expected, lower downlink throughputs  $S_{ap}$  are observed in comparison to uplink throughputs  $S_{wu}$  for the BEB and AWA schemes since they are both designed for adhoc networks. The plots show that at a high traffic load (i.e. 30 BSS) the downlink throughputs  $S_{ap}$  for BEB and AWA schemes are 0.06 and 0.09 with the corresponding uplink throughputs  $S_{wu}$  of 0.25 and 0.35 respectively. These resulted in the ratio between  $S_{ap}$  and  $S_{wu}$  for both schemes to be approximately 0.25, which reflects the simulation scenario of having 1 AP serving every 4 WUs. On the other hand, our TxPriority scheme with  $k = 1$  has an equal  $S_{ap}$  and  $S_{wu}$  of 0.22. An imbalance between  $S_{ap}$  and  $S_{wu}$  is noted for low BSS numbers due to the binomial approximations used in (5.20) to derive optimum CW size equations (5.24) and (5.25). Apart from this imbalance, the TxPriority scheme attains throughputs close to the theoretical values derived in (6.29) and (6.28) for  $S_{ap}$  and  $S_{wu}$  respectively.

Although the TxPriority scheme brings a balance between  $S_{ap}$  and  $S_{wu}$ , it does not compromise the overall throughput  $S$ , which matches the AWA scheme. In both cases, the throughput remained constant over increasing number of BSSs since the CW sizes are assigned on the number of active stations. The BEB scheme does not

consider the number of contending stations, it simply doubles its CW size at every unsuccessful transmission, and results in deteriorating throughput performance as the number of BSSs increase. Larger CW sizes also result in higher media access delays. Fig. 5.4 shows that the BEB scheme has longer delays than the AWA and TxPriority schemes. The media access delay is measured as the average time that a packet has to wait before its transmission (i.e. the backoff counter decrements to zero). Both BEB and AWA schemes have their DL access delays equal to their UL access delays. In contrast, DL delays in the TxPriority scheme are always less than UL delays because the assigned  $CW_{ap}$  size is less than the  $CW_{wu}$  size. Nonetheless, average overall delays of the TxPriority scheme is equal to the AWA scheme, and considerably better than the exponentially increasing delay of the BEB.

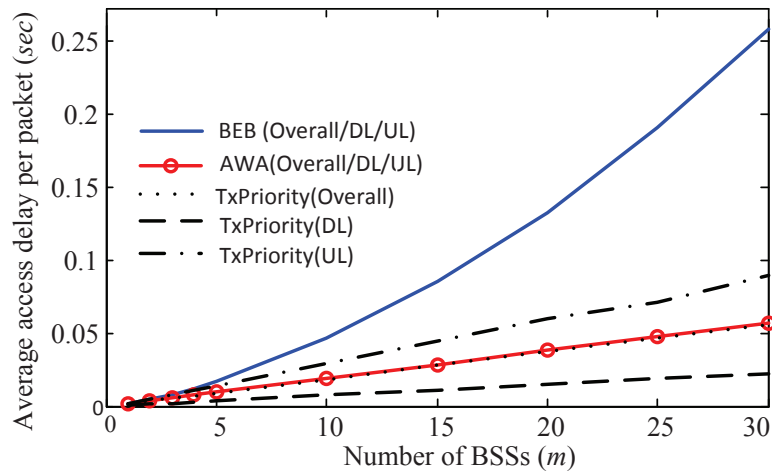


Figure 5.4: Media access delay per packet transmission vs. number of BSSs for BEB, AWA and TxPriority schemes

## 5.2 Adaptive Backoff Technique with Transmission Priority (ATxPriority) scheme

All stations, APs and WUs, in the wireless network aim to set an optimum CW size as formulated in ((5.24) and (5.25)) respectively to maximize their throughput. The optimum CW sizes depend on four parameters  $k, T, m$  and  $n$ . The priority factor  $k$  is set globally in accordance to the network demand. The packet transmission time  $T$  for each station is known from (5.13). However, the values of  $m$  and  $n$  vary with the number of active users in the network. The value of  $m$  can be estimated from the GPON network by observing the number of active ONTs at the integrated ONT-AP interface. Since this estimate  $m$  is only available to APs and not WUs, each AP will periodically broadcast the information to their associate WUs.

However, the value of  $n$  can only be estimated by observing the activity of the channel. Therefore, the following subsections propose a technique to estimate the values of  $n$  and consequently enable each station to periodically update their optimum CW size and contend for the channel accordingly.

### 5.2.1 Measurement of $P_{tr}$

The probability that there is a transmission on the channel can be approximated as,

$$\hat{P}_{tr} = \frac{F_B}{F_B + F_I} \quad (5.29)$$

where  $F_B$  is the number of times the channel is busy within an observation period (i.e. starting from the time a station first contends the channel until it completes transmission) and  $F_I$  is the total number of idle slots. Fig. 5.5 illustrates an example of the estimate for station Y. Station Y with a packet to transmit has randomly chosen a backoff counter of 10. The backoff counter is decremented while the channel

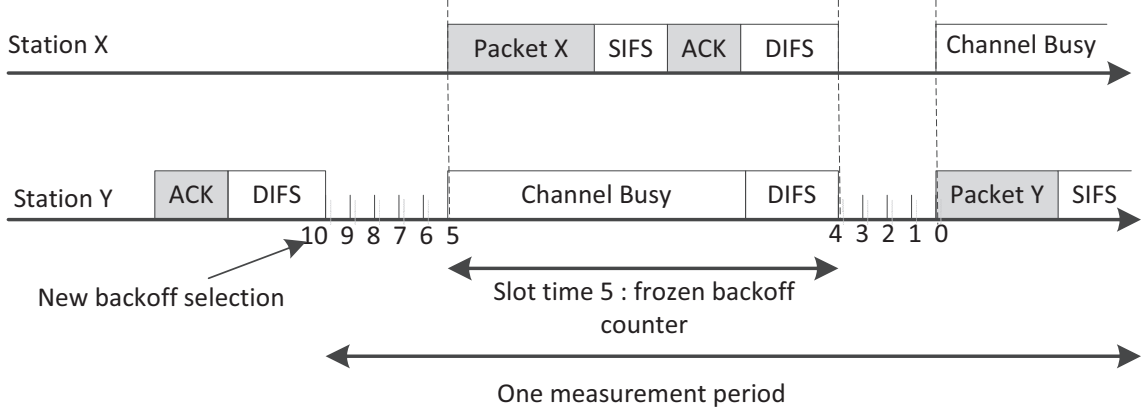


Figure 5.5: Estimating  $\hat{P}_{tr}$  over one observation period as measured by station Y.

is sensed idle. When the backoff counter is decremented to 5, the channel is sensed busy due to station X's transmission. As a result, the backoff counter is frozen at 5 until the transmission is complete (i.e: station X completes transmission) and the channel is sensed idle. Station Y waits a further DIFS period before decrementing the backoff counter to 4. Subsequently, the backoff counter is decremented until it reaches zero and station Y transmits. As such, the value of  $F_B$  observed by station Y is 2 (i.e. one time busy due to station X's transmission and the second due to its own transmission) and the value of  $F_I$  is observed to be 9. Hence, the  $\hat{P}_{tr}$  is evaluated to be  $2/11$ . The stochastic process of selecting the backoff counter makes the estimate  $\hat{P}_{tr}$  prone to error when measured over a single observation time. To reduce the error, the estimate is averaged over 10 observation periods and is given by,

$$\bar{P}_{tr} = \frac{\sum_{i=1}^{10} F_{B_i}}{\sum_{i=1}^{10} F_{B_i} + \sum_{i=1}^{10} F_{I_i}}. \quad (5.30)$$

Fig. 5.6 compares the  $\bar{P}_{tr}$  with the actual value of  $P_{tr}$  from (5.6) for a scenario of  $m = 15$  and  $n = 60$ . A standard deviation error of 4.4% is noted.

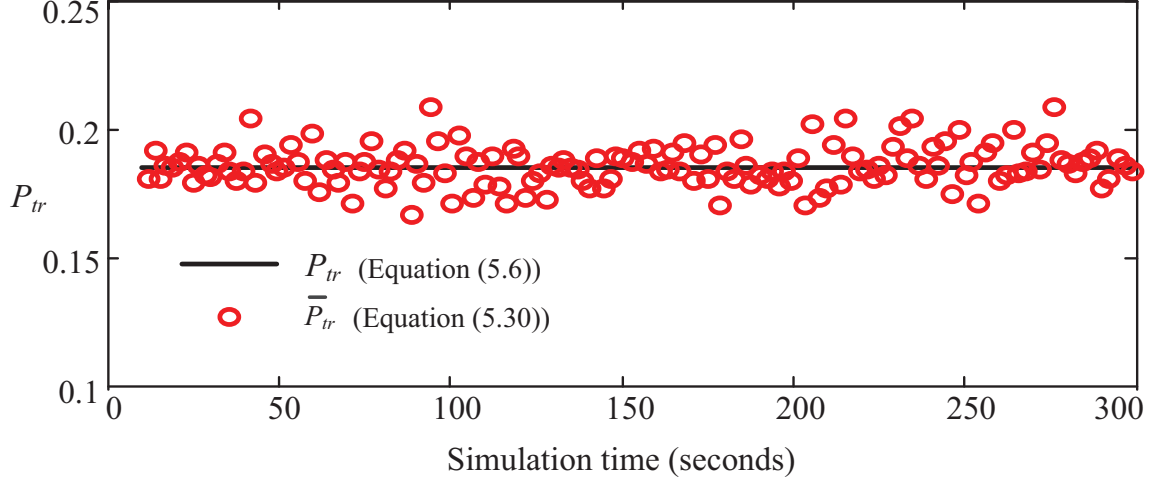


Figure 5.6: Average  $P_{tr}$  values as measured by one user (equation(5.30)) compared to theoretical  $P_{tr}$  values (equation(5.6))

### 5.2.2 Estimate of $n$

The raw estimate  $\hat{n}$  is approximated by employing first order binomial approximation into (5.6),

$$P_{tr} = np_{wu} + mp_{ap} - mn p_{ap} p_{wu} \quad (5.31)$$

and substituting using (5.4) and (5.5),

$$P_{tr} = \frac{2n}{CW_{wu} + 1} + \frac{2m}{CW_{ap} + 1} - \frac{4mn}{(CW_{wu} + 1)(CW_{ap} + 1)} \quad (5.32)$$

The ATxPriority algorithm to estimate  $n$  starts here. At time ( $t$ ) the smooth estimate  $\bar{P}_{tr}$  from (5.30) is applied to (5.32) to estimate the number of users,  $\hat{n}$ , (5.33).

$$\hat{n}(t) = \frac{(C\hat{W}_{wu} + 1)((C\hat{W}_{ap} + 1)\bar{P}_{tr}(t)) - 2m}{2(C\hat{W}_{ap} + 1 - 2m)}. \quad (5.33)$$

Furthermore, a smoother behaving estimate  $\bar{n}$  is obtained by exploiting a first order recursive filter of  $\hat{n}$ ,

$$\bar{n}(t) = \alpha\bar{n}(t-1) + (1-\alpha)\hat{n}(t) \quad (5.34)$$

where  $\alpha$  is a smoothing factor. A value of  $\alpha = 0.8$  is chosen since it has been shown in literature [56,60] and [57] as a good compromise between accuracy and precision.

The updated  $\bar{n}(t)$  evaluates the new estimate of the  $C\hat{W}_{ap}(t)$  and  $C\hat{W}_{wu}(t)$ , formulated in (5.24) and (5.25) as follows,

$$C\hat{W}_{ap}(t) \approx \frac{2\hat{Q}}{\sqrt{(m + \bar{n}(t))^2 + 2\hat{Q}} - (m + \bar{n}(t))} \quad (5.35)$$

$$C\hat{W}_{wu}(t) \approx \frac{\bar{n}(t)(C\hat{W}_{ap}(t) - 1)}{km} + 2 \quad (5.36)$$

where the  $\hat{Q}$  is calculated from (5.22) using  $\bar{n}(t)$ .

$$C\hat{W}_{wu} = C\hat{W}_{wu}(t) \quad (5.37)$$

and,

$$C\hat{W}_{ap} = C\hat{W}_{ap}(t). \quad (5.38)$$

The process (5.30) to (5.38) is then repeated with the new  $C\hat{W}(t)$ 's for the next time period with  $t = t + 1$ . As it stands the proposed adaptive technique does not converge to the optimum CW due to  $\hat{n}$  not reaching the correct value. Fig. 5.7 shows the effect of adaptation on one station from a group of 60 stations with all the other stations using the correct value of  $n = 60$  and inhibiting their correction algorithms. When the adapting station starts off with an initial estimate above the correct value, ( $\bar{n}(t = 0) = 70$ ), it further diverges until it reaches a stable value of  $\bar{n}(t \rightarrow \infty) = 200$ , far above the optimum value and resulting in a CW much larger than optimum. Similarly when starting with a lower estimate ( $\bar{n}(t = 0) = 50$ ) the estimate drops to close on zero, forcing a small CW. Both situations cause the measured  $P_{tr}$  to change and affect the estimates of the other stations. In particular the low CW causes the adapting station to hog the traffic which gives the impression to other stations of

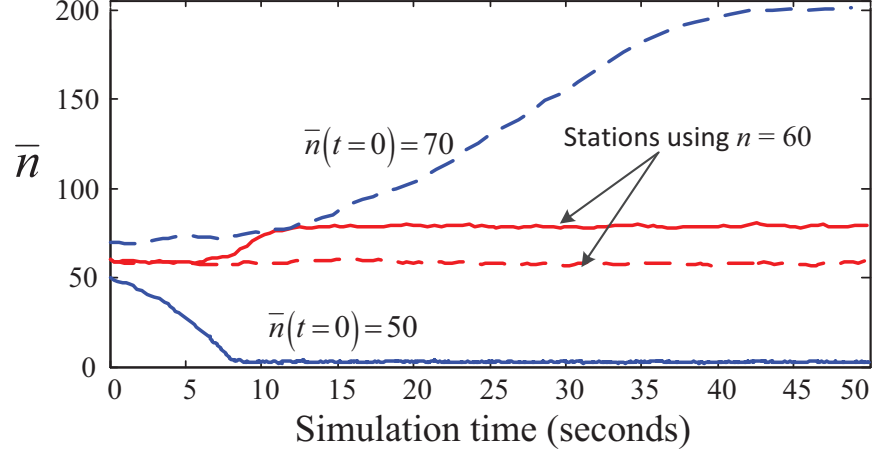


Figure 5.7: The convergence of  $\bar{n}$  for one station. Other stations use the known (ideal) value of  $n = 60$ . Initial condition:  $\bar{n}(t=0) = 50$ , solid; and  $\bar{n}(t=0) = 70$ , dashed.

more users accessing the channel, indicated by their estimates,  $\bar{n}$ , going over the actual value of  $n = 60$ .

### 5.2.3 The Convergence Function

In this section, a new convergence function,  $c(\bar{n})$ , is added into the computation of  $CW(t)$ . The convergence function acts as a correcting factor in estimating the  $\hat{n}$ . In what follows, an analysis is carried out to show that the convergence function for an adhoc network described in [60] is not appropriate for an infrastructure multiple APs scenario.

Equations (5.37) and (??) are replaced by:

$$C\hat{W}_{wu} = c(\bar{n})C\hat{W}_{wu}(t) \quad (5.39)$$

$$C\hat{W}_{ap} = c(\bar{n})C\hat{W}_{ap}(t) \quad (5.40)$$

where,

$$c(\bar{n}) = \left(1 + \frac{h}{\sqrt{\bar{n}(t)}}\right). \quad (5.41)$$

The convergence function acts as a correcting factor in estimating the  $\hat{n}$ . Under

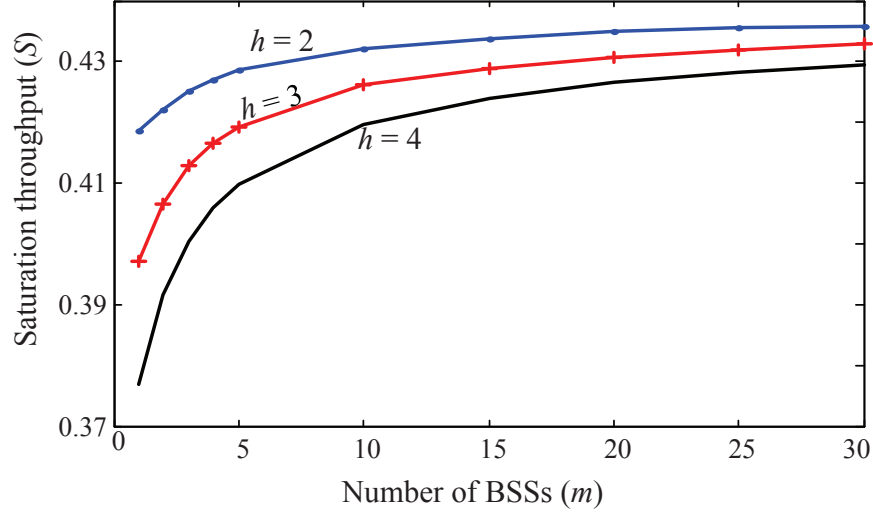


Figure 5.8: Effect of the convergence factor,  $h$  on system throughput as the number of BSSs increases.

conditions  $CW_{ap} \gg 1$  and  $CW_{wu} \gg 1$ , equation (5.33) can be simplified and rewritten as,

$$\hat{n}(t) = \frac{(C\hat{W}_{wu})((C\hat{W}_{ap})P_{tr} - 2m)}{2(C\hat{W}_{ap} - 2m)}. \quad (5.42)$$

The  $(\hat{\cdot})$  represents the estimate by the adapting station while  $P_{tr}$  is the actual value dominated by other stations which are assumed operating close to the optimum CW size in which case the assumption that they all have the same  $p_{ap}$  or  $p_{wu}$  is justified.

Substituting  $P_{tr}$  in (5.42) with equation (5.32) gives

$$\hat{n} = \frac{C\hat{W}_{ap}C\hat{W}_{wu}}{C\hat{W}_{ap} - 2m} \left( \frac{n}{CW_{wu}} + \frac{m}{CW_{ap}} - \frac{2mn}{CW_{ap}CW_{wu}} - \frac{m}{CW_{ap}} \right). \quad (5.43)$$

where  $n$  and  $m$  are the actual number of wireless users and access points, all (except

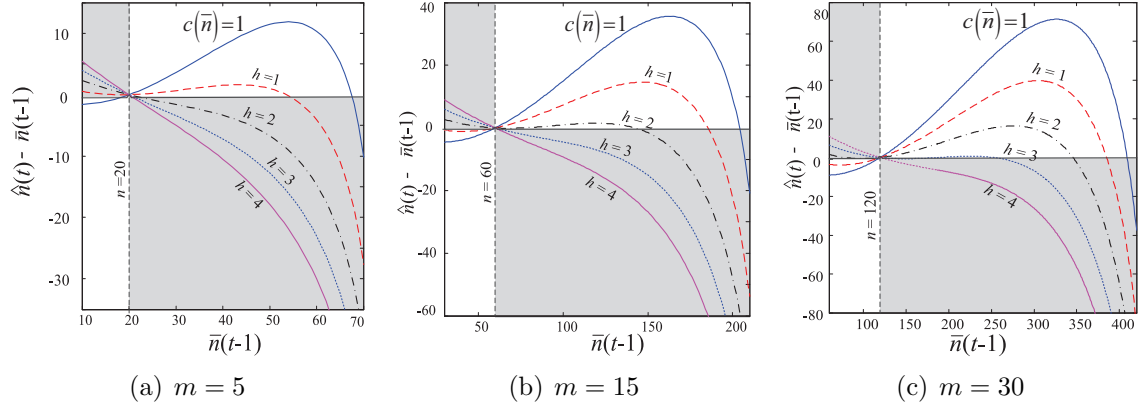


Figure 5.9: The change in  $\bar{n}$  per iteration vs.  $\bar{n}$  for different values of  $h$ , ( $c(\bar{n}) = (1 + \frac{h}{\sqrt{\bar{n}}})$ ).

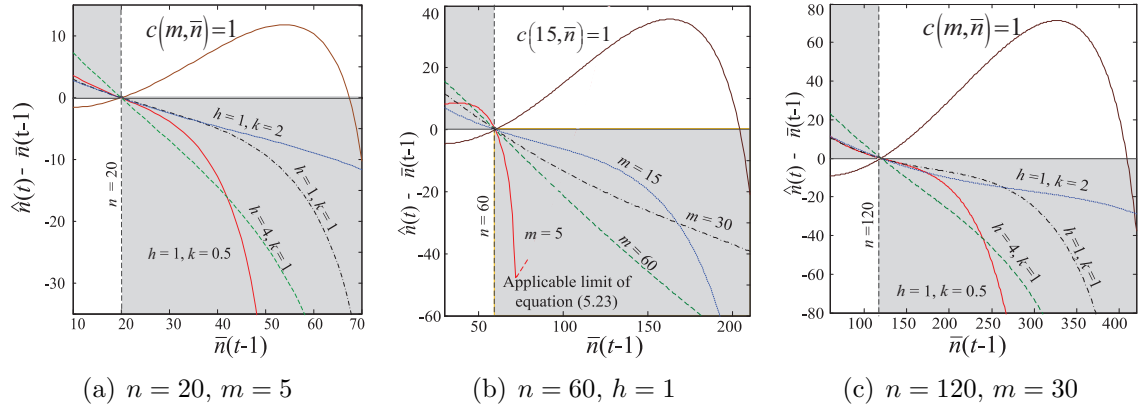


Figure 5.10: The change in  $\bar{n}$  per iteration vs.  $\bar{n}$  for different values of  $h, k$  and  $m$ , ( $c(m, \bar{n}) = (1 + \frac{h+2\log_{10}m}{\sqrt{\bar{n}}})$ ).

for the adapting station) operating with contention windows of  $CW_{wu}$  and  $CW_{ap}$

respectively. The convergence improves with the positive integer convergence factor,  $h$ , in (5.41). However, Fig. 5.8 indicates that the system throughput gradually decreases as the convergence factor increases. This observation is justified by (5.39)-(5.41), increasing the value of  $h$  will further increase the  $C\hat{W}$  size beyond the optimum value and result in throughput degradation. Therefore, lower values of  $h$  are preferred.

An analysis is carried out to investigate the compatibility of the convergence function with the formulated CW size. Fig. 5.9 plots  $\hat{n} - \bar{n}$  against  $\bar{n}$  as it deviates from the actual value of  $n$  for different sizes of  $m$  and varying values of  $h$ . To achieve effective convergence,  $\hat{n} - \bar{n} > 0$  (i.e.  $\hat{n} > \bar{n}$ ) is required when  $\bar{n} < n$  and  $\hat{n} - \bar{n} < 0$  (i.e.  $\hat{n} < \bar{n}$ ) is required when  $\bar{n} > n$ . The convergence region is graphically represented by the shaded areas in Fig. 5.9; while the non-shaded areas represent divergence. A stable value for  $\bar{n}$  exists when the curve crosses the zero correction line with a negative slope. The steeper the curve the stronger the stability. For example, with no correction factor,  $c(\bar{n}) = 1$ , the curve is almost completely in the divergence region. If  $\bar{n} < n$  then  $\bar{n}$  will keep reducing until it gets to 0 or if it is greater than  $n$  it will keep increasing until the curve re-enters the convergence region at a stable but incorrect value of  $\bar{n}$ . In Fig. 5.9(b) the incorrect value is  $\bar{n} = 200$ , way in excess of the actual value of  $n = 60$  but in agreement with the simulations of Fig. 5.7 which use the same values of  $n, m$  and  $k$ .

Fig. 5.9(a) illustrates the results for  $m = 5$  having  $n = 20$ . The line  $h = 1$  falls outside the shaded region and will not drive  $\bar{n}$  toward the actual value of  $n$ . Nonetheless, the lines  $h = 2$ ,  $h = 3$ , and  $h = 4$  all fall within the shaded region and will allow convergence,  $h = 2$  being the smallest results in the least throughput degradation and is considered to be the optimum choice. However, in Fig.5.9(b) and Fig. 5.9(c), for  $m = 15$  and  $m = 30$ , both with the same  $n/m = 4$  ratio, the optimum value of  $h$  increases to  $h = 3$  and  $h = 4$  respectively, indicating that the proposed scheme has to adaptively choose the optimum  $h$  for a particular size of  $m$ , thus,

increasing its complexity. This is because the convergence equation defined in (5.41) does not consider the number of APs ( $m$ ). Hence, a modified convergence function  $c(m, \bar{n})$  is proposed,

$$c(m, \bar{n}) = \left(1 + \frac{h + 2\log_{10}m}{\sqrt{\bar{n}(t)}}\right). \quad (5.44)$$

Fig. 5.10(a) and Fig. 5.10(c) show the results of the modified convergence function for the more extreme cases  $m = 5$  and  $m = 30$ . All lines now fall within the shaded regions for  $k$  between 0.5 and 2. As a result, the constant  $h = 1$  can be used as the optimum choice irrespective of the size of  $m$ . Fig. 5.10(b) shows the curves stay in the stable zones as the ratio  $n/m$  changes while holding the number of users constant at  $n = 60$ . The truncation of the  $m = 5$  curve for large  $\bar{n}$  is due to the invalidity condition (5.23). The maximum number of APs simulated was 60, but since the curves appear to be moving into more stable regions of the graph as  $m$  increases, the upper value of  $m$  for stability is likely to be much higher than this. However the situation is quite different for  $n$ , which is limited by condition (5.23). For large  $m$  the maximum value of  $n$  is set by the ratio  $n/m < ((k + 1)\sqrt{2T} - 1)$ . Using typical values of  $k = 1$  and  $T = 30$ , the maximum number of contending users,  $n < 14.4m$ , a figure that is unlikely to be exceeded in a GPON residential environment. For small  $m$  the  $n/m$  limit improves (increases) since the second term of (5.23) now dominates. Finally, the convergence function can be incorporated into the equations (5.35) and (5.36) to give the CW sizes as follows,

$$C\hat{W}_{ap} = \left(1 + \frac{1 + 2\log_{10}m}{\sqrt{\bar{n}}}\right) \frac{2\hat{Q}}{\sqrt{(m + \bar{n})^2 + 2\hat{Q}} - (m + \bar{n})} \quad (5.45)$$

and,

$$C\hat{W}_{wu} = \left(1 + \frac{1 + 2\log_{10}m}{\sqrt{\bar{n}}}\right) \left(\frac{\bar{n}(C\hat{W}_{ap} - 1)}{km} + 2\right). \quad (5.46)$$

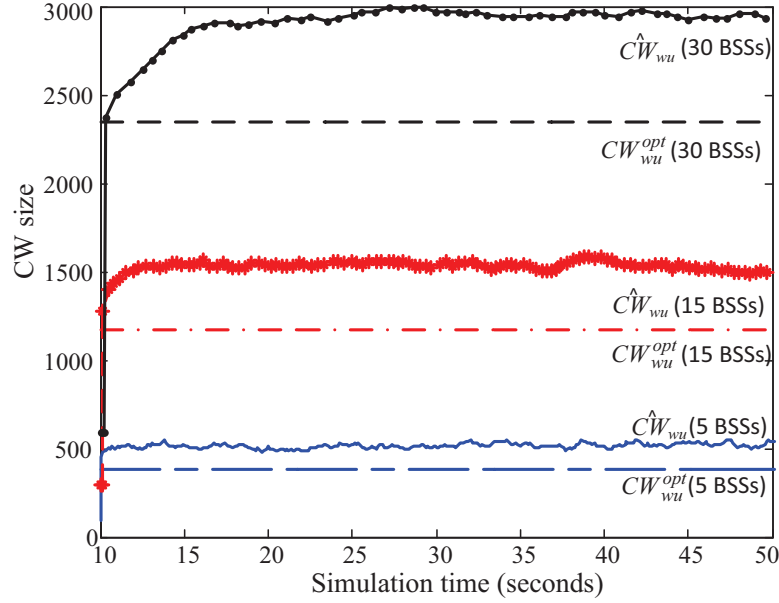


Figure 5.11: The convergence of  $\hat{C}W_{wu}$  toward  $CW_{wu}^{opt}$  of one station for 3 sizes of BSS

### 5.3 ATxPriority Performance

Fig. 5.11 illustrates the  $\hat{C}W_{wu}$  of one randomly selected station for simulation scenarios of 5 BSSs, 15 BSSs and 30 BSSs contending the channel. It is observed that all  $\hat{C}W_{wu}$  converge within 15 seconds. The  $\hat{C}W_{wu}$  for 5 BSSs converge almost instantaneously after the simulation starts. The converged values of  $\hat{C}W_{wu}$  are larger than the  $CW_{wu}^{opt}$  values by, 34%, 28% and 25% for 5 BSSs, 15 BSSs and 30 BSSs respectively; a combined effect of the convergence function and other approximations. The error percentages decrease as the size of BSSs increase due to the fact that the defined convergence function (5.44) is a decreasing one. However, as seen in Fig. 5.12, the overall system throughput of the proposed adaptive TxPriority (ATxPriority) scheme, only degrades by 3% compared to the TxPriority scheme.

Further, Fig 5.13 plots the cumulative distribution function (cdf) of all the WU stations'  $\hat{C}W_{wu}$  for 3 network sizes after the networks have converged. In common, the slopes of the obtained cumulative distribution functions are steep, corroborating

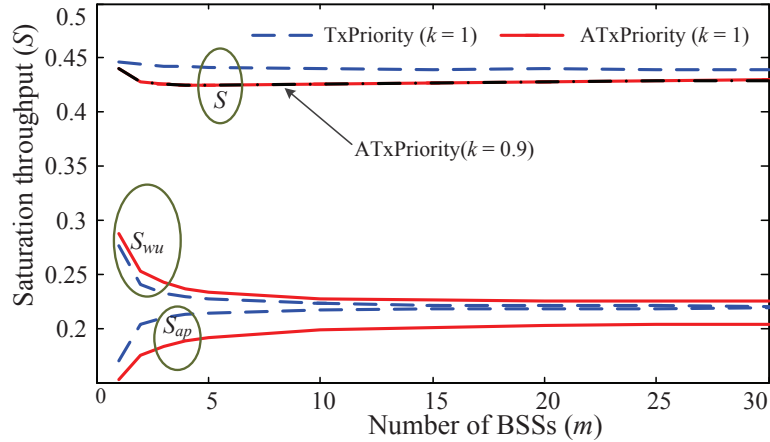


Figure 5.12: Comparison of normalized saturation throughput vs. number of BSSs between TxPriority and ATxPriority schemes.

the small standard deviations,  $\sigma_{C\hat{W}_{wu}}$ , of : 2.3%, 1.1% and 1.3% (relative to the measured means  $\mu_{C\hat{W}_{wu}}$ ) for 5 BSSs, 15 BSSs and 30 BSSs respectively. This leads to the conclusion that most WU stations within a network have an equal chance of transmission, thus, offering comparable fairness among all WUs.

Fig. 5.14 compares the measured transmission priority factor  $k_{mea}$  (UL/DL) of the ATxPriority scheme to the TxPriority scheme. A 10% reduction is observed. This is due to a higher degradation of the downlink throughput experienced by the ATxPriority scheme than its uplink throughput  $S_{wu}$ , as shown in Fig. 5.12. Equation (5.10) shows that the balance between the downlink throughput and the uplink throughput  $S_{wu}$  can be recovered by reducing the value of  $k$ . As illustrated in Fig. 5.14, a value of  $k = 0.9$  brings the measured transmission priority factor  $k_{mea} = 1$ . Nonetheless, the overall throughput of the ATxPriority remains unaltered (Fig. 5.12,  $k = 0.9$ ). Note the divergence at low BSS numbers in Fig. 5.12 and Fig. 5.14 is due to simplifications previously explained in Section 5.1.3

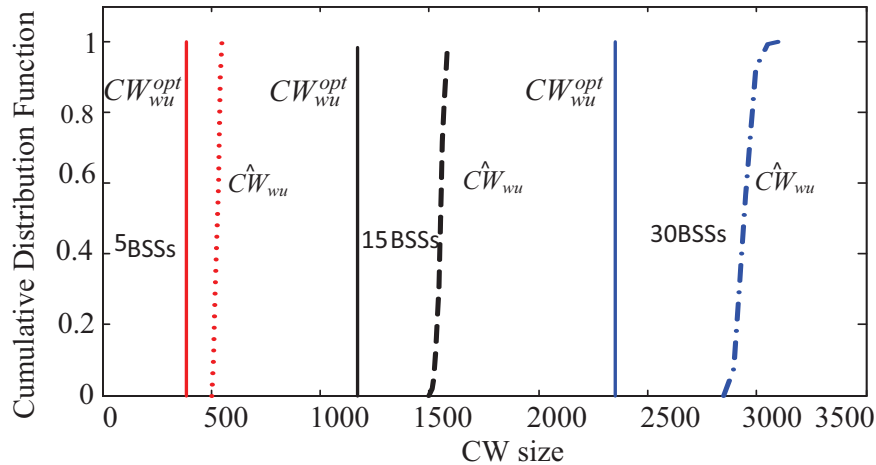


Figure 5.13: The cumulative distribution function of  $\hat{C}W_{wu}$  of contending WUs for three sizes of BSS after convergence.

## 5.4 Summary

The chapter proposes a transmission priority scheme with an adaptive backoff technique to enhance the WLAN performance of a Fi-Wi (GPON-WLAN) hybrid.

The TxPriority scheme introduces a transmission priority factor  $k$  to control the UL/DL fairness in multi-BSSs infrastructure WLAN networks. The optimum CW sizes for AP and WU are derived. Performance evaluations show that the TxPriority scheme is comparable in terms of overall throughput and delay to the adaptive window algorithm (AWA) developed for adhoc networks [60]. Nonetheless, it outperforms the legacy BEB scheme with 40% overall throughput improvement and a maximum 80% of delay reduction.

The adaptive backoff technique, ATxPriority, is introduced. This requires estimates of the number of APs ( $m$ ) and the number of WUs ( $n$ ). The first is directly estimated from GPON frame information and the second is estimated by measuring the activity on the WLAN channel. However, the studied behaviour of  $\bar{n}$  (estimate of  $n$ ) indicates that it does not converge to the correct value. Thus, a new convergence function,  $c(m, \bar{n})$ , is developed. Simulations show its robustness for practical values of

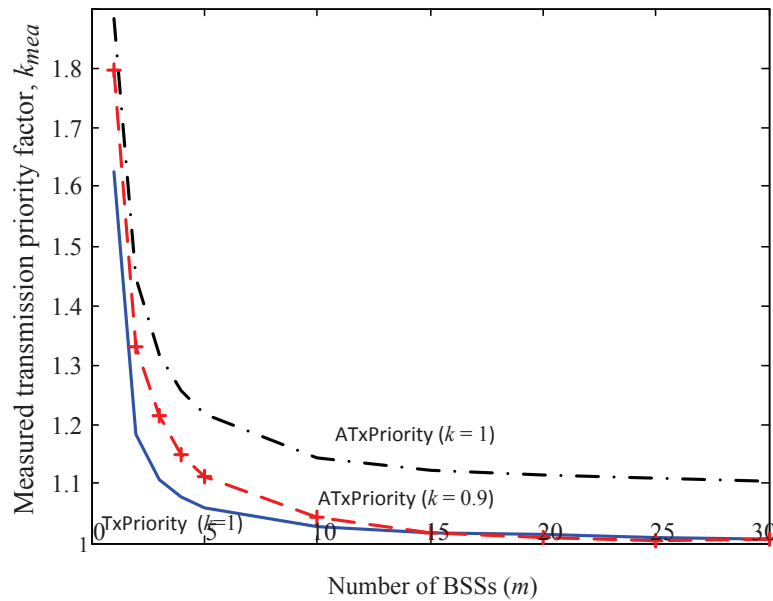


Figure 5.14: Comparison of the measured transmission ratio factor between TxPriority and ATxPriority schemes for different sizes of BSSs.

$k$ ,  $m$  and  $n$ ; but there is a small 3% reduction in overall throughput and a slight offset in  $k$ . The latter can be corrected by pre-compensation. The scheme shows uniform convergence among all WUs with a measured standard deviation of their CW sizes being less than 1.5%. The next chapter proposes an improved scheme which does not involve the intermediate step of estimating  $n$ .

# Chapter 6

## Transmission Priority Scheme using Idle Sense Method

This chapter proposes an improved transmission priority scheme that does not require the intermediate step of estimating number of WUs,  $n$ . Thus, avoiding any instability problems due to the inaccuracy of the estimate as described in the previous Chapter 5. The proposed method is realized using *Idle Sense* (IS) technique [67]. IS is a distributed control method for optimizing the contention window (CW) sizes of wireless stations in WLAN networks for maximum system throughput and fairness. Each station dynamically controls its CW size by monitoring the estimate number of idle slots between transmission attempts  $\hat{I}$  and comparing to a fixed target  $I_t$ .

IS is developed from the assumption that: minimizing time spent in the collision state and the contention state will maximize the throughput (Fig. 6.1). The probability of collision reduces as the contention time increases and vice versa. The optimum trade-off occurs when both times are equal [57]. Following [67] a cost function is formed

$$\begin{aligned} \text{Cost} &= \text{wasted time per transmission} \\ &= \frac{\sum \text{contention time} + \sum \text{collision time}}{\text{transmission time}}. \end{aligned} \tag{6.1}$$

$$Cost = \frac{\frac{T_c}{T_i} p_c + p_i}{p_s} \quad (6.2)$$

where  $p_i$  is the probability the slot is idle,  $p_s$  is the probability of successful transmission and  $p_c$  is the probability of collision;  $T_i$  is the slot time and  $T_c$  is the collision time (= transmission time + DIFS). The optimum number of idle slots per transmis-

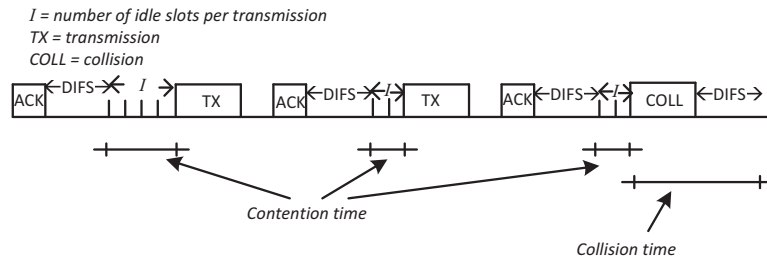


Figure 6.1: Non-productive (wasted) time.

sion is a function of the number of contending stations,  $n$ , but quickly converges to a constant as  $n$  goes to infinity. The converged value is used as the target ( $I_t$ ) for all stations irrespective of  $n$  values and it is defined from [67]

$$I_t = \frac{e^{-\Omega}}{1 - e^{-\Omega}} \quad (6.3)$$

The value for  $\Omega$  is obtained by numerically solving the first derivative of the cost function (setting to zero as  $n$  approaches  $\infty$ ):

$$1 - \Omega = \left(1 - \frac{T_i}{T_c}\right) e^{-\Omega} \quad (6.4)$$

where  $T_i$  and  $T_c$ , are functions of the MAC/PHY parameters for a given variant of the IEEE 802.11 WLAN standards.

Previous IS research assumed all stations have a similar CW size [67–70]. However, this assumption is not always valid in a practical deployment of WLAN. A station may have a larger CW size due to localized interference which only it can hear (e.g., a

bluetooth device or a microwave oven). Even when there is no interference, a station with no prior knowledge of channel history can contend the channel with significantly different CW size. Therefore, the chapter first investigates the robustness of the IS scheme in relation to varying CW sizes in an *ad hoc* network. The chapter then studies the robustness of the IS scheme when implemented in a multiple BSS Fi-Wi network incorporating the *Asymmetric Access Point* scheme of [69]. However, in the Fi-Wi network, an increase in the number of APs deteriorates the fairness between WUs, caused by the adjustment algorithm in IS. To overcome the problem, novel algorithms are proposed to achieve the desired fairness while maintaining maximum throughput.

The chapter is organized as follows. Section 6.1 describes the *Idle Sense* algorithm. Section 6.2 defines the bias in IS. Section 6.3 investigates the accuracy of  $\hat{I}$ . Section 6.4 identifies causes of the unfairness in IS and proposes a potential solution. Section 6.5 extends the idle sense method in multiple APs scenario and derives the optimum AP and WU contention window sizes. Section 6.6 evaluates the throughput performance of the proposed scheme when the WUs have different starting values of  $CW_{wu}$ . Section 6.7 studies the accuracy of  $\hat{I}$  with respect to the measurement period. Finally, Section 6.8 and 6.9 propose an AP self-adapting (APSA) and a WU adjustment (WUA) algorithms respectively to improve the fairness of the scheme.

## 6.1 Idle Sense

All stations in *Idle Sense* compare their estimated idle slots per transmission attempt  $\hat{I}$  with the target value  $I_t$  and adapt their CW size in a distributed manner using the additive increase multiplicative decrease (AIMD) algorithm. The initial proposal of IS in [67] applied AIMD to a transmission access probability  $p$ . However, the work in [68] observed that the method did not work well because a ceiling function is required to avoid  $p$  from becoming greater than 1. Thus, they proposed to directly apply AIMD

to the CW sizes. This avoided intermediate calculation of  $p$  and subsequently has become the standard adjustment algorithm for IS research [68–70].

```

/*Station observes I idle slots before transmission */
sum = sum + I;
trans = trans + 1 ;
if trans = M then
    /*Compute the estimate */
     $\hat{I} = \frac{sum}{M}$ ;
    sum  $\leftarrow$  0
    trans  $\leftarrow$  0
    /* Compare the estimate*/
    if  $\hat{I} < I_t$  then
        | CW = CW +  $\phi$ ;
    else
        | CW = CW(1 -  $\frac{1}{\psi}$ );
    end
    /*Adjust measurement period*/
    if  $|\hat{I} - I_t| < 0.75$  then
        | M =  $\frac{CW}{4}$ ;
    else
        | M  $\leftarrow$  5
    end
end

```

**Algorithm 1:** Full IS Algorithm ( $\phi = 6, \psi = 16, I_t = 3.26$  for IEEE 802.11a WLAN)

Estimating the number of idle slots per transmission,  $\hat{I}$ , involves continuously monitoring the channel over a number of transmit periods,  $M$ , which can be expressed as,

$$\hat{I} = \frac{\sum_{k=0}^M I_k}{M} \quad (6.5)$$

where  $I$  is the number of idle slots observed between two transmission attempts and  $M$  is the number of transmission attempts over which the measurement is taken.  $M$  determines the measurement uncertainty or variance in the estimate  $\hat{I}$  about its mean value,  $\bar{I}$ . The original work set  $M$  equal to 5 [67]. Despite fast convergence, the

shortcoming of using such a low value of  $M$  was inconsistent behaviour [68] caused by the large measurement variance. Note, when  $M$  is small a station can update its CW a number of times before it transmits itself, hence the fast convergence. To contend the channel, the station will use the current CW value for initialising its back-off counter.

As a solution to the large measurement variance, [68] refined the IS algorithm by making the value of  $M$  dependent on the accuracy of the estimate  $\hat{I}$ . If the difference between estimate  $\hat{I}$  and the target value  $I_t$  is within 0.75,  $M$  is increased to one quarter of the CW size, substantially reducing the measurement variance. Otherwise,  $M$  is maintained at 5 in order to speed up convergence when the estimate is clearly off target (algorithm 1). This dynamic adjustment of estimating period has become de facto in IS research [68–70].

## 6.2 Bias in Idle Sense Method

The AIMD principle of IS in [68] was applied directly to the CW. Stations additively increase their current CW by  $\phi$  slots when the channel is less idle ( $\hat{I} < I_t$ ) and multiplicatively decrease their CWs to  $CW(1 - \frac{1}{\psi})$  when the channel is more idle ( $\hat{I} > I_t$ ). The variable step size of the multiplicative decrement tends to force all stations to the same CW value. AIMD adjusts the CW in all subsequent IS works [69, 70].

$$CW_{new} = \begin{cases} CW_{old} - \frac{CW_{old}}{\psi} & \hat{I} > I_t \\ CW_{old} + \phi & \hat{I} < I_t \end{cases}, \quad (6.6)$$

In this section it is shown that the AIMD control algorithm becomes biased when the increment and decrement step sizes are not equal which can be proven as follows.

When the AIMD algorithm stabilises and CW sizes have converged to  $\overline{CW}$ , then

the long term reduction in CW size must equal the long term increment in CW size,

$$\begin{aligned}\phi U &= D \frac{\overline{CW}}{\psi} \\ \frac{U}{D} &= \frac{\overline{CW}}{\phi\psi}\end{aligned}\tag{6.7}$$

where  $U$  and  $D$  are the number of increments and decrements respectively. Therefore, the probability that a station decreases the CW size is given by,

$$P(\hat{I} > I_t) = \frac{D}{U + D} = \frac{\phi\psi}{\overline{CW} + \phi\psi}.\tag{6.8}$$

When the increment step size equals the decrement step size then  $\phi = \frac{\overline{CW}}{\psi}$ . From (6.8), it is clear that if  $\overline{CW} = \phi\psi$ , the station has reached the *equilibrium point*,  $\overline{CW}_{eq}$ , and obtained an equal chance of increasing or reducing the CW size. For example, following [68] to set  $\phi = 6$  and  $\psi = 16$  will result in  $\overline{CW}_{eq} = 96$ . When the *equilibrium point* occurs the median idle slot length  $I_{median} = I_t$ . If, as is normally the case,  $\bar{I} \approx I_{median}$ , then the mean idle sense value,  $\bar{I}$ , is operating close to the target,  $I_t$ , giving near optimum throughput. However, as the  $\overline{CW}$  increases above the equilibrium point (for example, due to an increased number of active stations), the decrementing step size ( $\overline{CW}/\psi$ ) is larger than the incrementing step size ( $\phi$ ) implying  $U > D$  when  $\overline{CW}$  reaches steady state. The probability of reduction  $P(\hat{I} > I_t)$  becomes less than 0.5 implying that the median  $I_{median}$  has reduced below  $I_t$  (or  $I_{median} < I_t$ ).  $I_{median}$ , and therefore  $\bar{I}$ , is biased away from the target value,  $I_t$ . The system is now operating at a slightly higher transmission probability per slot ( $P_{tr}$ ) and is no longer optimum for maximum throughput.

The bias in  $\bar{I}$  is dependant on  $\overline{CW}$  which, in turn is dependant on the number of active stations contending the channel, a variable quantity. In the next section, the estimation parameter which affects the accuracy of estimate  $\hat{I}$  is investigated.

### 6.3 The Accuracy of $\hat{I}$

An analysis is carried out to investigate the effect of  $M$  on the accuracy of the estimate. The estimation process is denoted as a negative binomial experiment considering the fact that the idle slots are measured until the number of transmission attempts reaches  $M$ . The  $x$  number of slots to produce  $M$  transmission attempts is the negative binomial random variable with probability distribution given by [104],

$$b^*(x; M, P_{tr}) = \binom{x-1}{M-1} (P_{tr})^M (1 - P_{tr})^{x-M} \quad (6.9)$$

where  $P_{tr}$  is the transmission probability. If there are  $n$  stations contending the channel,

$$P_{tr} = 1 - \left(1 - \frac{2}{\overline{CW} + 1}\right)^n \quad (6.10)$$

and  $(1 - P_{tr})$  is the probability that there is no transmission which indicates that the slot is idle. Intuitively, (6.9) can also be defined as a probability distribution of having  $(x - M)$  idle slots,

$$P(I \leq \frac{X - M}{M}) = \sum_{x=M}^X b^*(x; M, P_{tr}). \quad (6.11)$$

Fig. 6.2 compares the cumulative distribution function (cdf) of the average idle slots per transmission  $I$  for  $M = 5$  and  $M = 100$ . The difference between  $I_{median}|_{M=5}$  and  $\bar{I}$  is clearly visible for  $M = 5$ , but disappears as  $M$  increases as indicated by the  $M = 100$  curve. More importantly, the accuracy of the estimate increases as the mean estimate,  $\bar{I}|_{M=100}$ , is closer to the target value  $I_t$  (reduced bias) compared to  $\bar{I}|_{M=5}$ . Also, the increased slope indicates a lower variance between stations. Throughput and fairness is improved. The increased  $\bar{I}|_{M=100}$  suggests stations are contending the channel less and operating with increased  $\overline{CW}$  size and therefore from (6.8) the

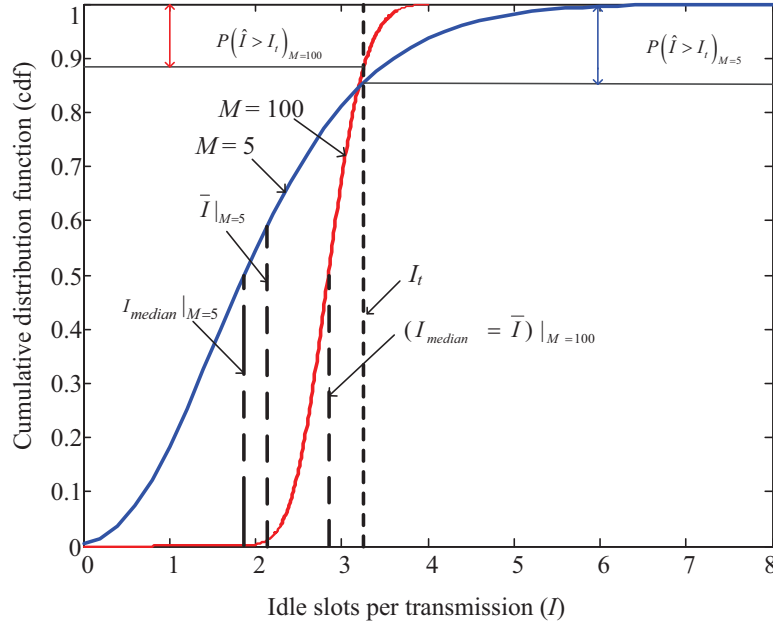


Figure 6.2: The cumulative distribution function of  $I$  when 100 stations contend the channel using the IS scheme ( $\phi = 6$  and  $\psi = 16$ ) in an adhoc network scenario with  $I_t = 3.26$ ,  $M = 5$  (blue) and  $M = 100$  (red).

probability of decreasing the CW size  $P(\hat{I} > I_t)_{M=100}$  is also reduced.

The above analysis clearly underpins the rational of using an adaptive  $M$  to give fast convergence followed by accurate estimates as per algorithm 1.

The following section demonstrates how the accuracy of  $\hat{I}$  affects the fairness between contending stations

## 6.4 Fairness Analysis

In IS [67–69], all contending stations use AIMD and select  $M$  as per algorithm 1. Importantly, they also assumed all stations have *similar* CW sizes. They try to reach the target value  $I_t$  and set the transmission probability to the target value  $P_{tr_t}$  given that,

$$I_t = \frac{1 - P_{tr_t}}{P_{tr_t}}. \quad (6.12)$$

Hence, from (6.10), the CW sizes of all stations should converge to the target  $CW_t$  value,

$$CW_t = \frac{2}{1 - (1 - P_{tr_t})^{\frac{1}{n}}} - 1. \quad (6.13)$$

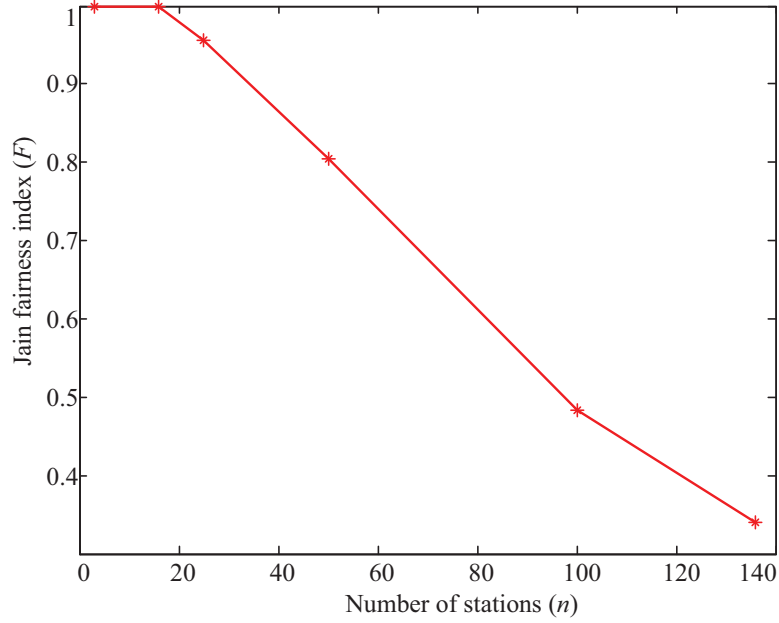


Figure 6.3: The Jain fairness index (6.14) vs. number of stations. All contending stations operate in a full IS scheme ( $\phi = 6$  and  $\psi = 16$ ) [68, 69].

Now, consider the behaviour of the IS algorithm when stations have *different* CW sizes. Ideally, by means of the IS algorithm, the CW sizes of all stations should converge to (6.13) irrespective of their initial CW states. However, our simulations show that as the number of stations increase, the CW sizes do not converge to  $CW_t$  and consequently degrade the fairness of channel utilization between all stations as depicted in Fig. 6.3. The Jain fairness index  $F$  defined in [105] is used, where,

$$F = \frac{(\sum_{i=0}^n \frac{2}{CW_{i+1}})^2}{n \sum_{i=0}^n (\frac{2}{CW_{i+1}})^2}. \quad (6.14)$$

The range of  $F$  lies within 0 to 1, the value closer to 1 implies better fairness

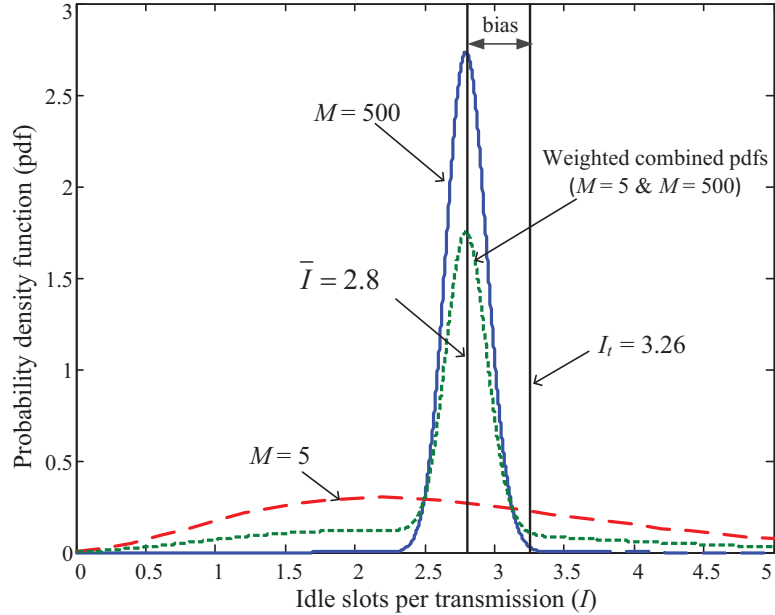


Figure 6.4: The probability distribution functions (pdfs) of  $I$  for 2 classes of stations, employing IS scheme ( $\phi = 6$  and  $\psi = 16$ ) with  $M = 5$  and  $M = 500$  respectively. The channel is set to operate with  $\bar{I} = 2.8$ .

performance. It is interesting to note that the problem only shows when the number of stations,  $n > 18$ . The IS authors in [68, 69] only simulated up to 20 stations and therefore missed the problem.

The poor fairness index is perceived because there exist two extreme classes of contending stations in the network. As an example, a system with two classes of stations is considered: one class with a small  $\overline{CW}$  operating with  $M = 5$  and a second class with large  $\overline{CW}$  operating with  $M = 500$ . In this example both classes of stations are contending the same channel (operating with  $\bar{I} = 2.8$ ) and periodically adjusting their  $CW$  sizes to allow the channel to reach the target value of  $I_t = 3.26$ . Fig. 6.4 shows the probability distribution function (pdf) plots for both classes of stations using (6.9). Stations with  $M = 500$  will estimate  $\hat{I}$  with accuracy as indicated by the narrow pdf (solid line). It is expected that the pdf curve will become even

narrower as  $M$  increases because it gives a longer estimation period and subsequently improves the accuracy of the estimate. Note that  $P(\hat{I} > I_t)$  of this pdf is almost zero denoting the stations have minimum chance to reduce their CW sizes. Conversely, they keep on incrementing their CW sizes as almost the whole pdf falls in  $P(\hat{I} < I_t)$  region. Consequently,  $M$  is increased, narrowing further the pdf( $I$ ) and making a reduction in CW even less likely. This positive feedback means the station will lose any chance to transmit at all. On the contrary, stations with  $M = 5$  have a wider pdf spread (dashed line) implying less accuracy in their estimate and causing  $P(\hat{I} > I_t)$  to be much higher than when  $M = 500$ . Therefore, this class of station has more chance to reduce their CW size and thus gain more transmission opportunities to hog the channel. The curve with dotted line in Fig. 6.4 is the weighted pdf of both classes to resemble the pdf of the overall network. It is assumed 60% of stations use  $M = 500$  while 40% use  $M = 5$ . The area under the dotted curve in the right tail ( $P(\hat{I} > I_t)$ ) gives the probability of decrements which was analytically derived in (6.8).

Fig. 6.5 shows the cdf of CW to demonstrate the behaviour of 136 stations that contend the channel using the IS scheme in an adhoc WLAN scenario. It is observed that the studied behaviour is consistent with the example in Fig. 6.4. At the beginning of the simulation ( $t = 0$  second) every station contends the channel with a CW size randomly chosen within the range  $(16, 2CW_t)(CW_{init}$ , blue line). After 50 seconds, the CW sizes of all stations do not converge to the common value but diverge from their initial values and create 2 classes of CW sizes (i.e., the first class dominates most of the channel bandwidth while the second class starves)( $CW|_{50secs}$  (full IS), blue dot-dashed line). As time approaches 100 seconds, the gap between the two classes of CW sizes widens, anticipating the instability of the scheme and deteriorating the fairness between all stations ( $CW|_{100secs}$  (full IS), blue dashed line).

Nevertheless, it is interesting to note that this problem does not occur for a smaller network scenario (i.e,  $n < 20$ ) as it maintains a fairness index close to 1, shown in

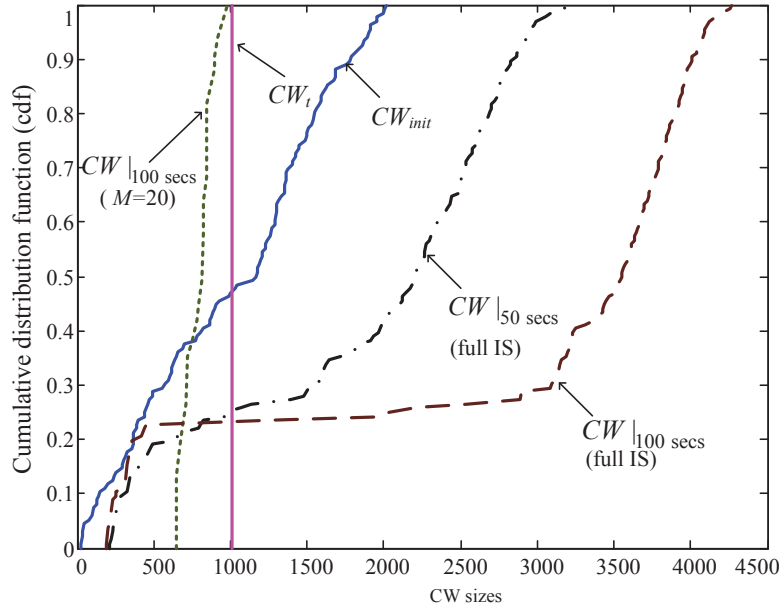


Figure 6.5: The cumulative distribution function of CW with 136 contending stations. OPNET simulation conditions: data frames of 8184 bits, full IS scheme ( $\phi = 6$  and  $\psi = 16$ ) [68, 69] in an adhoc IEEE 802.11a WLAN network, data rate of 54 Mbps and control rate of 6 Mps.

Fig. 6.3. This is because when the number of contending stations is small, the CW sizes of all stations converge to a relatively small  $\overline{CW}$  (as defined in (6.13)) which is close to the *equilibrium point* ( $\overline{CW}_{eq} = 96$ ). At this state, the bias is minimal. Fig. 6.6 shows the cdf of CW sizes for  $n = 16$  contending stations. It clearly shows that all stations converge to  $CW|_{100secs} = 111$ , close to the target ( $CW_t = 119$ ) even though their initial  $CW_{init}$  sizes were randomly selected over a very wide range of values ( $16, 20CW_t$ ) (blue line). Therefore, all stations gain optimum throughput and fairness.

The fairness problem in the IS scheme arises due to the combined effects of a bias in the AIMD algorithm and the varying length of  $M$ . Alternatively fairness can be improved by using a fixed value for  $M$  similar to [67] while keeping the CW based

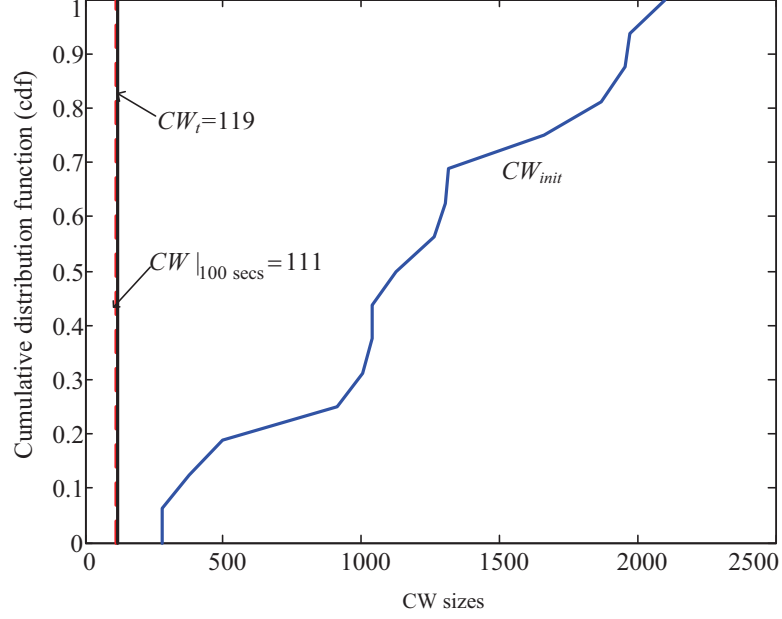


Figure 6.6: The cumulative distribution functions of CW when 16 stations contend the channel using full IS scheme ( $\phi = 6$  and  $\psi = 16$ ). (OPNET simulation conditions as per in Fig. 6.5)

AIMD algorithm as in [68,69]. The pdf( $\hat{I}$ ) is now the same for all stations. The probability of decrementing their CW's is therefore equal enabling all to converge to the common value irrespective of their initial values,  $CW_{init}$ . The solution is validated by setting  $M = 20^1$  for the traffic scenario described in Fig. 6.5. The  $CW|_{100sec}(M = 20)$  line (dotted) indicates stability with a well confined distribution having a mean value approximately 20% below the  $CW_t$ . The variation in CW translates to satisfactory fairness value between WUs of  $F = 0.985$ .

The results above apply to an adhoc WLAN network. The next section will extend the IS method to an infrastructure network with multiple BSSs, resembling the wireless side of a Fi-Wi network.

<sup>1</sup>the choice of M is further discussed in Section 6.7

## 6.5 *Idle Sense* with Transmission Priority in Multiple BSSs WLAN

The analysis is carried out by combining the principles of *Idle Sense* [67, 68] and *Asymmetric Access Point* [69] with the aim to give the APs priority bandwidth which is  $1/k$  time bigger than the WUs. The remaining bandwidth is thus shared by all WUs in a fair manner. Consider  $m$  APs and  $n$  WUs contending the WLAN channel with contention window sizes of  $CW_{ap}$  and  $CW_{wu}$  respectively. The same network scenario as described in the preceding Section 5.1 is assumed.

The optimum CW sizes for an AP and a WU are derived by first defining the probability of an idle slot (i.e., no transmission on the channel) as,

$$\begin{aligned} p_i &= (1 - p_{wu})^n (1 - p_{ap})^m \\ &\approx (1 - p_{wu})^n \left( \frac{km}{np_{wu} + km} \right)^m. \end{aligned} \quad (6.15)$$

where

$$1 - p_{ap} = \frac{km}{np_{wu} + km} \quad (6.16)$$

and (6.16) is obtained from

$$\frac{p_{ap}}{1 - p_{ap}} = \frac{np_{wu}}{km(1 - p_{wu})} \approx \frac{np_{wu}}{km}. \quad (6.17)$$

which is rearranged from (5.10) under condition  $\frac{p_{wu}}{1 - p_{wu}} \approx p_{wu}$ .

According to [69], when all contending stations  $n$  use *Idle Sense* with the access probability  $p$ , the number of idle slots between two transmissions is kept constant so that the probability of an idle slot  $p_i$  also remains constant. Thus, *Idle Sense*

maintains  $np = \Omega$  with  $\Omega$  being some constant and as  $n \rightarrow \infty$ ,

$$\begin{aligned} p_i^{opt} &= \lim_{n \rightarrow \infty} (1 - p)^n \\ &= \lim_{n \rightarrow \infty} \left(1 - \frac{\Omega}{n}\right)^n \\ &\approx e^{-\Omega}. \end{aligned} \tag{6.18}$$

In this studied scenario, only wireless users (WUs) use *Idle Sense*. The probability of an idle slot remains  $p_i^{opt} \approx e^{-\Omega}$ , and the access probability of WUs  $p_{wu}$  is such that  $np_{wu} = \beta$ , where  $\beta$  is another constant. Then, similar to (6.18),

$$\begin{aligned} \lim_{n \rightarrow \infty} (1 - p_{wu})^n &= \lim_{n \rightarrow \infty} \left(1 - \frac{\beta}{n}\right)^n \\ &\approx e^{-\beta}. \end{aligned} \tag{6.19}$$

Using (6.18) and (6.19) in (6.15) leads to

$$\Omega = \beta - m \ln(km) + m \ln(\beta + km). \tag{6.20}$$

The value for  $\beta$  can be obtained by numerically solved (6.20). The value of  $k, m^2$ , and  $\Omega^3$  are known. Then, from (6.16),

$$p_{ap} = \frac{\beta}{\beta + km} \tag{6.21}$$

and from (5.4),

$$CW_{ap} = \frac{2(\beta + km)}{\beta} - 1. \tag{6.22}$$

---

<sup>2</sup>The variable  $m$  can be estimated from the GPON frame format information as suggested in Subsection 2.3.1.

<sup>3</sup>The constant  $\Omega$  can be obtained by solving  $1 - \Omega = (1 - \frac{T_i}{T_c})e^{-\Omega}$ , a minimized cost function derived in [67].

Further, as stated before  $np_{wu} = \beta$ , then,

$$p_{wu} = \frac{\beta}{n} \quad (6.23)$$

and from (5.5),

$$CW_{wu} = \frac{2n}{\beta} - 1. \quad (6.24)$$

All variables in the CW size formulations above are assumed known and the required MAC and PHY parameters are listed in Table 5.2.

The derived formulations are validated in terms of saturation throughput. Bianchi's model in [48] is used to analyse the normalized saturation throughput,  $S$ . Refer to Appendix A for a full derivation of (6.25).

$$S = \frac{P_s P_{tr} T_{payload}}{(1 - P_{tr})T_i + P_s P_{tr} T_s + (1 - P_s)P_{tr} T_c} \quad (6.25)$$

where  $T_{payload}$  is the average time taken to transmit the payload,  $T_i$  is the idle slot time defined in the IEEE 802.11 standard [43],  $T_s$  is the average time the channel is sensed busy by each station due to a successful transmission and  $T_c$  is the average time the channel is sensed busy by each station due to a collision. The values of  $T_s$  and  $T_c$  solely depend on PHY and MAC layers parameters (defined in IEEE 802.11 standard as listed in Table 5.2) which can be expressed as,

$$T_s = T_{payload} + SIFS + T_{ACK} + DIFS \quad (6.26)$$

and

$$T_c = T_{payload} + DIFS \quad (6.27)$$

Table 6.1:  $CW_{ap}^{opt}$  (6.22) and  $CW_{wu}^{opt}$ (6.24) for varying sizes of BSSs.

$m$	$n$	$CW_{ap}$	$CW_{wu}$
1	4	16	57
2	8	30	117
3	12	45	176
4	16	60	236
5	20	75	296
10	40	150	595
15	60	225	894
20	80	299	1193
25	100	374	1492
30	120	449	1791

In addition, the uplink throughput  $S_{wu}$  and the downlink throughput  $S_{ap}$  are expressed as follows,

$$S_{wu} = \frac{P_s^{wu} P_{tr} T_{payload}}{(1 - P_{tr})T_i + P_s P_{tr} T_s + (1 - P_s)P_{tr} T_c} \quad (6.28)$$

and,

$$S_{ap} = \frac{P_s^{ap} P_{tr} T_{payload}}{(1 - P_{tr})T_i + P_s P_{tr} T_s + (1 - P_s)P_{tr} T_c}. \quad (6.29)$$

The throughputs are computed analytically using (6.25), (6.28) and (6.29) when every station employs a fixed value of  $CW_{ap}^{opt}$  and  $CW_{wu}^{opt}$  derived in (6.22) and (6.24) respectively. All variables in CW size formulations are assumed known in order to obtain the ideal throughputs, known as target throughput. Table 6.1 presents the optimal CW sizes for APs and WUs as the number of BSSs increases from 1 to 30 with the value of  $k$  sets to 1. Similar with the previous chapter, the WLAN operates in the IEEE 802.11a standard and every AP in each BSS serves 4 WUs.

Fig. 6.7 shows the target (theoretical) throughputs ( $S$ ,  $S_{wu}$  and  $S_{ap}$ ) when the

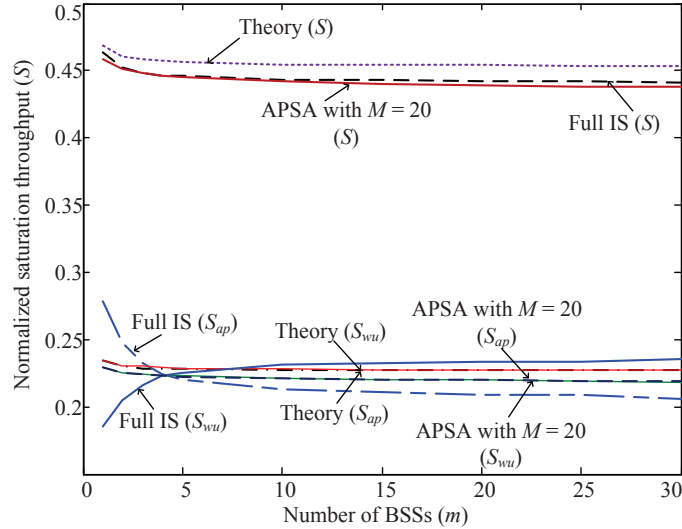


Figure 6.7: Normalized saturation throughput vs.  $m$ , number of BSSs (simulation and theory).

number of BSSs increases. The overlaid curves  $S_{wu}$  and  $S_{ap}$  are expected for  $k = 1$ .

## 6.6 Throughput Performance

This section evaluates the throughput performance of the proposed scheme when the WUs have different starting values of  $CW_{wu}$ . The WUs adaptively adjust their CW sizes using the *Idle Sense* algorithm while the APs fix their CW sizes to  $CW_{ap}^{opt}$  as computed in Table 6.1.

All WUs in IS compare their estimated idle slots per transmission attempt  $\hat{I}$  (6.5) with the target value  $I_t$  and adapt their  $CW_{wu}$  in a distributed manner using the additive increase multiplicative decrease (AIMD) algorithm. Based on the formulation derived in [67], the predefined target value  $I_t$  is set to 3.26 (in accordance to MAC and PHY IEEE 802.11a parameters, Table 5.2).

Fig. 6.7 indicates that the obtained total throughput  $S$  is within 97% of the target throughput when the WUs use IS as their adaptation mechanism. Furthermore, it

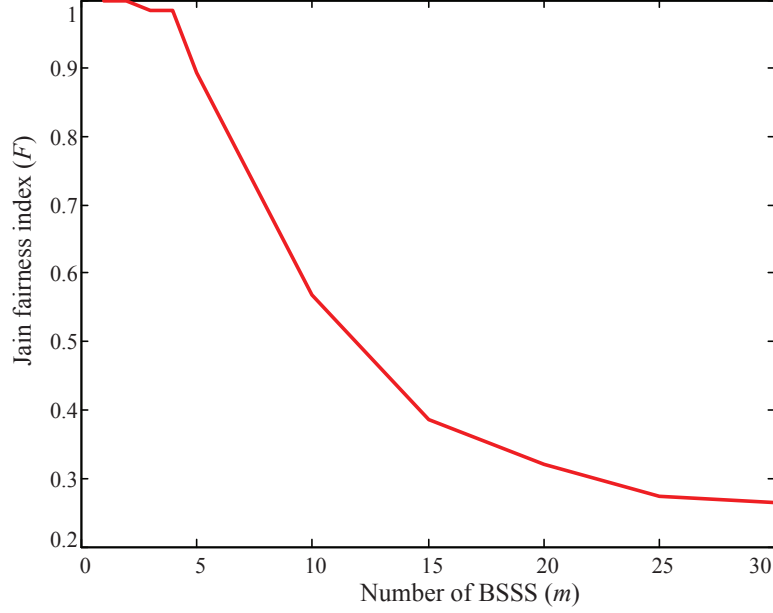


Figure 6.8: The Jain fairness index (6.14) vs.  $m$ , the number of BSSs. All WUs use full IS while the APs fixed  $CW_{ap}^{opt}$  as derived in (6.22)

is also observed that when the number of BSSs increase, the DL throughput  $S_{ap}$  is approximately 8% lower than its target throughput whereas the UL throughput  $S_{wu}$  is about 3% higher than its target throughput. Therefore, the resultant  $S_{wu}/S_{ap}$  ratio  $k_{mea}$  is nearly 8% lower than the target  $k$ . Overall, the obtained results are comparable to the respective target values with a minor difference, which is not significant, most probably resulted from the effect of the AIMD algorithm as discussed in Section 6.4.

However, it is surprising to note that the fairness in channel utilisation,  $F$ , deteriorates as the number of BSSs grows dropping below 0.5 when  $m \geq 12$  (Fig. 6.8). Similar to the adhoc case of Section 6.4, the figure shows that good fairness is only possible when the network size is small; ( $m \leq 5$ ).

According to the principle of IS, all contending stations, using the IS scheme, are trying to reach the target value  $I_t$  and set their transmission probabilities to the target  $P_{tr_t}$  given by (6.12)

Hence, from (5.6), the CW sizes of all WUs will ideally converge to the target value.

$$CW_{wu}^{opt} = \frac{2}{\left(\frac{1-(1-P_{irr_t})}{(1-CW_{ap}^{opt}+1)^m}\right)^{\frac{1}{n}}} - 1, \quad (6.30)$$

irrespective of their initial  $CW_{wu}$  states. However this is not always the case as shown next. When the network is large (large  $m$ , large  $n$ ), every WU adapts to a different value of CW as illustrated in Fig. 6.9. The figure shows the cdf of  $CW_{wu}$  for a network with  $m = 30$  APs having fixed  $CW_{ap}^{opt}$ , and  $n = 120$  WUs contending the channel using the IS scheme. At the beginning of the simulation ( $t = 0$  second) every WU contends the channel with a  $CW_{wu}^{init}$  size randomly chosen within the range  $(16, 2CW_{wu}^{opt})$ . After 50 seconds, the CW sizes of all WUs do not show any sign that they will converge to the common value but diverge away from the initial states. Finally, as time approaches 100 seconds, 2 classes of CWs are created where the first class dominates most of the channel bandwidth while the second class starves. The instability and poor fairness is similar to the adhoc case of section 6.4.

Despite the fact that one class of the WUs are starving and gaining poor throughput,  $S_{wu}$  does not deteriorate as it is supported by another class of WUs which hog the channel. Therefore, the resultant  $k_{mea}$  is still close to the target value and the channel utilization remains unaffected by the instability of the IS scheme. It is worth noting that the resultant  $S_{ap}$  also remains unaffected because all the APs use a fixed CW size.

## 6.7 The Choice of $M$

Similar to the study of adhoc WLANs (i.e., with  $m = 0$ ) in the preceding Section 6.4, the fairness problem between WUs using IS in multiple BSSs is due to the combined effects of a bias in the AIMD algorithm, and the varying sensing length,  $M$ , among

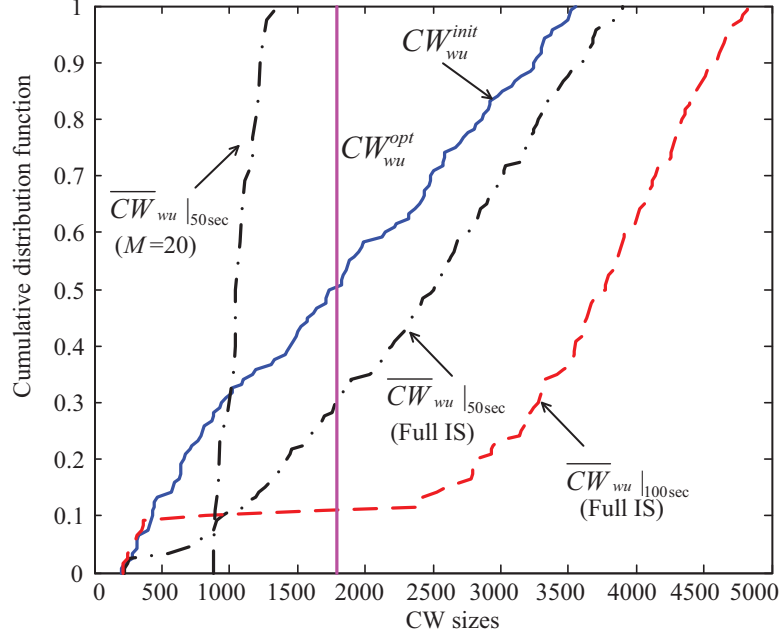


Figure 6.9: The cumulative distribution function of  $CW_{wu}$  with 120 WUs (from 30 BSSs) contending stations.

stations. Fixing  $M$  to a constant value will remove the instability in CW and improve fairness as demonstrated by the  $\overline{CW}_{wu|50sec}(M=20)$  line in Fig. 6.9 for  $M=20$ .

Table 6.2 summarizes the comparison between different values of  $M$  ( $M=5$ ,  $M=20$  and  $M=1000$ ) pertaining to their performance metrics. As expected the accuracy of the estimate  $\hat{I}$  increases with  $M$ . The mean of the estimate  $\bar{I} (= E(\hat{I}))$  for  $M=1000$  is within 4.6% of the target value,  $I_t$ , compared to 39% for  $M=5$ . It is also observed that lower  $\bar{I}$  estimates cause the  $CW_{wu}$  sizes to converge to lower than optimum values giving the WUs more chances to transmit. As a result, the  $S_{wu}$  increases and deteriorates the fairness between DL and UL transmissions. Note that  $CW_{ap}$  remains fixed. For example, with  $M=5$  resulted in  $\overline{CW}_{wu} = 862$  some 52% lower than target. Thus, allowing the WUs to gain higher throughput ( $S_{wu} = 0.293$ , 28% higher than target) and worsen the fairness between DL and UL as indicated by the 115% increase in  $k_{mea}$  to 2.15. Moreover, the reduction in  $\overline{CW}_{wu}$

Table 6.2: Performance comparison for  $M = 5, 20$  and 1000

$M$	5	20	1000	Target
$\bar{I}$	1.95	2.34	3.11	3.26
$\overline{CW}_{wu}$	862	1138	1677	1791
$S$	0.43	0.438	0.442	0.454
$S_{ap}$	0.137	0.168	0.213	0.227
$S_{wu}$	0.293	0.271	0.229	0.227
$k_{mea}$	2.15	1.61	1.08	1
Convergence time (s)	1.42	5.79	297.51	0

causes increased collisions which degrades the overall throughput by 5%; somewhat less than anticipated considering the almost halving of the  $\overline{CW}_{wu}$ .

Conversely, setting  $M = 1000$  improves all metrics.  $\overline{CW}_{wu}$  converges to within 7% of the optimum target value, and the fairness between UL and DL is significantly improved ( $k_{mea} = 1.08$ ), to within 8% of its target value.

In spite of higher  $M$  giving better performance, it requires a longer time to converge. The comparison summary in Table 6.2 reveals that the convergence time is directly proportional to  $M$ . For example, the convergence time for  $M = 1000$  is about 200 times longer than  $M = 5$ . Clearly, the benefits of better performance are offset by the downside of longer convergence time. Therefore, in this work,  $M = 20$  is chosen as a good compromise value. Although the fairness,  $k$ , is much improved (c.f.  $M = 5$ ), it is still 61% away from the designed value. In the following section, an alternative algorithm is proposed to improve the fairness without jeopardizing the convergence time.

## 6.8 AP Self-adapting algorithm

This section proposes the AP Self-Adapting (APSA) algorithm to assist the network to achieve the desired  $k$ . This approach requires every AP in the network to monitor the measured  $S_{wu}/S_{ap}$  ( $= k_{mea}$ ) in its respective BSS by counting the number of successfully transmitted packets,  $P_d$  (forming the DL throughput  $S_{ap}$ ) and the received packets,  $P_u$  (forming the UL throughput  $S_{wu}$ ). Each AP periodically adjusts its  $CW_{ap}$  after every  $P_{set}$  transmissions so that the observed  $k_{mea}$  will reach the desired  $k$ .

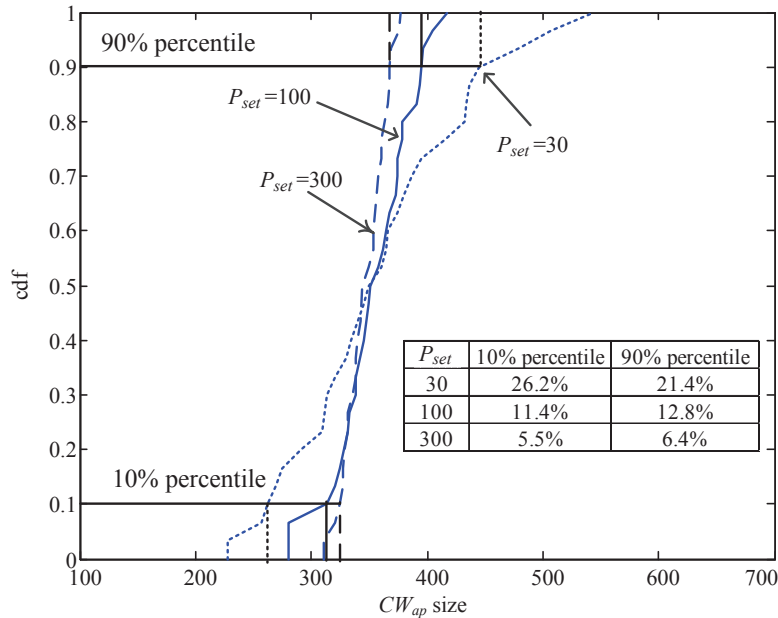


Figure 6.10: The cumulative distribution function of  $CW_{ap}$  with 120 WUs (from 30 BSSs) contending stations for different  $P_{set} = 30, 100$  and  $300$  ( $k = 1$  and  $\alpha = 1$ ).

The AP alters its CW size by  $\delta$  where,

$$\delta = \frac{P_u - k * P_d}{\max(k * P_d, P_u)} CW_{ap} \quad (6.31)$$

to equalize the discrepancy between  $k_{mea}$  and  $k$ . In order to provide a smoother behaviour of the obtained CW size, a smoothing factor  $\alpha$  is weighted into  $\delta$  where

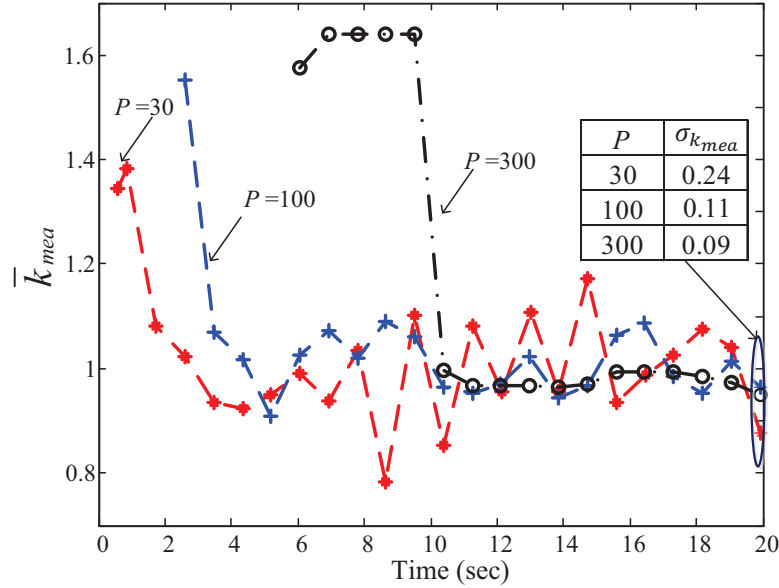


Figure 6.11: The convergence time for one AP in the network with 30 BSSs to reach the desired  $k = 1$  for different  $P_{set} = 30, 100$  and  $300$  with  $\alpha = 1$ .

$0 < \alpha \leq 1$ . Algorithm 2 describes APSA formally.

$$CW_{ap} = CW_{ap} + \alpha\delta \quad (6.32)$$

Next, the network performance is evaluated when the modified IS ( $M = 20$ ) and APSA schemes are incorporated together.  $P_{set}$  is a compromise between accuracy and convergence time, similar to  $M$  in the previous section. Fig. 6.10 shows the cdf of  $CW_{ap}$  for a system of 30 APs after convergence. The variation in  $CW_{ap}$  is directly attributed to the accuracy of estimating  $k_{mea}$  and hence  $P_{set}$ . The simulations show 80% of access points have CW's within  $\pm 6\%$ ,  $\pm 12\%$  or  $\pm 24\%$  of the mean value of  $\overline{CW}_{ap} = 348$  for  $P_{set} = 300, 100, 30$  respectively. A similar trend is shown for the deviation in  $k_{mea}$  after it has reached convergence (Fig. 6.11 table of  $\sigma_{k_{mea}}$ ). The convergence time however increases with  $P_{set}$  and is dominated by the time it takes

```

while active do
  if DATA received then
    |  $P_u = P_u + 1;$ 
  end
  if DATA transmitted then
    |  $P = P + 1;$ 
    if ACK received then
      |  $P_d = P_d + 1;$ 
    end
  end
  if  $P = P_{set}$  then
    |  $\Delta = (P_u - k * P_d) ;$ 
    |  $\delta = \frac{P_u - k * P_d}{\max(k * P_d, P_u)} CW_{ap};$ 
    |  $CW_{ap} = CW_{ap} - \alpha \delta ;$ 
    |  $P \leftarrow 0$ 
    |  $P_u \leftarrow 0$ 
    |  $P_d \leftarrow 0$ 
    |  $\delta \leftarrow 0$ 
  end
end

```

**Algorithm 2:** APSA Algorithm

to the first estimates as indicated by the waiting time before the starting transient. Once convergence starts it is generally fast and accurate. Here  $P_{set} = 100$  is chosen as 10 seconds convergence time is too long with  $P_{set} = 300$  and the spread of  $\pm 24\%$  in  $CW_{ap}$  is too large when  $P_{set} = 30$ .

Fig. 6.7 shows that the APSA algorithm exactly balances  $S_{wu}$  and  $S_{ap}$  when  $k = 1$ , irrespective of network size,  $m$ . Nonetheless, the 2.6% throughput degradation (relative to target) remains almost unchanged caused by the choice of  $M = 20$  in the IS section of the algorithm.

A corollary of the APSA algorithm was that the AP's  $CW_{ap}$  size was no longer fixed which might affect their fairness. Therefore, the fairness between APs is measured using (6.14) for different number of BSSs, with targets of  $k = 0.5, 1$  and  $2$ . Interestingly, it is apparent from the plots in Fig. 6.12 that the impact of APSA on

the fairness between APs is minimal as the measured  $F$  is maintained above 0.98 for all network scenarios in this study.

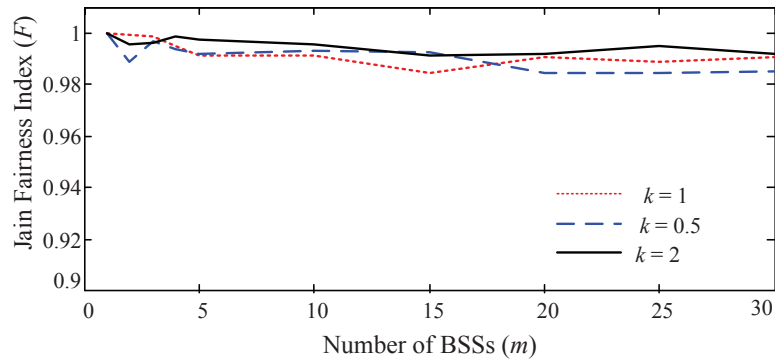


Figure 6.12: The fairness between 30 APs for networks with  $k = 0.5, 1$  and  $2$ .

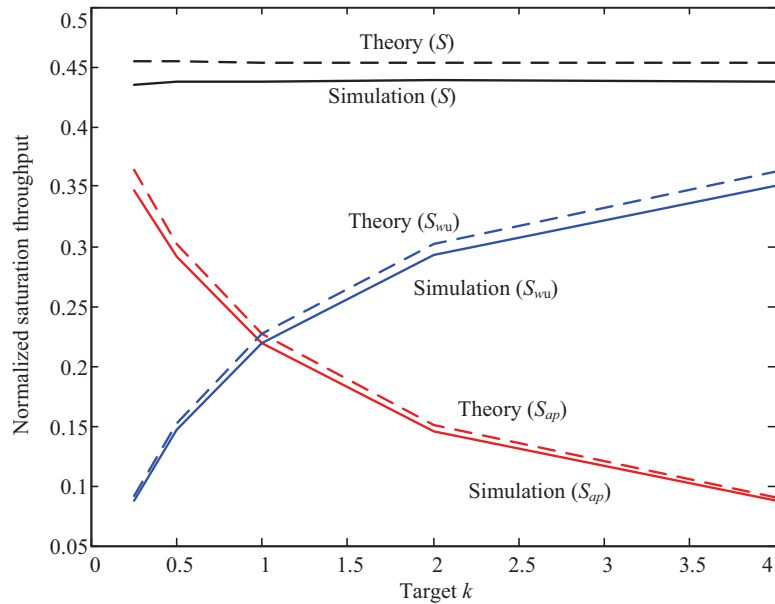


Figure 6.13: The normalized saturation throughputs (total, DL and UL) for 30 BSSs network scenario as the network's target  $k$  varies from 0.25 to 4.

Fig. 6.13 depicts the throughput performance of 30 BSSs when the target  $k$  varies from 0.25 to 4. It is evident that throughputs  $S_{ap}$  and  $S_{wu}$  are within 4% of the theoretical optimum, indicating  $k_{mea}$  also remains close to the set priority factor  $k$ .

Thus the APSA algorithm can handle a wide range of  $m$  and  $k$ .

Table 6.3: Equilibrium throughput for 5 BSSs having different target  $k$

		IS and APSA			IS,APSA and WUA		
$k$	$n^j$	$S_{ap}$	$S_{wu}$	$S$	$S_{ap}$	$S_{wu}$	$S$
1	4	0.039	0.039	0.078	0.044	0.045	0.089
1	4	0.039	0.038	0.077	0.044	0.045	0.089
0.5	4	0.078	0.039	0.117	0.059	0.029	0.088
0.5	4	0.078	0.039	0.117	0.059	0.029	0.088
2	4	0.020	0.039	0.059	0.030	0.059	0.089

Table 6.4: Equilibrium throughput for 5 BSSs having different target  $k$  and  $n^j$

			IS and APSA			IS,APSA and WUA		
$j$	$k$	$n^j$	$S_{ap}$	$S_{wu}$	$S$	$S_{ap}$	$S_{wu}$	$S$
1	1	2	0.020	0.020	0.040	0.046	0.045	0.091
2	1	6	0.059	0.057	0.116	0.045	0.043	0.088
3	0.5	2	0.039	0.019	0.058	0.060	0.029	0.089
4	0.5	6	0.119	0.057	0.176	0.060	0.029	0.089
5	2	4	0.020	0.038	0.058	0.030	0.059	0.089

Further, the performance of the IS+APSA scheme is evaluated when 5 BSSs operate in the same spectrum but with different priority factors  $k$ , as specified in Table 6.3. By comparing the throughput columns,  $S_{ap}$  and  $S_{wu}$  (without WUA), every BSS achieves the target  $k$ , corroborating the effectiveness of the APSA and IS algorithms. Every AP plays its role to maintain the  $k_{mea}$  within the set target  $k$  in its BSS while all the WUs equally share the remaining bandwidth using the IS scheme. Therefore, each BSS gains equal uplink throughput  $S_{wu}$  (column 2) irrespective of the target  $k$ . However, the downlink throughput  $S_{ap}$  is inversely proportional to the target  $k$  (i.e., the higher  $k$ , the lower the downlink throughput  $S_{ap}$ ), validating the impact of the APSA algorithm. For instance, for the case  $k = 0.5$ , the AP keeps on reducing its CW size in order to ensure its capacity ( $S_{ap}$ ) is twice the uplink capacity

( $S_{wu}$ ) while for  $k = 2$ , it keeps on increasing its CW size to ensure  $S_{ap}$  is half of the  $S_{wu}$ . This unbalance behaviour affects the throughput fairness amongst BSSs as demonstrated in Table 6.3 (column 3). The two BSSs with  $k = 0.5$  dominate 52% of the total throughput leaving two BSSs with  $k = 1$  and one BSS with  $k = 2$  to obtain 35% and 13% of the total throughput respectively. Fi-Wi users might not be happy with this situation. Each user (BSS) expects their share of the cake (channel) irrespective of what  $k$  value they choose to operate at. The following section suggests a technique to equalize the fairness amongst BSSs.

## 6.9 Wireless User Adjustment Algorithm (WUA)

The WUA algorithm introduces a mechanism to ensure the chance of a WU to transmit is dependent on the target  $k$  set in its respective BSS so that the total throughput per BSS across the network is fairly equalized. Consider a network which comprises of  $m$  BSSs. Each  $BSS^j$  ( $j = 1, 2, 3 \dots m$ ) has one  $AP^j$  with  $n^j$  number of WUs and it independently sets the target  $k^j$ . Every  $j^{th}$  BSS has a probability of  $p_s^j$  of a successful transmission in either downlink or uplink directions, given from (5.10) as,

$$p_s^j = \left(1 + \frac{1}{k_j}\right) p_{swu}^j \quad (6.33)$$

where  $p_{swu}^j$  is the probability that any one of the  $n^j$  WUs successfully transmits a packet without incurring any collision,

$$p_{swu}^j = n^j p_{wu}^j (1 - p_c). \quad (6.34)$$

Note that  $p_c$  is the probability of a collision which is assumed constant across the network because all the contending stations use the same transmission rate and packet

size. Moreover,  $p_{wu}^j$  is the probability of WUs from  $BSS^j$  transmitting after contending the channel with the contention window size of  $CW_{wu}^j$ .

$$p_s^j = \left(1 + \frac{1}{k_j}\right) n^j p_{wu}^j (1 - p_c). \quad (6.35)$$

By the principle of *Idle Sense*, all WUs have an equal chance of transmission (i.e.,  $p_{wu}^{j-1} = p_{wu}^j = p_{wu}^{j+1}$ ), causing  $p_s^j$  (6.35) to vary with  $k_j$  and  $n^j$ , the number of WU's per  $BSS^j$ . Thus, to give throughput fairness amongst BSSs,  $p_s^j$  must be scaled to remove the dependence on these two parameters. It is chosen,

$$p_s^* = p_s^j \frac{2}{n^j \left(1 + \frac{1}{k_j}\right)} \quad (6.36)$$

such that when  $k = 1$  and  $n^j = 1$  there is no scaling. To achieve this,  $p_{wu}^j$  in (6.35) is altered at the WU to

$$p_{wu}^{j*} = \frac{2p_{wu}^j}{n^j \left(1 + \frac{1}{k_j}\right)} \quad (6.37)$$

by scaling the CW. Substituting (5.5) into (6.37) and assuming  $CW \gg 1$

$$CW_{wu}^{j*} = CW_{wu}^j \frac{n^j \left(1 + \frac{1}{k_j}\right)}{2}. \quad (6.38)$$

In summary, the above analysis suggests that every WU scales its current  $CW_{wu}$  (after being updated by IS) with a factor of  $\frac{n^j \left(1 + \frac{1}{k_j}\right)}{2}$  before contending the channel. The WU only needs to know local information pertaining to its BSS's  $n^j$  and  $k^j$ . The former is available by monitoring the traffic from the AP and identifying its address fields and the latter, must be periodically broadcast from the  $AP^j$ .

The simulation scenario described in Table 6.3 is repeated employing the WUA algorithm. The uplink throughput  $S_{wu}$  in each BSS varies with the set priority target  $k^j$ , and  $n^j$  such that every BSS is forced to have an equal throughput,  $S$  (column 6)

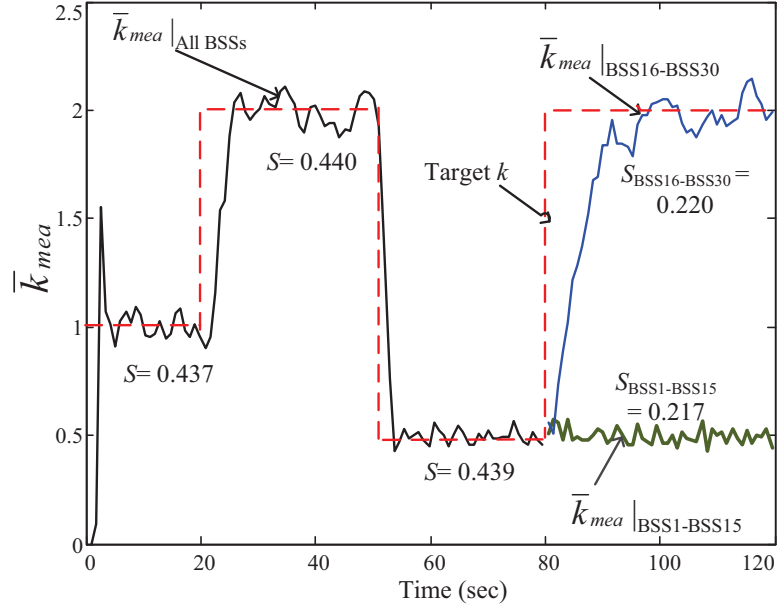


Figure 6.14: The network (30 BSSs) responds to the changes of the target  $k$  ( $\alpha = 1$ ).

irrespective of  $k^j$ . Note the measured  $k_{mea}$  remains close to the target value,  $k^j$ .

The previous simulations assumed the number of users per BSS is fixed at  $n^j = 4$ . Table 6.4 shows results for variable  $n^j$  per BSS. There are still  $m = 5$  AP's and  $n = 20$  WUs, but the WUs are no longer evenly spread between the BSSs. In all cases the the APSA algorithm maintains the measured  $k_{mea} = \frac{S_{wu}}{S_{ap}}$  close to target, while the IS algorithm keeps a constant throughput per WU. The total throughput  $S$  per BSS, (column 3) is now dependant on both  $n^j$  and  $k$ . Finally fairness is restored between BSSs when the WUA algorithm is included. Also note the total throughput,  $S$ , is independent of  $n^j$ , which means the more WUs, the less throughput each gets.

Finally, the robustness of the network is evaluated when all  $m = 30$  APs and  $n = 120$  WUs in the combined IS, APSA and WUA schemes. The plot in Fig. 6.14 demonstrates the convergence behaviour of the  $\bar{k}_{mea}$  when the target  $k$  changes across the network. It is evident that the proposed scheme quickly responds to the changes in  $k$ : 5 seconds are required for the network to change from  $k = 1$  to  $k = 2$  and a

similar time to change from  $k = 2$  to  $k = 0.5$ . However, a somewhat longer 12 sec is required for 15 BSSs to reach  $k_{mea} = 2$  (from  $k_{mea} = 0.5$ ) while the other 15 BSSs remain at their  $k = 0.5$  setting. At this state, despite the  $k$  difference, both classes of BSSs have almost equal capacities, within 1% of each other as indicated by  $S_{BSS}$  values in the plot.

## 6.10 Summary

The chapter first studied the behaviour of the *Idle Sense* scheme when all stations use different CW sizes to contend the channel. *Idle Sense* seeks to maintain the average number of idle slots per transmission,  $I$ , at an optimum level for maximum throughput. The analysis shows that the AIMD algorithm used in IS generates a bias in the mean idle slot operating point,  $\bar{I}$ , compared to the target  $I_t$  which is inversely related to the  $\overline{CW}$  size.

The effect of the averaging length (in number of transmissions  $M$ ) on the accuracy of the estimate  $\hat{I}$  is investigated. The estimation process is modelled as a negative binomial distribution process. Although higher  $M$  improves the accuracy of an estimate, it lessens the chance of a station reducing its CW size due to bias in the AIMD algorithm caused by other stations operating on lower values of  $M$ . Therefore, two extreme classes of stations (small and large CW sizes) are formed, causing instability and unfairness.

The IS fairness problem is therefore caused by the combined effects of a bias in the AIMD algorithm, and the varying sensing period (controlled by  $M$ ) among stations.

Further, the IS scheme was adapted to improve the performance of multiple BSS WLANs in a Fi-Wi network. Priority is given to the APs by using constant  $CW_{ap}$  sizes (analytically derived) while the WUs equally share the remaining bandwidth using the IS adaptation method. Instability in the IS scheme is stabilised by forcing

all WUs to a fixed IS sensing period ( $M = 20$ ). As a result, the fairness between WUs is improved but UL/DL fairness,  $k_{mea}$ , remains a problem. Thus, every AP uses the APSA algorithm to periodically adjust its  $CW_{ap}$  to maintain a desired priority factor  $k$ . However, the IS+APSA algorithm generates unfairness between BSSs with different  $k$  targets. The WUA algorithm recuperates the fairness between BSSs by scaling the current  $CW_{wu}$  based on the required  $k^j$  and the number of BSS users,  $n^j$ .

The combined IS+APSA+WUA scheme is well fitted for the WLAN networks with multiple BSSs sharing the same frequency channel. The network achieves the desired fairness between UL and DL as well as between BSSs while maintaining throughputs within 4% of theoretical optimum. The network responds to changes in  $k$  within a few seconds.

# Chapter 7

## Conclusions and Future Works

### 7.1 Conclusions

The thesis aims at enhancing WLAN performance of the Fi-Wi (GPON-WLAN) networks by capitalizing on the information gained from both optical and wireless media. The proposed schemes are focused on providing solutions for multiple BSS WLAN networks to gain maximum throughput while achieving the desired fairness (i.e., between uplink and downlink transmissions, between WUs or amongst BSSs). These specific aims are addressed in chapters as follows,

- *To study the media access control (MAC) protocol of the GPON and identify potential traffic indicator(s) that can be used in the WLAN enhancement.*

Chapter 2 explores the architectures and protocols of GPON. The study reveals that the broadcast nature of GPON's architecture allows users to obtain three traffic indicators : upstream traffic size, downstream traffic size and total number of active ONTs. These traffic indicators can be exploited to enhance the performance in the wireless side of Fi-Wi networks.

- *To study the MAC protocol of the existing IEEE 802.11 WLAN and identify the factors that affect the throughput performance.*

The foundation for the thesis is built in Chapter 3 through a critical review of the relevant subjects in WLAN. The IEEE 802.11 WLAN standards and their medium access control protocols are introduced. The throughput performance was evaluated by means of OPNET simulations and identified that the binary exponential backoff (BEB) algorithm adopted in the MAC protocol is the key factor in the throughput degradation. Existing adaptive backoff schemes are critically reviewed and the schemes are classified according to the traffic indicators used in the proposed algorithms. In addition, a literature survey of transmission priority schemes provides understanding of the techniques to improve the fairness between uplink and downlink transmissions. The chapter finally addresses recent developments in Fi-Wi networks.

- *To modify the legacy binary exponential backoff (BEB) algorithm in a WLAN in order to allow the network to gain optimum capacity and to investigate the causes of fairness problem in a multiple BSSs network scenario.*

Inspired by the findings from the preceding chapters, Chapter 4 proposes a hybrid Fi-Wi network by integrating GPON with a ‘closed’ WLAN. The term ‘closed’ indicated that the network operator has a dedicated spectrum allocation, shared by all WLAN APs in a highly dense populated area. The chapter then proposes an optimized constant contention window (OCCW) scheme for non-saturated multiple BSS WLANs which resemble the wireless side of a Fi-Wi network. OCCW modified the standard BEB algorithm by assigning the constant CW size based on traffic intensity, to achieve the best throughput performance. Traffic information obtained from the GPON is used by the WUs as an indicator to select the optimum CW size. In comparison to BEB, OCCW

improved the throughput by up to 50% and the delay reduced by a factor of 5. However, the OCCW scheme did not do justice to the downlink transmissions in such an infrastructure WLAN. Therefore, the APPriority scheme was proposed to give APs more transmission opportunities. Simulations showed that selecting a smaller CW size for an AP than that of a WU allowed the AP to select smaller backoff slots than a WU. This resulted in an improved downlink throughput and consequently brought fairness between uplink and downlink transmissions. Interestingly, both schemes show that problems of throughput and fairness occur under heavily loaded conditions, when the channel reaches saturation. Therefore, the remainder of the thesis deals exclusively with the saturated condition.

- *To derive expressions that optimize the CW sizes of an access point (AP) and wireless users (WUs) for maximum throughput while achieving the desired fairness between uplink and downlink transmissions.*

Subsequently, Chapter 5 further improves the enhancement techniques by deriving the expressions for the optimum CW sizes of the AP and WU to obtain maximum saturation throughput. An adjustable transmission priority factor  $k$  is introduced to allow the network to achieve the desired fairness between UL and DL transmissions. The adaptive backoff technique is introduced and it requires estimates of the number of APs ( $m$ ) and the number of WUs ( $n$ ). The first is directly estimated from GPON frame information and the second is estimated by measuring the activity on the WLAN channel. In addition, a new convergence function,  $c(m, \bar{n})$ , is added to overcome the instability problem caused by the estimate  $\bar{n}$ . The scheme demonstrates robustness for practical values of  $k$ ,  $m$  and  $n$  with a minimal 3% throughput degradation (from optimum).

- *To develop a distributed algorithm that dynamically tracks changes in the network while maintaining optimum CW sizes in a robust and simple way.*

Chapter 6 studies *Idle Sense*, a method which does not require the intermediate step of estimating  $n$ . However, an analytical study reveals that when the contending stations use different CW sizes to initiate the contention, two classes of stations are formed: those that dominate transmissions and those that starve. Instability arises when a bias from the AIMD convergence process interacts with the adaptive idle slot sensing mechanism. Therefore, the IS scheme is simplified by forcing all stations to a fixed IS sensing period. The IS technique is then applied to a Fi-Wi network by allowing WUs to equally share the remaining bandwidth using the IS adaptation method after the desired priority has been given to APs, through the use of a constant CW size (analytically derived). Despite achieving fairness between WUs, the network failed to reach the desired  $k$ . Therefore, the APSA algorithm is introduced to allow every AP to periodically adjust its  $CW_{ap}$  to reach the desired priority  $k$ . In addition, the WUA algorithm is proposed to mitigate unfairness (due to IS+APSA) between BSSs with different  $k$  targets. The combined IS+APSA+WUA scheme enables the network with multiple BBSSs to achieve the desired fairness between UL and DL as well as between BSSs while maintaining throughputs within 4% of theoretical optimum.

It is worth noting that all the schemes proposed in this thesis are compatible with the DCF protocol adopted by all 802.11 family members [106, 107]. The schemes improve the integration of fiber-wireless networks as this ensures each station in the BSS is given a fair transmission opportunity so that the huge bandwidth capacity provided by the GPON (backhaul) can be fully utilised. The findings of this thesis can make a significant contribution to the advancement of Fi-Wi networks, specifically in the wireless media. In the long term, Fi-Wi networks hold great promise of

changing the way people communicate by replacing commuting with teleworking. Indirectly, they will contribute to a reduction in fuel consumption and thereby protect the environment.

## 7.2 Future Works

Future work should concentrate on eliminating many of the assumptions associated with this work, namely:

- Assumption of closed spectrum, means that other (non participating) WLAN users are forbidden. The effect of loosening this constraint would increase the applicability of the system by enabling operation on license free bands as per normal WiFi systems.
- Assumption of all GPON traffic going through the wireless access point. Direct connections of equipment to the ONT (avoiding the wireless ) would give the impression that more data is flowing through the wireless medium than actually was. A method of identifying wireless and directly connected data sources would be needed.
- Assumption that all stations from all BSSs can overhear each other, although not necessarily having enough SNR to demodulate the payloads (no hidden nodes etc.). Protocol modifications might be necessary to improve robustness in such situations.
- Assumption that the GPON network boundary contains no interfering sources. In reality neighbouring GPONs with different OLTs (head-end) will cause interference to boundary BSSs without their traffic data being monitored on the fibre. A study of boundary conditions would be necessary.

- Assumption that only one frequency channel is available. Multiple channels would allow some FDMA and reduce interference, but how best to deploy the added resource is an open question.

# Appendix A

## Full Derivation of Saturation Throughput $S$

Considering the fact that the contention of a radio channel can evolve between 3 states : idle  $i$ , collision  $c$ , and successful transmission  $s$ , which gives,

$$p_i + p_c + p_s = 1. \quad (\text{A.1})$$

By definition, normalized saturation throughput  $S$  is expressed as the fraction of time the channel is used to successfully transmit payload bits,

$$S = \frac{p_s T_{\text{payload}}}{p_i T_i + p_c T_c + p_s T_s}. \quad (\text{A.2})$$

Note that collision and successful transmission states give impression that the channel is busy indicating that there is at least one transmission on the channel. Hence, the transmission probability  $P_{tr}$  is,

$$P_{tr} = p_c + p_s, \quad (\text{A.3})$$

which further yields,

$$P_c + P_s = 1, \quad (\text{A.4})$$

where,

$$P_c = \frac{P_c}{P_{tr}} \quad (\text{A.5})$$

and

$$P_s = \frac{P_s}{P_{tr}}. \quad (\text{A.6})$$

Corroborating (A.1) and (A.3) gives,

$$p_i = 1 - P_{tr}. \quad (\text{A.7})$$

Finally, using (A.2), (A.5), (A.6) and (A.7), the normalized saturation throughput  $S$  is derived,

$$S = \frac{P_s P_{tr} T_{payload}}{(1 - P_{tr})T_i + P_s P_{tr} T_s + (1 - P_s)P_{tr} T_c}.$$

# References

- [1] L. G. Kazovsky, N. Cheng, W.-T. Shaw, D. Gutierrez, and S.-W. Wong, *Broadband Optical Access Networks*, John Wiley & Sons, 2011.
- [2] OECD, “The development of fixed broadband networks,” OECD Publishing, Tech. Rep. OECD Digital Economy Papers No. 239, 2014.
- [3] Cisco, “Cisco visual networking index: Forecast and methodology, 2013-2018,” Cisco, Tech. Rep., June 2014.
- [4] R. S. Tucker *et al.*, “Broadband facts, fiction and urban myths,” *Telecommunications Journal of Australia*, vol. 60, no. 3, pp. 43–1, 2010.
- [5] M. Maier, “Fiber-wireless (FiWi) broadband access networks in an age of convergence: Past, present, and future,” *Advances in Optics*, Hindawi Publishing Corporation, 2014.
- [6] F. Effenberger, D. Clearly, O. Haran, G. Kramer, R. D. Li, M. Oron, and T. Pfeiffer, “An introduction to PON technologies [topics in optical communications],” *Communications Magazine, IEEE*, vol. 45, no. 3, pp. S17–S25, 2007.
- [7] F. Effenberger, J.-i. Kani, and Y. Maeda, “Standardization trends and prospective views on the next generation of broadband optical access systems,” *Selected*

- 
- Areas in Communications, IEEE Journal on*, vol. 28, no. 6, pp. 773–780, Aug 2010.
- [8] Commscope , “GPON-EPON comparison,” White paper, Commscope.Inc, Tech. Rep., 2013.
- [9] M. Scott, “Protocols for fibre to the home,” *Doctoral Training Centre*, 2010.
- [10] D. Nowak and J. Murphy, “FTTH: The overview of existing technologies,” in *OPTO-Ireland International Society for Optics and Photonics*, 2005, pp. 500–509.
- [11] ITU-T Recommendation G.984.1, “Gigabit-capable pasive optical networks (G-PON): General characteristics,” *ITU-T Study Group*, 2008.
- [12] ITU-T Recommendation G.984.2, “Gigabit-capable passive optical networks (G-PON): Physical media dependent (PMD) layer specification,” *ITU-T Study Group*, 2008.
- [13] ITU-T Recommendation. G.984.3, “Gigabit-capable passive optical networks (GPON):transmission convergence layer specification,” *ITU-T Study Group*, 2008.
- [14] ITU-T Recommendation G.984.4, “Gigabit-capable passive optical networks (G-PON): ONT management and control interface specification,” *ITU-T Study Group*, 2008.
- [15] S. Bindhaiq, A. S. M. Supaat, N. Zulkifli, A. B. Mohammad, R. Q. Shaddad, M. A. Elmagzoub, and A. Faisal, “Recent development on time and wavelength-division multiplexed passive optical network (TWDM-PON) for next-generation

- passive optical network stage 2 (NG-PON2),” *Optical Switching and Networking*, no. 0, pp. –, 2014. [Online]. Available: <http://www.sciencedirect.com/science/article/pii/S1573427714000733>
- [16] M. Hernandez, A. Arcia, R. Alvizu, and M. Huerta, “A review of XDMA-WDM-PON for next generation optical access networks,” in *Global Information Infrastructure and Networking Symposium (GIIS), 2012*, Dec 2012, pp. 1–6.
- [17] F. Beltrn, “Fibre-to-the-home, high-speed and national broadband plans: Tales from down under,” *Telecommunications Policy*, no. 0, pp. –, 2013. [Online]. Available: <http://www.sciencedirect.com/science/article/pii/S0308596113001225>
- [18] L. G. Kazovsky, W.-T. Shaw, D. Gutierrez, N. Cheng, and S.-W. Wong, “Next-generation optical access networks,” *J. Lightwave Technol.*, vol. 25, no. 11, pp. 3428–3442, Nov 2007. [Online]. Available: <http://jlt.osa.org/abstract.cfm?URI=jlt-25-11-3428>
- [19] M. Maier, M. Levesque, and L. Ivanescu, “NG-PONs 1 2 and beyond: the dawn of the uber-fiwi network,” *Network, IEEE*, vol. 26, no. 2, pp. 15–21, March 2012.
- [20] M. S. Ahsan, M. Lee, S. H. S. Newaz, and S. Asif, “Migration to the next generation optical access networks using hybrid WDM/TDM-PON,” *Journal of Networks*, vol. 6, no. 1, 2011.
- [21] N. Cvijetic, “OFDM for next-generation optical access networks,” *Lightwave Technology, Journal of*, vol. 30, no. 4, pp. 384–398, Feb 2012.
- [22] Y. Lu, Y. Gong, Y. Wei, M. Hu, X. Zhou, and Q. Li, “A smooth and gradual evolution to next generation pon based on simple line-coding,” *Photonics Technology Letters, IEEE*, vol. 26, no. 5, pp. 512–515, March 2014.

- 
- [23] I. Cale, A. Salihovic, and M. Ivekovic, “Gigabit passive optical network-GPON,” in *Information Technology Interfaces, 2007. ITI 2007. 29th International Conference on*, IEEE, 2007, pp. 679–684.
- [24] Huawei, “GPON fundamentals [online],” Huawei Technologies, Tech. Rep., 2010. [Online]. Available: <http://www.huawei.com>
- [25] M. Driberg, “Channel assignment strategies for throughput enhancement in high density wireless local area networks,” Ph.D. dissertation, Victoria University, 2010.
- [26] O. Bejarano, E. W. Knightly, and M. Park, “IEEE 802.11 ac: From channelization to multi-user mimo,” *IEEE Communications Magazine*, p. 85, 2013.
- [27] K. Ross. Jim Kurose, *Computer Networking A Top-Down Approach*, M. Hirsch, Ed., Addison Wesley, 2010.
- [28] IEEE Standard for Information technology-, “Telecommunications and information exchange between systems Local and metropolitan area networks—Specific requirements Part 11: Wireless LAN Medium Access Control (MAC) and Physical Layer (PHY) Specifications,” *IEEE Std 802.11-2012 (Revision of IEEE Std 802.11-2007)*, vol., no., pp.1,2793, March 29 2012.
- [29] G. Bianchi, S. Choi, and I. Tinnirello, “Emerging technologies in wireless LANs: theory, design, and deployment”, *Cambridge University Press*, 2008, ch. Performance understanding of IEEE 802.11 DCF and IEEE 802.11e EDCA.
- [30] R. Moraes, P. Portugal, F. Vasques, and J. A. Fonseca, “Limitations of the IEEE 802.11 e edca protocol when supporting real-time communication,” in *Factory Communication Systems, 2008. WFCS 2008. IEEE International Workshop on*, 2008, pp. 119–128.

- 
- [31] G. Cena, L. Seno, A. Valenzano, and C. Zunino, “On the performance of IEEE 802.11 e wireless infrastructures for soft-real-time industrial applications,” *Industrial Informatics, IEEE Transactions on*, vol. 6, no. 3, pp. 425–437, 2010.
- [32] Intel, “Helping define IEEE 802.11 and other wireless LAN standards.” [Online]. Available: <http://www.intel.com/content/www/us/en/standards/802-11-wireless-LAN-standards-study.html>
- [33] T. Paul and T. Ogunfunmi, “Wireless LAN comes of age: Understanding the IEEE 802.11 n amendment,” *Circuits and Systems Magazine, IEEE*, vol. 8, no. 1, pp. 28–54, 2008.
- [34] C.-Y. Wang and H.-Y. Wei, “IEEE 802.11 n MAC enhancement and performance evaluation,” *Mobile Networks and Applications*, vol. 14, no. 6, pp. 760–771, 2009.
- [35] W.-F. Alliance, “802.11n draft 2.0: Longer-range, faster-throughput, multimedia-grade Wi-Fi networks,” Wi-Fi Alliance, Tech. Rep., 2007.
- [36] E. Perahia and M. X. Gong, “Gigabit wireless LANs: an overview of IEEE 802.11 ac and 802.11 ad,” *ACM SIGMOBILE Mobile Computing and Communications Review*, vol. 15, no. 3, pp. 23–33, 2011.
- [37] R. C. Daniels, J. N. Murdock, T. S. Rappaport, and R. W. Heath, “60 ghz wireless: Up close and personal,” *Microwave Magazine, IEEE*, vol. 11, no. 7, pp. 44–50, 2010.
- [38] Q. Chen, J. Tang, D. T. C. Wong, X. Peng, and Y. Zhang, “Directional cooperative MAC protocol design and performance analysis for IEEE 802.11 ad WLANs,” *Vehicular Technology, IEEE Transactions on*, vol. 62, no. 6, pp. 2667–2677, 2013.

- 
- [39] B. Schluz, “802.11ad? WLAN at 60 GHz a technology introduction,” Rohde and Schwarz amd Co., Tech. Rep., 2013.
- [40] E. Perahia, C. Cordeiro, M. Park, and L. L. Yang, “IEEE 802.11 ad: Defining the next generation multi-Gbps Wi-Fi,” in *Consumer Communications and Networking Conference (CCNC), 2010 7th IEEE IEEE*, 2010, pp. 1–5.
- [41] B. Patil, Y. Saifullah, S. Faccin, and S. Sreemanthula, *IP in Wireless Networks*, Prentice Hall , 2003.
- [42] N. Gupta, P. Kuman *et al.*, “A performance analysis of the 802.11 wireless LAN medium access control,” *Communications in Information & Systems*, vol. 3, no. 4, pp. 479–304, 2003.
- [43] IEEE 802.11, “Wireless LAN medium access control (MAC) and physical layer (PHY) specifications,” IEEE, 1999.
- [44] M. Youssef, A. Vasan, and R. E. Miller, “Specification and analysis of the DCF and pcf protocols in the 802.11 standard using systems of communicating machines,” in *Network Protocols, 2002. Proceedings. 10th IEEE International Conference on*, 2002, pp. 132–141.
- [45] Q. Liu, D. Zhao, and D. Zhou, “An analytic model for enhancing IEEE 802.11 point coordination function media access control protocol,” *European Transactions on Telecommunications*, vol. 22, no. 6, pp. 332–338, 2011.
- [46] B. Sikdar, “An analytic model for the delay in IEEE 802.11 pcf MAC-based wireless networks,” *Wireless Communications, IEEE Transactions on*, vol. 6, no. 4, pp. 1542–1550, 2007.

- 
- [47] INVOCOM, “PCF Scheme,” *Internet Based Vocational Training of Communication Students, Engineers and Technicians*, 2004. [Online]. Available: [http://www.invocom.et.put.poznan.pl/~invocom/C/P1-4/p1-4\\_en/p1-4\\_8\\_2.htm](http://www.invocom.et.put.poznan.pl/~invocom/C/P1-4/p1-4_en/p1-4_8_2.htm)
- [48] G. Bianchi, “Performance analysis of the IEEE 802.11 distributed coordination function,” *Selected Areas in Communications, IEEE Journal on*, vol. 18, no. 3, pp. 535–547, 2000.
- [49] OPNET Modeler 16.1, [www.opnet.com](http://www.opnet.com).
- [50] N.-O. Song, B.-J. Kwak, J. Song, and M. Miller, “Enhancement of IEEE 802.11 distributed coordination function with exponential increase exponential decrease backoff algorithm,” in *Vehicular Technology Conference, 2003. VTC 2003-Spring. The 57th IEEE Semiannual*, vol. 4, IEEE, 2003, pp. 2775–2778.
- [51] V. Bharghavan, A. Demers, S. Shenker, and L. Zhang, “Macaw: a media access protocol for wireless LAN’s,” in *ACM SIGCOMM Computer Communication Review*, vol. 24, no. 4, ACM, 1994, pp. 212–225.
- [52] M. Al-Hubaishi, T. Alahdal, R. Alsaqour, A. Berqia, M. Abdelhaq, and O. Alsaqour, “Enhanced binary exponential backoff algorithm for fair channel access in the IEEE 802.11 medium access control protocol,” *International Journal of Communication Systems*, 2013.
- [53] J. Wang and M. Song, “An efficient traffic adaptive backoff protocol for wireless MAC layer,” in *Wireless Algorithms, Systems and Applications, 2007. WASA 2007. International Conference on*, IEEE, 2007, pp. 169–173.
- [54] L. Ma, Q. Zhang, F. An, and X. Cheng, “DIAR: A dynamic interference aware routing protocol for IEEE 802.11-based mobile ad hoc networks,” in *Mobile Ad-hoc and Sensor Networks*, pp. 508–517, Springer Berlin Heidelberg, 2005.

- 
- [55] T. Li, T. Tang, and C. Chang, “A new backoff algorithm for IEEE 802.11 distributed coordination function,” in *Fuzzy Systems and Knowledge Discovery, 2009. FSKD'09. Sixth International Conference on*, vol. 3, IEEE, 2009, pp. 455–459.
- [56] F. Cali, M. Conti, and E. Gregori, “IEEE 802.11 protocol: design and performance evaluation of an adaptive backoff mechanism,” *Selected Areas in Communications, IEEE Journal on*, vol. 18, no. 9, pp. 1774–1786, 2000.
- [57] F. Cali, M. Conti, and E. Gregori, “Dynamic tuning of the IEEE 802.11 protocol to achieve a theoretical throughput limit,” *IEEE/ACM Transactions on Networking (ToN)*, vol. 8, no. 6, pp. 785–799, 2000.
- [58] P. Chatzimisios, V. Vitsas, A. C. Boucouvalas, and M. Tsoulfa, “Achieving performance enhancement in IEEE 802.11 WLANs by using the DIDD backoff mechanism,” *International Journal of communication systems*, vol. 20, no. 1, pp. 23–41, 2007.
- [59] K. Hong, S. Lee, K. Kim, and Y. Kim, “Channel condition based contention window adaptation in IEEE 802.11 WLANs,” *Communications, IEEE Transactions on*, vol. 60, no. 2, pp. 469–478, 2012.
- [60] G. Bianchi, L. Fratta, and M. Oliveri, “Performance evaluation and enhancement of the CSMA/CA MAC protocol for 802.11 wireless LANs,” in *Personal, Indoor and Mobile Radio Communications, 1996. PIMRC'96., Seventh IEEE International Symposium on*, vol. 2, IEEE, 1996, pp. 392–396.
- [61] M. Ibrahim and S. Alouf, “Design and analysis of an adaptive backoff algorithm for IEEE 802.11 DCF mechanism,” in *NETWORKING 2006. Networking Technologies, Services, and Protocols; Performance of Computer and Communication Networks; Mobile and Wireless Communications Systems*, Springer, 2006,

- pp. 184–196.
- [62] H.-M. Liang, S. Zeadally, N. K. Chilamkurti, and C.-K. Shieh, “A novel pause count backoff algorithm for channel access in IEEE 802.11 based wireless LANs,” in *Computer Science and its Applications, 2008. CSA’08. International Symposium on*, IEEE, 2008, pp. 163–168.
- [63] S.-W. Kang, J.-R. Cha, and J.-H. Kim, “A novel estimation-based backoff algorithm in the IEEE 802.11 based wireless network,” in *Consumer Communications and Networking Conference (CCNC), 2010 7th IEEE*, IEEE, 2010, pp. 1–5.
- [64] A. Balador, A. Movaghar, S. Jabbehdari, and D. Kanellopoulos, “A novel contention window control scheme for IEEE 802.11 WLANs.” *IETE Technical Review*, vol. 29, no. 3, 2012.
- [65] Q. Nasir and M. Albalt, “History based adaptive backoff (HBAB) IEEE 802.11 MAC protocol,” in *Communication Networks and Services Research Conference, 2008. CNSR 2008. 6th Annual*, IEEE, 2008, pp. 533–538.
- [66] D.-J. Deng, C.-H. Ke, H.-H. Chen, and Y.-M. Huang, “Contention window optimization for IEEE 802.11 DCF access control,” *Wireless Communications, IEEE Transactions on*, vol. 7, no. 12, pp. 5129–5135, 2008.
- [67] M. Heusse, F. Rousseau, R. Guillier, and A. Duda, “Idle sense: An optimal access method for high throughput and fairness in rate diverse wireless LANs,” *SIGCOMM Comput. Commun. Rev.*, vol. 35, no. 4, pp. 121–132, Aug. 2005. [Online]. Available: <http://doi.acm.org/10.1145/1090191.1080107>

- 
- [68] Y. Grunenberger, M. Heusse, F. Rousseau, and A. Duda, “Experience with an implementation of the idle sense wireless access method,” in *Proceedings of the 2007 ACM CoNEXT conference*, ACM, 2007, p. 24.
- [69] E. Lopez-Aguilera, M. Heusse, Y. Grunenberger, F. Rousseau, A. Duda, and J. Casademont, “An asymmetric access point for solving the unfairness problem in WLANs,” *Mobile Computing, IEEE Transactions on*, vol. 7, no. 10, pp. 1213–1227, 2008.
- [70] M. Nassiri, M. Heusse, and A. Duda, “A novel access method for supporting absolute and proportional priorities in 802.11 WLANs,” in *INFOCOM 2008. The 27th Conference on Computer Communications*, IEEE, 2008.
- [71] J. Deng, P. K. Varshney, and Z. J. Haas, “A new backoff algorithm for the IEEE 802.11 distributed coordination function,” in *Communication Networks and Distributed Systems Modelling and Simulation (CNDS '04)*, IEEE, 2008.
- [72] G. Chockler, M. Demirbas, S. Gilbert, C. Newport, and T. Nolte, “Consensus and collision detectors in wireless ad hoc networks,” in *Proceedings of the twenty-fourth annual ACM symposium on Principles of distributed computing*, ACM, 2005, pp. 197–206.
- [73] B. H. S. Abeysekera, T. Matsuda, and T. Takine, “Dynamic contention window control mechanism to achieve fairness between uplink and downlink flows in IEEE 802.11 wireless LANs,” *Wireless Communications, IEEE Transactions on*, vol. 7, no. 9, pp. 3517–3525, 2008.
- [74] Y. Gao and L. Dai, “Optimal downlink/uplink throughput allocation for IEEE 802.11 DCF networks,” *IEEE Wireless Communications Letters*, vol. 2, no. 6, pp. 627–630, 2013.

- 
- [75] M. Bottigliengo, C. Casetti, C.-F. Chiasserini, and M. Meo, “Smart traffic scheduling in 802.11 WLANs with access point,” in *Vehicular Technology Conference, 2003. VTC 2003-Fall. 2003 IEEE 58th*, vol. 4, IEEE, 2003, pp. 2227–2231.
- [76] C. Wang, “Achieving per-flow and weighted fairness for uplink and downlink in IEEE 802.11 WLANs,” *EURASIP Journal on Wireless Communications and Networking*, vol. 2012, no. 1, pp. 1–9, 2012.
- [77] F. Micó, J. Villalón, A. Valverde, P. Cuenca, and J. Delicado, “Guaranteed access mode for downlink traffic over IEEE 802.11 WLANs,” in *Wireless and Mobile Networking Conference (WMNC), 2011 4th Joint IFIP*, IEEE, 2011, pp. 1–7.
- [78] S. W. Kim, B.-S. Kim, and Y. Fang, “Downlink and uplink resource allocation in IEEE 802.11 wireless LANs,” *Vehicular Technology, IEEE Transactions on*, vol. 54, no. 1, pp. 320–327, 2005.
- [79] S. Shin and H. Schulzrinne, “Balancing uplink and downlink delay of VoIP traffic in WLANs using adaptive priority control (APC),” in *Proceedings of the 3rd international conference on Quality of service in heterogeneous wired/wireless networks*, ACM, 2006, p. 41.
- [80] P. Clifford, K. Duffy, D. J. Leith, and D. Malone, “On improving voice capacity in 802.11 infrastructure networks,” in *Proceedings of IEEE WirelessCom 2005*, IEEE, 2005.
- [81] G. Min, J. Hu, and M. E. Woodward, “Modeling and analysis of TXOP differentiation in infrastructure-based WLANs,” *Computer Networks*, vol. 55, no. 11, pp. 2545–2557, 2011.

- 
- [82] W.-S. Lim, D.-W. Kim, and Y.-J. Suh, "Achieving fairness between uplink and downlink flows in error-prone WLANs," *Communications Letters, IEEE*, vol. 15, no. 8, pp. 822–824, 2011.
- [83] Y. Xiao, "Performance analysis of priority schemes for IEEE 802.11 and IEEE 802.11e wireless LANs," *Wireless Communications, IEEE Transactions on*, vol. 4, no. 4, pp. 1506–1515, 2005.
- [84] F. Keceli, I. Inan, and E. Ayanoglu, "Weighted fair uplink/downlink access provisioning in IEEE 802.11e WLANs," in *Communications, 2008. ICC'08. IEEE International Conference on*, IEEE, 2008, pp. 2473–2479.
- [85] J. Jeong, S. Choi, and C.-k. Kim, "Achieving weighted fairness between uplink and downlink in IEEE 802.11 DCF-based WLANs," in *Quality of Service in Heterogeneous Wired/Wireless Networks, 2005. Second International Conference on*, 2005, pp. 10–pp.
- [86] L. Zhang, P. Sénac, E. Lochin, and M. Diaz, "Cross-layer based congestion control for WLANs," in *Proceedings of the 5th International ICST Conference on Heterogeneous Networking for Quality, Reliability, Security and Robustness*, ICST (Institute for Computer Sciences, Social-Informatics and Telecommunications Engineering), 2008, p. 35.
- [87] L. Zhang, P. Sénac, E. Lochin, and M. Diaz, "A cross-layer architecture to improve mobile host rate performance and to solve unfairness problem in WLANs," *Telecommunication Systems*, vol. 53, no. 3, pp. 343–356, 2013.
- [88] S. H. Rhee and X. Lei, "AP-initiated reservations for performance enhancement in 802.11 MAC," *Wireless Personal Communications*, pp. 1–12, 2014.

- 
- [89] J. Hecht, “Ultrafast fibre optics set new speed record,” *New Scientist*, April, 2011 [Online]. Available: <http://www.newscientist.com/article/mg21028095.500-ultrafast-fibre-optics-set-new-speed-record.html#.VNHNRMiUeom>
- [90] J. Johny and S. Shashidharan, “Design and simulation of a radio over fiber system and its performance analysis,” in *Ultra Modern Telecommunications and Control Systems and Workshops (ICUMT), 2012 4th International Congress on*, IEEE, 2012, pp. 636–639.
- [91] B. O. Obele and M. Kang, “Fixed mobile convergence: a self-aware QoS architecture for converging WiMax and GEAPON access networks,” in *Next Generation Mobile Applications, Services and Technologies, 2008. NGMAST’08. The Second International Conference on*, IEEE, 2008, pp. 411–418.
- [92] M. Milosavljevic, Y. Shachaf, P. Kourtessis, and J. M. Senior, “Interoperability of GPON and WiMax for network capacity enhancement and resilience,” *Journal of Optical Networking*, vol. 8, no. 3, pp. 285–294, 2009.
- [93] G. Shen and R. Tucker, “Fixed mobile convergence (FMC) architectures for broadband access: Integration of EPON and WiMAX,” in *Asia-Pacific Optical Communications*, International Society for Optics and Photonics, 2007, pp. 678 403–678 403.
- [94] Y. Yan, H. Yu, and L. Dittmann, “Wireless channel condition aware scheduling algorithm for hybrid optical/wireless networks,” in *AccessNets*, Springer, 2009, pp. 397–409.
- [95] M. Maier, N. Ghazisaidi, and M. Reisslein, “The audacity of fiber-wireless (FiWi) networks,” in *AccessNets*, Springer, 2009, pp. 16–35.

- 
- [96] S. Sarkar, S. Dixit, and B. Mukherjee, “Hybrid wireless-optical broadband-access network (WOBAN): a review of relevant challenges,” *Lightwave Technology, Journal of*, vol. 25, no. 11, pp. 3329–3340, 2007.
- [97] N. Ghazisaidi and M. Maier, “Fiber-wireless (FiWi) access networks: Challenges and opportunities,” *Network, IEEE*, vol. 25, no. 1, pp. 36–42, 2011.
- [98] F. Aurzada, M. Lévesque, M. Maier, and M. Reisslein, “Fiwi access networks based on next-generation PON and gigabit-class WLAN technologies: A capacity and delay analysis,” 2013.
- [99] M. Maier, “FiWi access networks: Future research challenges and moonshot perspectives,” in *Communications Workshops (ICC), 2014 IEEE International Conference on*, 2014, pp. 371–375.
- [100] W. H. W. Hassan, M. Faulkner, and H. King, “Integration of a modified distributed coordination function (DCF) in wireless LAN using IEEE 802.11n to mitigate interference and optimise transmission capacity in full duplex gigabits passive optical network (GPON),” in *Information, Communications and Signal Processing (ICICS) 2011 8th International Conference on*, IEEE, 2011, pp. 1–4.
- [101] W. H. W. Hassan, H. King, and M. Faulkner, “Modified backoff technique in fiber-wireless networks,” in *Personal Indoor and Mobile Radio Communications (PIMRC), 2012 IEEE 23rd International Symposium on*, 2012, pp. 431–435.
- [102] J. Wang and M. Song, “An efficient traffic adaptive backoff protocol for wireless MAC layer,” in *Wireless Algorithms, Systems and Applications, 2007. WASA 2007. International Conference on*, IEEE, 2007, pp. 169–173.

- [103] W. H. W. Hassan, H. King, S. Ahmed, and M. Faulkner, "Modified back-off technique with transmission priority scheme in fiber-wireless networks," in *AFRICON, 2013*, IEEE, 2013, pp. 1–4.
- [104] R.E Walpole, R.H Myers, S.L. Myers, "Some Discrete Probability Distributions," in *Probability and Statistics for Engineers and Scientists*, 6th ed. New Jersey, Prentice Hall International, 1998, ch. 5, sec. 5.5, pp. 132-134.
- [105] R. Jain, D.-M. Chiu, and W. Hawe, "A quantitative measure of fairness and discrimination for resource allocation in shared computer system,? Digital Equipment Corp., Tech. Rep., 1984.
- [106] S. Mangold, S. Choi, P. May, O. Klein, G. Hiertz, and L. Stibor, "IEEE 802.11e Wireless LAN for Quality of Service," in *Proc. European Wireless*, vol. 2, pp. 32-39, 2002.
- [107] D. Skordoulis, Q. Ni, H-H. Chen, A.P. Stephens, C. Liu, and A. Jamalipour, "IEEE 802.11n MAC frame aggregation mechanisms for next-generation high-throughput WLANs," *IEEE Wireless Communications*, pp. 40-47, 2008.